HAL
open science

Contribution for the ergonomic analysis using virtual human

Liang Ma

To cite this version:

Liang Ma. Contribution for the ergonomic analysis using virtual human. Robotics [cs.RO]. Ecole Centrale de Nantes (ECN), 2009. English. NNT : . tel-01385176

HAL Id: tel-01385176

https://hal.science/tel-01385176v1

Submitted on 20 Oct 2016

HAL is a multi-disciplinary open access archive for the deposit and dissemination of scientific research documents, whether they are published or not. The documents may come from teaching and research institutions in France or abroad, or from public or private research centers.

L'archive ouverte pluridisciplinaire **HAL**, est destinée au dépôt et à la diffusion de documents scientifiques de niveau recherche, publiés ou non, émanant des établissements d'enseignement et de recherche français ou étrangers, des laboratoires publics ou privés.

Ecole Centrale de Nantes

École Doctorale

Sciences Pour Ingénieur, Géosciences, Architecture

Année 2009 N°B.U.:

Thèse de Doctorat

Spécialité: Génie Mécanique

Présentée et soutenue publiquement par:

Liang MA

le 19 Octobre 2009

à l'École Centrale de Nantes

Titre

Contributions pour l'analyse ergonomique de mannequins virtuels

JURY

Rapporteurs:	Georges DUMONT	Maître de Conférences & HDR, ENS Cachan Bretagne
	Ronan BOULIC	Adjoint scientifique & HDR, EPFL
Examinateurs:	Etienne DOMBRE	Directeur de Recherche CNRS, LIRMM
	Fouad BENNIS	Professeur, École Centrale de Nantes
	Damien CHABLAT	Chargé de recherche CNRS & HDR, IRCCyN
	Philippe WENGER	Directeur de Recherche CNRS, IRCCyN
	Zhizhong LI	Professeur, Université Tsinghua
	Wei ZHANG	Professeur associé & HDR, Université Tsinghua
Invité:	François GUILLAUME	Ingénieur de Recherche, EADS Innovation Works

---

Directeur de Thèse: Fouad BENNIS

Laboratoire: Institut de Recherche en Communications et Cybernétique de Nantes

Co-directeur: Damien CHABLAT

Laboratoire: Institut de Recherche en Communications et Cybernétique de Nantes N° ED 498-59

Abstract

Physical fatigue in occupational activities leads to potential musculoskeletal disorder (MSD) risks, and it has received great attention to model the fatigue in order to prevent potential risks in ergonomics. Meanwhile, virtual human techniques have been used a lot in industrial design in order to consider human factors and ergonomics as early as possible. However, fatigue effect is considered sufficiently neither in conventional ergonomics tools nor in virtual human simulation tools. In this thesis, we are focusing on the modeling of muscle fatigue and recovery processes in manual handling operations, its potential applications, and the integration of fatigue effect into human operation evaluation and human simulation tools.

At first, a simplified muscle fatigue model is proposed based on motor-unit pattern in muscle physiology to predict the reduction of physical strength in manual handling operations. Theoretical approach and experimental approach are used to validate the fatigue model. In theoretical way, comparisons have been made between the proposed model and existing maximum endurance models in static cases and other muscle fatigue models in dynamic cases. From theoretical analysis, fatigue resistance for a specific muscle group of a certain population can be determined by regression method. Secondly, in experimental method, a total of 40 subjects carried out the simulated drilling operation under posture constraints. Along the working process, the simulated job static strengths were measured as an index of the physical fatigue, and the posture of the upper limb was also captured in the operation. It has been found that the fatigue of most of the subjects followed the exponential function predicted by the fatigue model. At last, the fatigue model is integrated into our new virtual human simulation framework for evaluating industrial operations and predicting human posture in multi-objective optimization method.

The fatigue and recovery model proposed in this thesis is useful for evaluating physical fatigue in manual handling operations, analyzing human posture, identifying the human fatigue and recovery properties, and optimizing the design of manual handling operations.

Résumé

La fatigue physique dans les activités professionnelles conduit à des risques éventuels de troubles musculo-squelettiques (TMS). Les recherches en ergonomie ont pour objectif la prévention des risques potentiels. Ainsi, la simulation de mannequins virtuels a été beaucoup utilisée dans l'industrie, afin d'examiner les facteurs humains et l'ergonomiques dès que possible. Cependant, l'effet de la fatigue n'est pas encore suffisamment considéré ni dans les analyses ergonomiques conventionnelles, ni dans les outils de simulation. Dans cette thèse, nous nous concentrons sur la modélisation de la fatigue et la récupération musculaire dans les opérations de manutention, et ses applications potentielles, et l'intégration de ses effets dans les évaluations des opérations et des outils de simulation.

Dans un premier temps, un modèle simplifié de la fatigue musculaire est proposé sur la base de paramètres physiologiques pour prédire la réduction de la force physique dans les opérations de manutention. Une approche théorique et une approche expérimentale ont été utilisées pour valider ce modèle. Dans la première approche, des comparaisons ont été faites entre notre modèle et les modèles d'endurance pour des cas statiques et des cas dynamiques. De l'analyse théorique, la résistance à la fatigue pour un groupe de muscles d'une certaine population ne peut être déterminée par la méthode de régression. Dans la deuxième approche, 40 ouvriers ont effectué la simulation d'opérations de perçage sous contraintes posturales. Outre le processus de travail, les forces exercées par les ouvriers dans la simulation des perçages ont été mesurées comme un indice de la fatigue physique, et la posture des membres supérieurs a également été mesurée grâce à un système de capture de mouvements. Il a été constaté que la fatigue de la plupart des sujets a suivi la fonction exponentielle prédite par le modèle de la fatigue. Enfin, le modèle de fatigue est implémenté dans notre logiciel de simulation de mannequin pour évaluer des opérations de manutention et faire de la prédiction de postures de travail avec une méthode d'optimisation multi-objectifs.

Les modèles de fatigue et de récupération proposés dans cette thèse sont utiles pour évaluer la fatigue physique lors d'opérations de manutention, pour analyser la posture de travail, pour identifier les propriétés de fatigue musculaire, et pour optimiser la planification des opérations de manutention.

Remerciements

Je voudrais remercier sincèrement M. Jean-François Lafay et M. Michel Malabre pour leur accueil à l'Institut de Recherche en Communications et Cybernétique de Nantes, où j'ai effectué tous mes travaux. Je remercie également M. Philippe Wenger, responsable de l'équipe Méthodes de Conception en Mécanique.

Je tiens tout d'abord à remercier M. Fouad Bennis et M. Damien Chablat, mes directeurs de thèse. Je tiens à leur exprimer toute ma reconnaissance pour leur disponibilité, leur encadrement professionnel, leurs qualités scientifiques, et leur grande gentillesse. Je n'oublierai jamais leur accueil et leur encadrement lors de mes études en France.

Je souhaite adresser aussi mes remerciements à M. Wei Zhang, qui était encadrant de ma thèse en Master, pour son aide à la recherche scientifique, à la rédaction de ma thèse, et à mon intégration professionnelle.

Je remercie très sincèrement tous les membres du jury pour leurs remarques constructives, et surtout les rapporteurs M. Georges Dumont et M. Ronan Boulic pour l'intérêt qu'ils ont manifesté à l'égard de mon travail.

Je tiens à remercier la Région des Pays de la Loire et EADS pour leurs financements et sans lesquels ce travail n'aurait jamais vu le jour. Je remercie aussi M. François Guillaume pour ses contributions à la valorisation de nos recherches.

Je remercie aussi tous les membres des équipes MCM et Robotique au sein desquelles j'ai eu la possibilité d'accomplir ce travail dans une ambiance très agréable, surtout mes collègues de bureaux successifs, M. Benoît Guédas, M. Daniel Kanaan, M. Sébastien Briot et M. Guillaume Moroz.

Je veux aussi adresser mes remerciements à tous mes amis à Nantes, en France, en Allemagne, aux Etat-Unis et en Chine.

Finalement, je remercie chaleureusement mon épouse Tiantian Wang et mes parents.

Dedication

dedicated to my wife

dedicated to my parents

Contents

Abstract **i**

Résumé **ii**

Acknowledgment **iii**

Dedication **iv**

Contents **v**

General introduction **1**

Purpose 1

Project description 2

Thesis structure 2

1 Literature review **3**

1.1 Musculoskeletal disorders 3

1.1.1 Definition of MSD 3

1.1.2 Conventional methods to prevent MSD 4

1.2 Computer-aided ergonomics 8

1.2.1 Development of Computer-Aided Ergonomics 8

1.2.2 Virtual human simulation 9

1.3 Muscle fatigue models 13

1.3.1 Muscle fatigue mechanism and measurement 14

1.3.2 Muscle fatigue model 15

1.4 Conclusions from literature review 19

1.4.1 Problematic analysis in DHM 19
1.4.2 Fatigue analysis solutions in DHM 20

2 Framework for objective work analysis 23
2.1 Introduction 23
2.2 Structure of the framework 25
2.3 Virtual human status 27
2.4 Input modules and their technical specifications 28
2.4.1 Human motion input module 28
2.4.2 Visualization of human simulation 32
2.4.3 Force and interaction information 33
2.4.4 Personal factors 34
2.5 Output modules 34
2.5.1 Posture analysis 34
2.5.2 Posture prediction 35
2.6 Summary 36

3 Muscle fatigue model and its theoretical validation 37
3.1 Introduction 37
3.2 Muscle fatigue model and its explanation 39
3.2.1 Muscle fatigue model 39
3.2.2 Explanation of the fatigue model 41
3.3 Validation in comparison to MET models 42
3.3.1 Mathematical principle of the validation 42
3.3.2 Results and discussion 48
3.4 Validation in comparison to other dynamic models 49
3.4.1 Comparison with Freund's model 50
3.4.2 Comparison with Wexler's model 50
3.4.3 Comparison with Liu's model 51
3.4.4 Discussion 53
3.5 Fatigability of different muscle groups 53
3.5.1 Regression for determining the fatigability 53
3.5.2 Results and discussion 54
3.5.3 Discussion on fatigue resistance 61
3.5.4 Limitations 65

3.6 Summary 65

4 Muscle fatigue model: experimental validation 67

4.1 Introduction 67
4.2 Material and methods 69
4.2.1 EADS drilling case and its simplification 69
4.2.2 Experiment design 70
4.2.3 Subjects 71
4.2.4 Material 72
4.2.5 Experiment procedure 73
4.3 The fatigue model and regression 74
4.3.1 The fatigue model 74
4.3.2 Regression analysis 75
4.3.3 Torque estimation 76
4.3.4 Interface in Matlab 77
4.4 Results 77
4.4.1 General descriptive findings 77
4.4.2 Individual force and torque analysis 78
4.4.3 Posture change in the work 81
4.5 Discussion 84
4.5.1 Experiment design 84
4.5.2 Fatigue model and rates of fatigue 84
4.5.3 Posture changes 85
4.5.4 Study limitations 85
4.6 Summary 86

5 Application cases in computer-aided ergonomics 89

5.1 Introduction 89
5.2 Digital human modeling 91
5.2.1 Kinematic modeling of virtual human 91
5.2.2 Dynamic modeling of virtual human 91
5.2.3 Biomechanical modeling of virtual human 95
5.2.4 Graphical modeling of virtual human 96
5.2.5 Workflow for fatigue analysis 96
5.3 Physical fatigue assessment in posture analysis 98

5.3.1 Operation description 98
5.3.2 Endurance time prediction 99
5.3.3 Fatigue evaluation 102
5.3.4 Experiment validation 103
5.3.5 Discussion 104
5.4 Multi-objective posture prediction 105
5.4.1 Mathematical description 105
5.4.2 Results 109
5.4.3 Discussion 111
5.5 Summary 113

6 Muscle recovery model 115
6.1 Introduction 115
6.2 Muscle recovery model 116
6.2.1 Mathematical description of recovery model 116
6.2.2 Analysis of the recovery model 119
6.3 Application 122
6.3.1 Rest-allowance Model 122
6.3.2 Recovery process during manual handling operation 124
6.4 Discussion 125
6.4.1 Recovery model 125
6.4.2 Rate of recovery from individual 127
6.5 Summary 128

7 General conclusions and perspectives 129
7.1 Conclusions 129
7.2 Perspectives 130

Bibliography 132

Appendices 145

A Modified Denavit-Hartenberg notation 147

B Newton-Euler inverse dynamics for posture analysis 151
B.1 Mathematical description of task 151

B.2 Geometric modeling of arm 151
B.3 Parameters for dynamic modeling of arm 154
B.4 Calculation of torques at joints 154

C Joint strength change based on posture change 159

D Original experiment data 161

E Publications 163

List of Figures

1.1 OWAS evaluation chart, adapted from Chatizwa (1996) 5
1.2 RULA work assessment worksheet (McAtamney and Corlett, 1993) 6
1.3 Diagram of Rodgers' muscle fatigue analysis, adapted from Rodgers (2004) 7
1.4 Main frame of 3DSSPP 10
1.5 Graphical example of Jack 11
1.6 Graphical example of Santos^{TM} 12
1.7 Graphical example of AnyBody 12
1.8 Physical fatigue process under a constant external load 14
1.9 Schematic illustration of muscle fatigue mechanism adapted from Vøllestad (1997) . 15

2.1 Schematic representation of evaluations in virtual reality 24
2.2 Framework of Objective Work Evaluation System 26
2.3 Human status in human simulation tools 28
2.4 Schematic structure of the motion capture system 30
2.5 Posture comparison between real postures and postures in simulation 31

3.1 Endurance time in general models and dynamic model 43
3.2 *ICC* of general models 45
3.3 Endurance time in shoulder endurance models and dynamic model 45
3.4 *ICC* of shoulder endurance models 46
3.5 Endurance time in elbow endurance models and dynamic model 46
3.6 *ICC* of elbow endurance models 47
3.7 Endurance time in hip and back models and dynamic model 47
3.8 *ICC* of hip/back models 48
3.9 Maximum exertable force and time relationship in Wexler's Model 51

3.10 Comparison between the experimental result of the active motor model and dynamic model in the maximum effort . . . 52
3.11 ICC diagram for MET general models before regression . . . 55
3.12 ICC diagram for MET general models after regression . . . 55
3.13 ICC diagram for MET elbow models before regression . . . 57
3.14 ICC diagram for MET elbow models after regression . . . 57
3.15 ICC diagram for MET shoulder models before regression . . . 57
3.16 ICC diagram for MET shoulder models after regression . . . 57
3.17 ICC diagram for hip/back shoulder models before regression . . . 58
3.18 ICC diagram for hip/back shoulder models after regression . . . 58
3.19 Normal distribution test for the general model . . . 59
3.20 Normal distribution test for the elbow model . . . 59
3.21 MET prediction using Dynamic model in comparison with general static models . . . 60
3.22 MET prediction using Dynamic model in comparison with elbow static models . . . 60
3.23 MET prediction using Dynamic model in comparison with shoulder static models . . . 61
3.24 MET prediction using Dynamic model in comparison with hip/back static models . . . 61

4.1 Schematic layout of experiment design . . . 69
4.2 Schema of the decrease of the physical capacity in a continuous operation . . . 70
4.3 Participant in the experiment . . . 72
4.4 Complete FASTRAK System . . . 73
4.5 Force schema in the drilling operation . . . 73
4.6 Experiment layout in VRHIT laboratory Tsinghua University . . . 74
4.7 Matlab interface for experiment analysis . . . 77
4.8 Force measurement results and the mean values and standard deviations at each time instant . . . 78
4.9 General regression result of the decrease of the measured forces . . . 79
4.10 Force regression analysis from representative subject data ($r_{force} = 0.9926$) . . . 81
4.11 Torque regression analysis from representative subject data ($r_{torque} = 0.9940$) . . . 82
4.12 Joint flexion angles in different work steps . . . 83
4.13 Posture change in the drilling operation . . . 83

5.1 Geometrical modeling of virtual human . . . 92
5.2 Elbow static strength depending on the human elbow and shoulder joint position, α_s, α_e [deg] . . . 96

5.3 Virtual skeleton composed of 3DS models 97
5.4 Workflow for the fatigue evaluation 97
5.5 Drilling case in CATIA 98
5.6 Endurance time prediction for shoulder with average fatigue resistance 100
5.7 Endurance time prediction for the elbow with average fatigue resistance 100
5.8 Endurance time for the population with average strength for shoulder joint 101
5.9 Endurance time for the population with average strength for elbow joint 101
5.10 Fatigue evaluation after drilling a hole in a continuous drilling process 102
5.11 Joint discomfort example 107
5.12 Posture prediction 109
5.13 MOO prediction in Pareto front 110
5.14 Posture prediction under consideration of fatigue effect 112

6.1 Recovery curves of joint from different fatigue levels 118
6.2 Recovery curves of joint under different rates of recovery 118
6.3 Schematic illustration of recovery time for different parameters after a fatiguing contraction, adapted from Westgaard and Winkel (1996) 121
6.4 Rest allowance profiles using the theoretical approach 123
6.5 Holding time and recovery time using the theoretical approach 123
6.6 Rest allowance profiles using the existing RA models 125
6.7 Fatigue and recovery in a work cycle 126
6.8 Fatigue and recovery in a work cycle 126

A.1 Associated notations to a tree structure 148
A.2 Geometrical parameters for a body with more than two joints 149

B.1 Geometric modeling of the arm 152
B.2 Dynamic forces exerted on joint body 156

C.1 Shoulder joint flexion strength of adult male population 160

List of Tables

1.1 Pen-paper-based observational techniques 5
1.2 Comparison of available virtual human simulation tools 13
1.3 Description of parameters in Wexler's Muscle Fatigue Model (Ding et al., 2000a) . . 16
1.4 Parameters in Active Motor model 19

2.1 Comparison of different evaluation methods in real and virtual environment 25

3.1 Parameters in Dynamic Fatigue model 40
3.2 Static validation results r and ICC between Eq. 3.8 and the other existing MET models in the literature (El ahrache et al., 2006) 44
3.3 Static validation results 56
3.4 Fatigue resistance m of different MET models 59

4.1 Participant characteristics 71
4.2 Pearson's correlation r and rate of fatigue in force output and joint torque estimation 79
4.3 Statistical analysis of rate of fatigue k 80
4.4 Fatigue resistances of shoulder MET models 81
4.5 Posture change in the experiment [deg] 82
4.6 Correlation between Pearson's correlations in force and torque and the individual posture changes 86

5.1 Geometric modeling parameters of the overall human body 93
5.2 Body segment lengths as a proportion of body stature (Chaffin et al., 1999; Tilley and Dreyfuss, 2002) 94
5.3 Percentage distribution of total body weight according to different segmentation plans (Chaffin et al., 1999) 94

5.4 Maximum endurance time of shoulder and elbow joints for drilling work 99
5.5 Normalized shoulder joint strength in the drilling operation 103
5.6 Normalized torque strength reduction for the population with higher fatigue resistance 103

6.1 Rest allowance (RA) models (adapted from El ahrache and Imbeau (2009)) 124

A.1 Functions of the joints in human geometrical model 150

B.1 Geometric modeling parameters for the right arm 153
B.2 Coordinates of several center points in corresponding joint coordinates system 154
B.3 Dynamic modeling parameters for arm 158

D.1 Individual force measurement results 161
D.2 Force measurement results and the mean values and standard deviations at each time instant 162

General introduction

Contents

Purpose 1
Project description 2
Thesis structure 2

Purpose

Although automation techniques have been used greatly in modern manufacturing technologies, human manual handling operations are still required thanks to the dexterity and the flexibility of human beings, especially in assembly and maintenance operations. During those manual handling operation, there are lots of ergonomic issues concerning the operators. The sustained incorrect posture, heavy external load, and some other factors might generate potential physical exposure risks to human body. Fatigue caused by the physical load is one of the important reasons responsible for musculoskeletal disorders (MSDs).

Increasing global industrial competition and rapidly changing customer demands have resulted in great changes in production methods and the configuration of manufacturing systems. Under this background, computer aided ergonomics has been developed from the 80s of last century to accelerate the design process with consideration of ergonomics. In previous studies, conventional ergonomic tools have been integrated into digital human modeling tools to enhance the evaluation efficiency. However, physical fatigue is not yet considered and modeled enough in those commercialized tools. Therefore, how to model the physical fatigue and integrate it into computer aided ergonomics (CAE) to prevent MSD risks is the main aim of our research.

Project description

The content of this thesis is based on the Project EADS which is financially supported by the European Aeronautic Defence & Security Company (EADS, France) and Région des Pays de la Loire (France). This is a project under the collaboration between École Centrale de Nantes (France) and Tsinghua University (PR China).

The evaluation of the human work is the main concern of the ergonomics. The overall purpose of the project is to analyze human tasks globally taking account of ergonomics, especially fatigue (Stress, Workload, and Fatigue) aspects of the human in the context of aircraft industry. In the context of the development of new product, it is necessary to analyze as early as possible the human tasks in order to be able to realize the needed modifications.

Typical manual handling operations in aircraft assembly tasks are set for evaluating the different work aspects. The physical fatigue should be evaluated and predicted in concrete cases using digital human modeling techniques; the evaluated result should be consistent to the result from experiments under simulated working conditions.

Thesis structure

This thesis is mainly focusing on the evaluation of physical fatigue and its application in CAE. Firstly, the state of the art (Chapter 1) for fatigue evaluation in CAE is presented in literature review with the analysis of problematic. Secondly, the framework of the overall human evaluation is presented and discussed in Chapter 2 based on the conclusion from the literature review. Thirdly, a simplified physical fatigue model is developed and validated in Chapter 3 and Chapter 4. The application case of the fatigue model is demonstrated by analyzing a concrete EADS drilling task in Chapter 5. Furthermore, a new recovery model is proposed and applied in EADS case to determine work-rest allowance in Chapter 6. At last, conclusions and perspectives for the overall research work are presented.

Chapter 1

Literature review

Contents

1.1 Musculoskeletal disorders 3
1.2 Computer-aided ergonomics 8
1.3 Muscle fatigue models 13
1.4 Conclusions from literature review 19

1.1 Musculoskeletal disorders

1.1.1 Definition of MSD

Although automation techniques have been employed widely in industry, there are still many manual operations, especially in assembly and maintenance jobs thanks to the dexterity and the flexibility of human being (Forsman et al., 2002). Among these manual handling operations, there are occasionally physical operations with high strength demands. Musculoskeletal disorder (MSD) is one of the major health problems for the workers involved in those operations.

Definition 1 Musculoskeletal disorders
Injuries and disorders to muscles, nerves, tendons, ligaments, joints, cartilage and spinal discs and it does not include injuries resulting from slips, trips, falls or similar accidents (Maier and Ross-Mota, 2000)

From the report of Health, Safety and Executive in UK (HSE, 2005) and the report of Washington State Department of Labor and Industries (SHARP, 2005), over 50% of workers in industry have suffered from MSDs. In European Union, It was estimated that 40 millions workers suffered from MSDs and the finanical loss caused by MSDs was about between 0.2% to 5% GDP by some estimation (Buckle et al., 1999). Only in France, The MSD makes up the vast proposition of the occupational

diseases (OD) and the statistics reported that the MSD exceeded about 70% of total occupational diseases (EuropGip, 2006) from 2001 to 2005.

There are numerous "risk factors" associated with the work-related MSDs, including physical work load factors (e.g., force, posture, movement, and vibration) (Burdorf, 1992), psychosocial factors (Bongers et al., 1993), and individual factors (Armstrong et al., 1993). The level of exposure to physical workload can be normally assessed with respect to intensity (or magnitude), repetitiveness, and duration.

It is believed that physical fatigue resulting from the physical work is one of the risk factors for MSDs. According to the statement in *Occupational Biomechanics* (Chaffin et al., 1999, p. 48), "Since muscle fatigue reduces muscle power, induces discomfort and pain, and in the long term, is believed to contribute to Cumulative Trauma Disorders (CTDs), it is important to quantify fatigue and to determine the limits of acceptable muscle loads.", and the similar statement in Armstrong et al. (1993), "physical work requirements and individual factors determine muscle force and length characteristics as a function of time, which in turn determines muscle energy requirements. Muscle energy requirements in turn can lead to fatigue, which then can lead to muscle disorders.". In Buckle and Devereux (2002), cumulative reduction of capacity was also discussed as one of pathomechanisms of work-related neck and upper limb MSDs. Overexertion of muscle force or frequent high muscle load is the main reason for muscle fatigue, and furthermore, it results in acute muscle fatigue, pain in muscles and severe functional disability in muscles and other tissues of the human body. Hence, it is necessary for ergonomists to find an efficient method to assess the extent of various physical exposures on muscles and to predict muscle fatigue in the work design stage.

1.1.2 Conventional methods to prevent MSD

In order to assess physical risks to MSDs, several ergonomics tools have been developed and most of them were listed, classified and compared in Li and Buckle (1999). These methods can be categorized into observation methods and direct methods.

Observational methods

Observational methods (see Table 1.1) for posture analysis, such as Posturegram, Ovako Working Posture Analyzing System (OWAS, Fig. 1.1), Posture Targeting and Quick Exposure Check for work-related musculoskeletal risks (QEC), were developed for analyzing whole body postures. In all these four methods, posture is taken as one of the most important factors to assess the physical exposure. In the first three methods mentioned, body posture is categorized into different types with different risk levels according to the recorded position. The differences between these methods are the rules to

classify the body positions. In the QEC method, posture of different body parts is scaled into different exposure levels. In combination with posture, other physical factors such as force, repetition and duration of movement, are also taken into consideration to assess physical work load in OWAS and QEC methods.

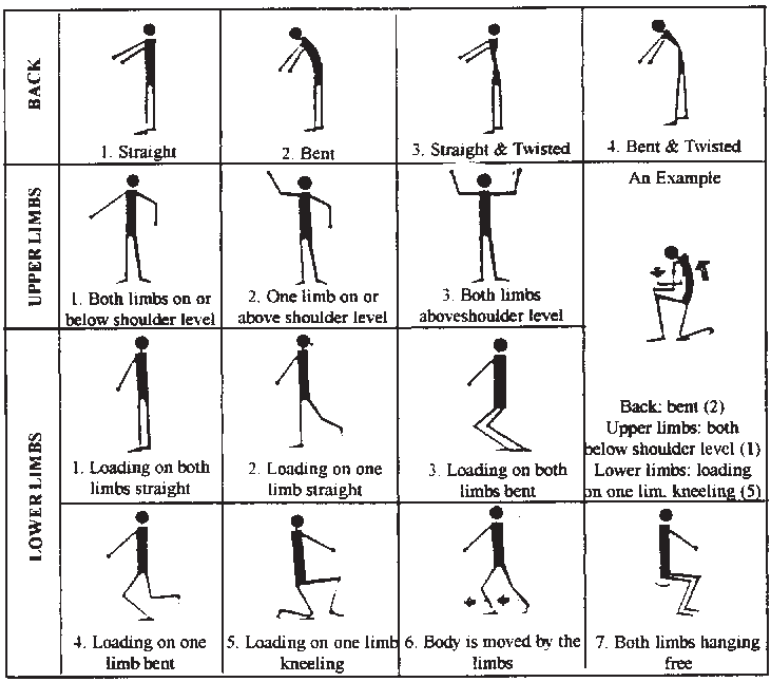

Figure 1.1: OWAS evaluation chart, adapted from Chatizwa (1996)

In spite of these general posture analysis tools, some special tools are designed for specific parts of the human body. For example, Rapid Upper Limb Assessment (RULA, Fig. 1.2) is designed for assessing the severity of postural loading for the upper extremity. This method has the same concept as OWAS, but particularly suited for sedentary jobs (McAtamney and Corlett, 1993). It uses a ranking system to rate different postures, different movements and repetition/duration of the task. The similar systems include HAMA (Hand-Arm-Movement Analysis) and PLIBEL (method for the identification of musculoskeletal stress factors that may have injurious effects) (Stanton et al., 2004, ch. 3). "In general, these observational methods are mainly posture-based. They are relatively inexpensive to carry out, and the assessments can be made without disruption to the workforce" (Li and Buckle, 1999).

Similar to these methods for posture analysis, there is one tool available for fatigue analysis and that is muscle fatigue analysis (MFA, Fig. 1.3) (Rodgers, 2004). This technique was developed by Rodgers and Williams to characterize the discomfort described by workers on automobile assembly lines and fabrication tasks (Rodgers, 1987). In this method, each body part is scaled into four effort levels according to its working position, and meanwhile the duration of the effort and frequency

Table 1.1: Pen-paper-based observational techniques for assessing physical strain at work (adapted from Li and Buckle (1999))

Techniques	Basic features and field of applications
Posturegram	Body postures are categorized and recorded by time sampling on to cards as digital numbers. Whole body posture evaluation for static tasks.
OWAS	Categorized body postures in digital numbers, including force; time sampling, has action categories. Whole body posture analysis.
Posture Targeting	Postures are marked as angles and directions together with work activities by time sampling. Whole body posture recording for static tasks.
QEC	Estimate exposure levels for body postures, repetition of movement, force/load and task duration for different body regions, with a hypothesized score table for their interactions. Assessing the change in exposure for both static and dynamic tasks.
RULA	Categorized body posture as coded numbers,including force and muscle activities;time sampling, with action categories. Upper limb assessment.
HAMA	Record the types of motion, grasps, hand position and features of load handled; the data is linked to work activities. Upper limb assessment.
PLIBEL	Checklist with questions answered for different body regions. Identification of risk factors
REBA	Score the body postures, estimate the load, with action levels. Risk assessment of the entire body for non sedentary tasks.

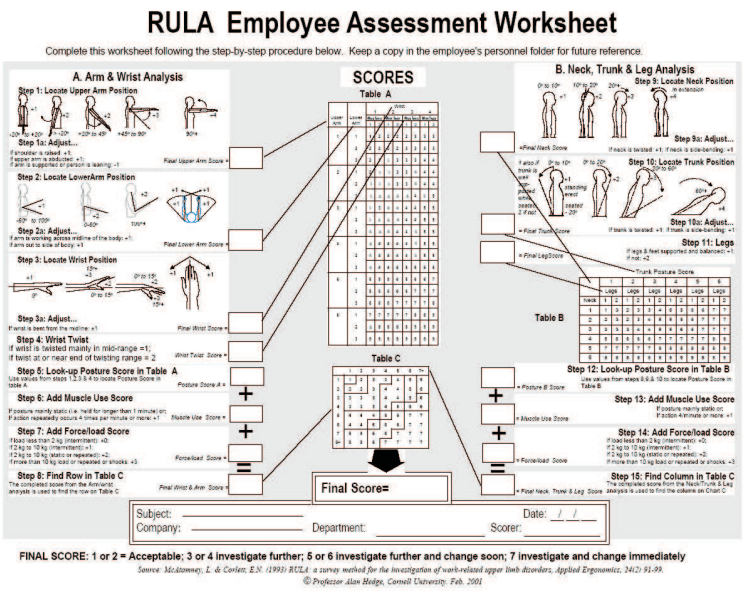

Figure 1.2: RULA work assessment worksheet (McAtamney and Corlett, 1993)

(frequency of alternating task and recovery) are both scaled into four effort levels. The combination of the three factors' levels can determine "priority to change" score. The task with a high priority score needs to be analyzed and redesigned to reduce the MSD risks (Stanton et al., 2004, ch. 12).

Rodgers Muscle Fatigue Analysis by Task

Task

	Effort Level (If the effort cannot be exerted by most people, enter 4 for Effort and VH for Priority)			**Scores**			**Priority**
Region	Light -- **1**	Moderate -- **2**	Heavy -- **3**	**Effort**	**Dur**	**Freq**	
Neck	Head turned partly to side, back or slightly forward	Head turned to side; head fully back; head forward about 20°	Same as Moderate but with force or weight; head stretched forward				
Shoulders	Arms slightly away from sides; arms extended with some support	Arms away from body, no support; working overhead	Exerting forces or holding weight with arms away from body or overhead	Right			
				Left			
Back	Leaning to side or bending arching back	Bending forward; no load; lifting moderately heavy loads near body; working overhead	Lifting or exerting force while twisting; high force or load while bending				
Arms / Elbow	Arms away from body, no load; light forces lifting near body	Rotating arms while exerting moderate force	High forces exerted with rotation; lifting with arms extended	Right			
				Left			
Wrists / Hands / Fingers	Light forces or weights handled close to body; straight wrists; comfortable power grips	Grips with wide or narrow span; moderate risk angles, especially flexion; use of gloves with moderate forces	Pinch grips; strong wrist angles; slippery surfaces	Right			
				Left			
Legs / Knees	Standing, walking without bending or leaning; weight on both feet	Bending forward, learning on table; weight on one side; pivoting while exerting force	Exerting high force while pulling or lifting; crouching while exerting force	Right			
				Left			
Ankles / Feet / Toes	Standing, walking without bending or leaning; weight on both feet	Bending forward, leaning on table; weight on one side; pivoting while exerting force	Exerting high force while pulling or lifting; crouching while exerting force	Right			
				Left			

Continuous Effort Duration	< 6 s **1**	6 - 20 s **2**	20 - 30 s **3**	> 30 s **4** (Enter VH for Priority)
Effort Frequency	< 1 / min **1**	1 - 5 / min **2**	> 5 - 15 / min **3**	> 15 / min **4** (Enter VH for Priority)

Figure 1.3: Diagram of Rodgers' muscle fatigue analysis, adapted from Rodgers (2004)

After listing these available methods, physical exposure to MSD can be evaluated with respect to intensity (or magnitude), repetitiveness, and duration (Li and Buckle, 1999; Westgaard and Winkel, 1996). While these methods can be used to assess physical jobs, there are still several limitations.

- Even just for a lifting job, the evaluation results of five tools (National Institute for Occupational Safety and Health (NIOSH) lifting index, American Conference of Industrial Hygienists - The Threshold Limit Values (ACGIH TLV), 3D Static Strength Prediction Program (3DSSPP), WA L&I, Snook lifting assessment instruments) for the same task were different, and sometimes even contradictory (Russell et al., 2007). That is because the evaluation techniques lack precision and their reliability of the system is a problem for assessing the physical exposures due to their intermittent recording procedures (Burdorf, 1992).

- Secondly, most of the traditional methods have to be carried out on site, therefore, there is no immediate result from the observation. It is also time consuming for later analysis. Further-

more, subjective variability can influence the evaluation results when using the same observation methods for the same task (Lämkull et al., 2007).

- Thirdly, it is time consuming to carry out these observational methods in work place, especially for the pen-paper based methods. Effort after data collection is required to analyze the obtained data. Furthermore, it is not applicable during the design of the workspace.

- The last limitation is that only intermittent posture positions and limited working conditions are considered in these methods, which means that they are suitable for analyzing a static working process and they are not less suitable to estimate the detailed MSD risks.

Self-reported methods

Besides these objective posture analysis tools, there are several self-report methods to assess the physical load or body discomfort, such as "body map" (Corlett and Bishop, 1976), rating scales (Borg, 1998), questionnaires or interviews (Wiktorin et al., 1993), and checklists (Corlett, 1995). These tools are also important because ergonomists need to concentrate themselves on the feeling of the workers. Several authors even insist that "If the person tells you that he is loaded and effortful, then he is loaded and effortful whatever the behavioral and performances measures may show" (Li and Buckle, 1999).

For muscle fatigue, Ratings of Perceived Exertion (RPE) and Swedish Occupational Fatigue Inventory (SOFI) based on PRE were developed to rate the workload in practice (Borg, 1998; Åhsberg et al., 1997; Åhsberg and Gamberale, 1998). SOFI consists of five aspects: lack of motivation, sleepiness, physical discomfort, lack of energy, and physical exertion, and it is used to measure fatigue as a perception of either mental or physical character (Åhsberg and Gamberale, 1998). The concept of perceived exertion and the associated methods for measuring fatigue is: "the human sensory system can function as an efficient instrument to evaluate the work load by integrating many peripheral and central signals of strain" (Borg, 2004).

These subjective assessments of body strain and discomfort have been the most frequently used form due to the ease of use and apparent face validity. However, subjective ratings are vulnerable to many influences. This kind of approach has lower validity (Burdorf and Laan, 1991) and reliability (Wiktorin et al., 1993).

Definition 2 Definition of Ergonomics (International Ergonomics Association, 2000)
Ergonomic research is performed by those who study human capabilities in relationship to their work demands. Information derived from these studies contributes to the design and evaluation of tasks, jobs, products, environments and systems in order to make them compatible with the needs, abilities and limitations of people.

1.2 Computer-aided ergonomics

1.2.1 Development of Computer-Aided Ergonomics

Ergonomics oriented manual operation design and analysis is one of the key methods to improve manual work efficiency, safety, comfort, as well as job satisfaction. As discussed in the previous section, conventional ergonomics methods are time-consuming, and they are not precise enough due to their intermittent principle while obtaining the original data. Therefore, Computer Aided Ergonomics (Karwowski et al., 1990) has been developed to make an appropriate design for manual operations and to solve the problem which has been encountered by several organizations in a variety of industries: the human element is not being considered early or thoroughly enough in the life cycle of products, from design to recycling.

With the development of powerful computation capability of computer, CAE offers new possibilities to integrate conventional ergonomic knowledge and develop new methods into the work design process. Different approaches have been adopted to enhance the speed of the ergonomic evaluation. As mentioned in Karwowski et al. (1990), ergonomics expert systems, ergonomic oriented information systems, computer models of human, etc. have been taken into computer supported ergonomic design. Using realistic virtual human in computer simulation is one key method to take account of the early consideration of ergonomics issues in the design and reduce the design cycle time and cost (Badler, 1997; Hou et al., 2007).

1.2.2 Virtual human simulation

In order to evaluate human work conditions objectively and quickly, virtual human techniques (digital human modeling) have been developed to facilitate the ergonomic evaluation, such as Jack (Badler et al., 1993), ErgoMan (Schaub et al., 1997), 3DSSPP (Chaffin, 1969), and Santos (VSR Research Group, 2004; Vignes, 2004), AnyBody(Damsgaard et al., 2006), etc.

The main functions of virtual human simulation tools are posture analysis and posture prediction.

Posture analysis techniques have been used in fields of automotive, military, and aerospace. These human modeling tools rely mainly on visualization to provide information about body posture, reach-

ability and field of view (Lämkull et al., 2007). These tools are capable of determining the workspace of virtual human (Yang et al., 2008), assessing the visibility and accessibility of an operation (Chedmail et al., 2003), evaluating postures (Bubb et al., 2006), etc.

Conventional motion time methods (MTM) can be integrated into virtual human simulation systems to assess the work efficiency (Hou et al., 2007). The effort of combining these virtual human tools with existing posture analysis methods has also been done. In Jayaram et al. (2006), a method to link virtual environment (Jack) and a quantitative ergonomic analysis tool (RULA) in real time for occupational ergonomics studies was presented, and it acknowledged that ergonomic evaluation could be carried out in real time using their prototype system.

From the physical aspect, the moment load at each joint (e.g., 3DSSPP) and even the force of each individual muscle (e.g., AnyBody, force determination in Pontonnier and Dumont (2008)) can be determined, and the posture is predictable for reach operations (Yang et al., 2006b) based on inverse kinematics and optimization methods. Overall, the human motion can be simulated and analyzed based on the workspace information, virtual human strength information, and other aspects. However, there are still several limitations in the existing virtual human simulation tools. The detailed analysis of the existing available tools are given in the following description.

3DSSPP

3DSSPP (3D Static Strength Prediction Programme, see Fig. 1.4) is a tool developed in University of Michigan (Chaffin et al., 1999). Originally, this tool was developed to predict population static strengths and low back forces resulting from common manual exertions in industry. The biomechanical models in 3DSSPP are meant to evaluate very slow or static exertions (Chaffin, 1997). It predicts static strength requirements for tasks such as lifts, presses, pushes, and pulls. The output report includes the percentiles of men and women who have the strength to perform the described job, spinal compression forces, and data comparisons to NIOSH guidelines. The posture can be predicted based on empirical motion tracking data in combination with inverse kinematics (Zhang and Chaffin, 2000). However, they do not allow dynamic exertions to be simulated, and in addition there is no fatigue model integrated into this tool for fatigue evaluation and prediction.

JACK

Jack (see Fig. 1.5) (Badler et al., 1993, p. 268) is a human modeling and simulation software solution that helps organizations in various industries improve the ergonomics of product designs and refine workplace tasks. With Jack, users are able to assign a virtual human in a task and analyze the posture and other performance of the task using existing posture analysis tools, like OWSA and so

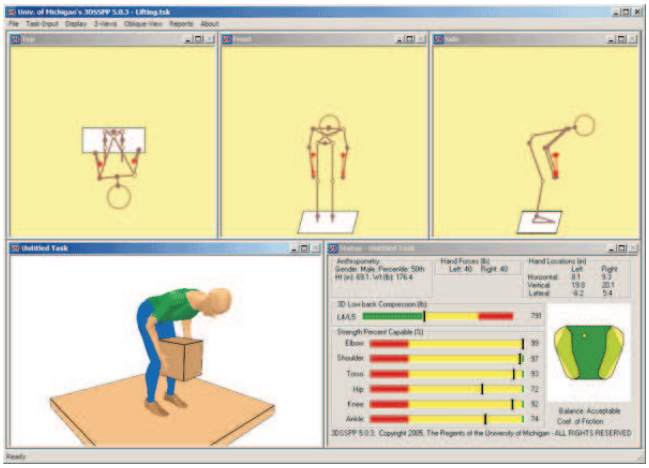

Figure 1.4: Main frame of 3DSSPP

on. PTMs (Predetermined Time Measurement Systems) are also integrated to estimate the standard working time for a specified task. The motion of the virtual human can be driven by scripts based on inverse kinematics and strength guided motion (Badler et al., 1993). In this virtual human tool, the fatigue term is considered in motion planning to avoid a path that has a high torque value that must be maintained over a prolonged period of time. However, the reduction of the physical capacity is not modeled in this tool, although the work-rest schedule can be determined using its extension package.

Figure 1.5: Graphical example of Jack

Santos^{TM}

Within VSR (Virtual Soldier Research) in the Center for Computer Aided Design at the University of Iowa, another virtual human, Santos^{TM} (see Fig. 1.6), has been developed originally for military applications. In this research, the posture prediction is based on MOO (multiple-objective optimization) with three objective terms of human performance measures: potential energy, joint displacement and joint discomfort (Yang et al., 2004). In Santos^{TM}, fatigue is modeled using the physiological muscle

fatigue model in a series of publications (Ding et al., 2000a, 2002, 2003a) (details will be discussed in section 1.3). Due to the physiological mechanism of this muscle fatigue model, it requires dozens of variables to construct the mathematical model for a single muscle. Meanwhile, the parameters for this muscle fatigue model are only available for quadriceps. Therefore, this model is too complex to be integrated into ergonomics application since it requires lots of computational effort for model identification. In addition, in the posture prediction method of this virtual human tool, the fatigue effect is not integrated.

Figure 1.6: Graphical example of Santos^{TM}

AnyBody

AnyBody (see Fig. 1.7) is a system capable of analyzing the musculoskeletal system of humans or other creatures as rigid-body systems. A modeling interface is designed for the muscle configuration, and optimisation method is used in the package to resolve the muscle recruitment problem in the inverse dynamics approach (Damsgaard et al., 2006). In this system, the recruitment strategy is stated in terms of normalized muscle forces. ”However, the scientific search for the muscle recruitment criterion is still ongoing, and it may never be established.” (Damsgaard et al., 2006). Furthermore, in the optimization criterion, the capacities of the musculoskeletal system are assumed as constants, and no limitations from the fatigue are taken into account.

The comparison of the previous virtual human tools is given in Table 1.2.

Figure 1.7: Graphical example of AnyBody

Table 1.2: Comparison of available virtual human simulation tools

	3DSSPP	AnyBody	Jack	Santo^{TM}
Posture Analysis	✓	✓	✓	✓
Joint effort analysis	✓	✓	✓	✓
Muscle force analysis		✓		
Posture prediction	✓	✓	✓	✓
Empirical data based	✓			
Optimization method based	✓	✓	✓	✓
Single objective optimization	✓	✓	✓	
Multi-objective optimization				✓
Joint discomfort guided			✓	✓
Fatigue effect in optimization			✓	✓

1.3 Muscle fatigue models

As discussed in section 1.1, MSD might result from physical fatigue caused by the repetitive manual operations. Therefore, it is necessary to develop appropriate models to reproduce the performance of muscle skeleton system to predict physical fatigue.

Furthermore, it has been stated in section 1.2 that physical fatigue evaluation has not yet been well considered in the literature. Here, the basic conceptions about fatigue and the existing models in the literature are given and discussed.

In the literature, the fatigue is defined as below.

Definition 3 Muscle fatigue

Any exercise-induced reduction in the capacity to generate force or power output.(Vøllestad, 1997)

The general process of physical fatigue is illustrated in Fig. 1.8. Assume in a static posture, the load of the joint is constant Γ_{load}. At the very beginning of the operation, the joint has the maximum strength Γ_{max}. Along time, the joint strength $\Gamma_{cem}(t)$ at each time instant t decreases from the maximum strength. The Maximum Endurance Time (MET) is the duration from the start to the time instant at which the strength decreases to the torque demand resulting from external load. Once the external load is over the current force capacity, potential physical risks might occur in the tissues of human body.

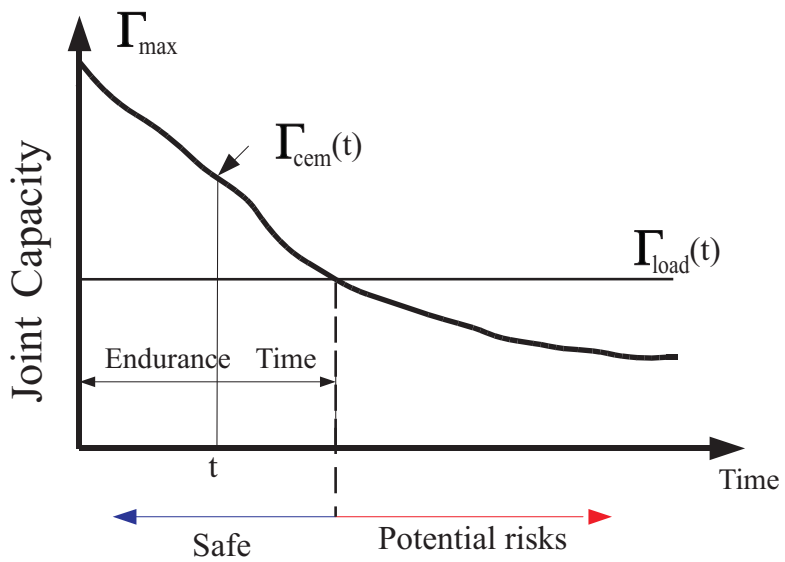

Figure 1.8: Physical fatigue process under a constant external load

1.3.1 Muscle fatigue mechanism and measurement

Muscle is made of muscle fibers. Production of force and movement is realized by contraction of muscle fibers driven by central nervous system command. The basic functional unit of muscle is the motor unit which consists of a motoneuron and the muscle fibers that it innervates. Motoneurons are the major efferent neurons that supply muscle fibers with control commands from the central nervous system (CNS).

A sequence of events in Fig. 1.9 results in voluntary force and each of these events is a potential limiting factor for force (Vøllestad, 1997). A command signal which is initiated voluntarily is sent by CNS to the muscle. For voluntary contraction, the stimulus is transmitted from the brain through the descending pathways to the motoneurons and the fibers that they control in form of an electrical impulse. If the command exceeds a threshold, chemical reaction (release of Ca^{2+} and binding of Ca^{2+}) will take place in muscle and it will trigger action potentials of motor units. All the related information in these events can be used to measure the force output and indicate the fatigue directly or indirectly.

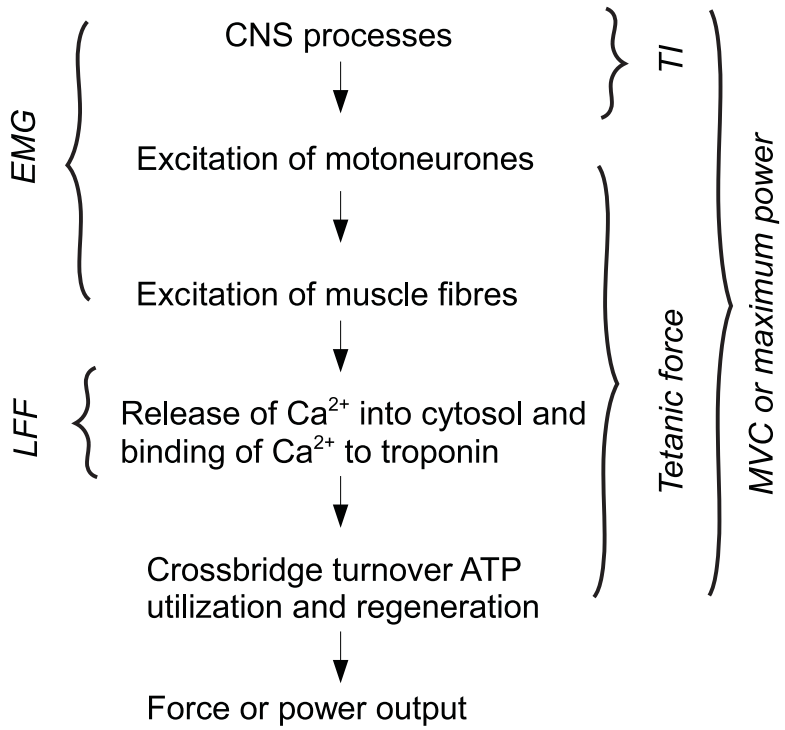

Figure 1.9: Schematic illustration of muscle fatigue mechanism adapted from Vøllestad (1997)

As stated in Vøllestad (1997), muscle fatigue can be measured in direct assessment methods by measuring the reduction of tetanic force, low frequency fatigue (LFF),the maximal voluntary contraction (MVC) or power output, which are the final output of the muscle force generation. Electromyography (EMG), endurance time, and twitch interpolation (TI) can be used to test the fatigue indirectly.

Based on these measurements under maximal or sub maximal contractions, different fatigue models can be established.

1.3.2 Muscle fatigue model

For objectively predicting muscle fatigue, several muscle fatigue models and fatigue indices have been proposed in the literature. In general, one or several terms are created to represent the reduction process of the muscle or joint in the existing models.

Wexler's model - Ca^{2+} cross bridge mechanism

In a series of publications (Wexler et al., 1997; Ding et al., 2000b,a, 2003b), Wexler and his colleagues have proposed a new muscle fatigue model based on Ca^{2+} cross-bridge mechanism and verified the model with stimulation experiments.

The first equation in Eq. 1.1 represents the dynamics of the rate limiting step of the formation of the calcium-troponin complex C_N. The second one in Eq. 1.1 stands for the nonlinear summation of calcium when stimulated with two closely spaced pulses. The third one describes the force generation in function of these parameters: C_N and A. The description of these variables and their definitions can be found in Table 1.3.

$$\begin{cases} \dfrac{dC_N}{dt} = \dfrac{1}{\tau_c}\sum_{i=1}^{N} R_i(-\dfrac{t-t_i}{\tau_c}) - \dfrac{C_N}{\tau_c} \\ R_i = 1 + (R_0 - 1)\exp(-\dfrac{t_i - t_{i-1}}{\tau_c}) \\ \dfrac{dF}{dt} = A\dfrac{C_N}{K_m + C_N} - \dfrac{F}{\tau_1 + \tau_2\dfrac{C_N}{K_m + C_N}} \end{cases} \tag{1.1}$$

It was noticed that the parameters A, R_0 and τ_c underwent significant changes while the muscle was fatiguing, and they were used as fatigue terms in the model. It was assumed that there was one time constant governing the rate of recovery from fatigue and arrived at the following three differential fatigue equations (Eq. 1.2).

$$\begin{cases} \dfrac{dA}{dt} = -\dfrac{A - A_{rest}}{\tau_{fat}} + \alpha_A F \\ \dfrac{dR_0}{dt} = -\dfrac{R_0 - R_{0rest}}{\tau_{fat}} + \alpha_{R_0} F \\ \dfrac{d\tau_c}{dt} = -\dfrac{\tau_c - \tau_{crest}}{\tau_{fat}} + \alpha_{\tau_c} F \end{cases} \tag{1.2}$$

The values of A_{rest}, $R_{0,rest}$ and $\tau_{c,rest}$ are obtained when the muscle is under non-fatigue conditions. At present, there are only parameters available for human quadriceps muscle.

Table 1.3: Description of parameters in Wexler's Muscle Fatigue Model (Ding et al., 2000a)

Name	Unit	Description
C_N		normalized amount of Ca^{2+} -troponin complex
F	N	mechanical force
t_i	ms	time of ith stimulation
n		Total number of stimuli in train before time t
τ_c	ms	Time constant controlling the rise and decay of C_N
R_0		Mathematical term characterizing the magnitude of enhancement in C_N from the following stimuli
A	N/ms	Scaling factor
τ_1	ms	Time constant of force decline at the absence of strongly bound cross-bridge
τ_2	ms	Time constant of force decline due to extra friction between actin and myosin resulting from the presents of cross-bridge
α_A	ms^{-2}	Coefficient for force model parameter A in fatigue model
α_{R_0}	$N^{-1}ms^{-1}$	Coefficient for force model parameter R_0 in fatigue model
α_{τ_c}	N^{-1}	Coefficient for force model parameter τ_c fatigue model
τ_{fat}	ms	Time constant controlling the recovery of the three force model parameters during fatigue

Because this model is mainly based on the physiological mechanism, it seems complex for ergonomic application due to its large number of variables. For example, only for quadriceps, there are more than 20 variables to describe the muscle fatigue mechanism. Furthermore, there are only parameters available for quadriceps, which makes it difficult to integrate it for full body application. This model was integrated into virtual soldier research (VSR) system to simulate the movement of legs by lifting loads using quadriceps (Vignes, 2004), and the results showed Wexler's Model could predict muscle fatigue correctly, but it still needs to be generalized for the other muscles.

Giat's model - force-pH relationship

Another muscle fatigue model based on force-pH relationship was developed in Giat et al. (1993). This fatigue model was obtained by curve fitting of the pH level with time t in the course of stimulation and recovery. Komura et al. (1999, 2000) have employed this model in computer graphics to visualize the muscle capacity and then to evaluate the feasibility of the movement.

When a large amount of force is required to the muscle, the muscle fibers in the muscles are recruited. This causes the intracellular pH level inside the muscle to decline, and then the maximum force generation capacity decreases during the fatigue phase. When the muscle is at rest, the pH level increases, and the capacity of force increases during the recovery phase. Based on this phenomena, Giat et al. (1993) developed a muscle fatigue model describing the relationship between the exertable force and the pH level.

The decay of pH level during the fatigue phase can be calculated by the following function with the constant parameters c_1, c_2, c_3, c_4 (Eq. 1.3).

$$pH^F(t) = c_1 - c_2 \tanh(c_3(t - c_4)) \tag{1.3}$$

The pH level during recovery is calculated similar to the fatigue phase, and it is formulated by Eq. 1.4.

$$pH^R(t) = d_1 + d_2 \tanh(d_3(t - d_4)) \tag{1.4}$$

with the constants d_1, d_2, d_3, and d_4.

The force output is fitted by Eq. 1.5 with d_5, d_6, and d_7 as constants.

$$f_{pH}(pH) = d_5(1 - e^{d_6(pH - d_7)}) \tag{1.5}$$

The equation 1.5 is normalized by the force obtained at the beginning of the experiment:

$$f_{pH}^N = \frac{f_{pH}(pH(t))}{f_{pH}(pH(t_0)} \tag{1.6}$$

However, this model did not evaluate the muscle fatigue in the whole working process. Meanwhile in this pH muscle fatigue model, although the force generation capacity can be mathematically analyzed, all the influences on fatigue from muscle forces are not well considered.

Rodríguez's model - half-joint endurance

Rodríguez proposed a half-joint fatigue model in Rodríguez et al. (2003a,b) and Rodríguez and Boulic (2008), more exactly a fatigue index, based on mechanical properties of muscle groups. This fatigue model was used to calculate the fatigue at joint level: two half-joints, and the fatigue level is expressed as the actual holding time normalized by maximum holding time of the half-joint (Eq. 1.7 to Eq. 1.9).

For each joint, the normalized torque T_N is calculated as the ratio of joint torque τ and joint strength st. From these elements we can deduce the normalized torque, T_N, and exploit the general force-time relationship expressed as a regression line, valid for several muscle groups. The maximum holding time mht gives the longest period of time during which the posture can be sustained before reaching an unbearable level of fatigue. The fatigue level simply expresses the ratio of the holding time ht by the maximum holding time mht.

$$T_N = \frac{\tau}{st} \tag{1.7}$$

$$mht = \exp(2.7 - 0.0448 T_N) \tag{1.8}$$

$$fatigue\ level = \frac{ht}{mht} \tag{1.9}$$

With this model, it is able to apply a posture optimization algorithm to adapt human posture during a working process dynamically when fatigue appears. However, it cannot predict individual muscle fatigue due to its half-joint principle because the movement of a joint is activated by several muscles. The maximum holding time equation of this model was from static posture analysis and it is mainly suitable for evaluating static postures.

Liu's model- motor units pattern model

In Liu et al. (2002), a dynamic muscle model is proposed based on motor units pattern of muscle. In this model, three phenomenological parameters (B, F, and γ) are introduced to construct the muscle model to describe the activation, fatigue and recovery process. But there were only parameters available under maximum voluntary contraction situation of the right hand which is rare in manual handling work, and furthermore, there is still no application of this model in ergonomics field.

The generated force is proportional to the activated motor units in the muscle. The brain effort B, fatigue property F and recovery property R of the muscle can decide the number of activated motor

units. The relationship is expressed by Eq. 1.10. The parameters in this equation are explained in Table 1.4.

$$\begin{cases} \dfrac{\mathrm{d}M_A}{\mathrm{d}t} &= B\,M_{uc} - F\,M_A + R\,M_F \\ \dfrac{\mathrm{d}M_F}{\mathrm{d}t} &= F\,M_A - R\,M_F \\ M_{uc} &= M_0 - M_A - M_F \end{cases} \tag{1.10}$$

Table 1.4: Parameters in Active Motor model

Item	Unit	Description
F	s^{-1}	fatigue factor, fatigue rate of motor units
R	s^{-1}	recovery factor, recovery rate of motor units
B	s^{-1}	brain effort, brain active rate of motor units
M_0		total number of motor units in the muscle
M_A		number of activated motor units in the muscle
M_F		number of fatigued motor units in the muscle
M_{uc}		number of motor units still in the rest
β		B/F
γ		R/F

1.4 Conclusions from literature review

1.4.1 Problematic analysis in DHM

Shortcoming in conventional ergonomic tools

Although conventional ergonomic evaluation tools have been integrated into DHM and some assessments in DHM tools provide indexes, because of the intermittent recording procedures of the conventional posture analysis methods, the evaluation result cannot analyze the fatigue effect in details. In this case, new fatigue evaluation tools should be developed and integrated into virtual human simulation to evaluate the fatigue precisely.

Shortcoming of CAE in fatigue evaluation

Fatigue is one main reason for MSD, and fatigue affects actions in our daily life. However, there is no integration of physical fatigue model in most of the human simulation tools.

The physical capacity is often treated as constant. For example, the joint strength is assigned as joint maximum moment strength in 3DSSPP, and the strength of each muscle is set proportional to its physiological cross section area (PSCA) in AnyBody. The physical capacity keeps constant in the simulation, and the fatigue effect along time is not considered enough. However, the change of the physical status can be experienced everyday by everyone, and different working procedures generate different fatigue effects. Furthermore, it has been reported that the motion strategy depends on the physical status, and different strategies were taken under fatigue and non-fatigue conditions (Chen, 2000; Fuller et al., 2008).

Therefore, it is necessary to create a virtual human model with a variable physical strengths for the simulation.

Shortcoming in fatigue models

Some fatigue models have been incorporated into some virtual human tools to predict the variable physical strength. For example, Wexler's fatigue model (Ding et al., 2000b) has been integrated into Santos^{TM} (Vignes, 2004), and Giat's fatigue model (Giat et al., 1993) has been integrated based on Hill's muscle model (Hill, 1938) in the computer simulation by Komura et al. (2000). However, either the muscle fatigue model has too many variables for ergonomic applications (e.g. Wexler's model), or there is no clear physiological principle for the fatigue decay term (Xia and Frey Law, 2008) in the previous studies. It is necessary to propose a simplified fatigue model interpretable in muscle physiological mechanism for ergonomics applications.

1.4.2 Fatigue analysis solutions in DHM

As conclusions of the previous part, findings of previous research indicate:

1. Manual handling operations may have potential ergonomic injury risk relevant to the load, and posture. Static postures involving repeated and prolonged low force contraction of skeletal muscles result in physical fatigue and furthermore MSDs in muscle tissues.

2. Conventional ergonomic posture analysis methods are time-consuming and they are not suitable for physical fatigue prediction.

3. Fatigue evaluation is not considered enough in current available virtual human simulation tools.

4. Fatigue models in the literature either requires too much effort for model identification or are not suitable for ergonomic application;

5. The influence from the physical work is not well modeled or considered in the virtual human simulation tools.

Therefore, in order to analyze the physical work in details and predict the physical exposures, especially muscle fatigue, a new digital human model, concerning the overall dynamic working process, should be developed to assess and predict the potential MSD risks objectively. This concern became the main content of our research work.

In this thesis, we are going to present our framework in which human posture can be analyzed and predicted with consideration of the fatigue effect. The fatigue effect is modeled by a new simple dynamic muscle fatigue model. In this fatigue model, temporal parameters, physical factors, and personal factors are considered from the macroscopic view. This model is validated theoretically and experimentally. The application case under this framework with the fatigue model is used to show the applicability of our method in posture analysis and posture prediction.

Chapter 2

Framework for objective work analysis

Contents

2.1 Introduction 23
2.2 Structure of the framework 25
2.3 Virtual human status 27
2.4 Input modules and their technical specifications 28
2.5 Output modules 34
2.6 Summary 36

2.1 Introduction

The aim of the dissertation is to analyze the ergonomic aspects of manual handling operations. Different methods can be used to realize the objective evaluation. Traditionally, ergonomic evaluations are carried out in field under real working environment. Recently, virtual reality has emerged as one technology supporting simulation based engineering for workspace design and work design (Nomura and Sawada, 2001). With virtual reality, more and more evaluation tasks have been carried out under virtual environment, and it takes less time and less cost to evaluate the operations and verify the workspace design under virtual conditions. Detailed discussion can be found in Wilson (1999).

According to the schema ((Hu and Zhang, 2008), Fig. 2.1), work evaluation methods can be classified into four groups based on their nature: 1) **RO**: objective evaluation methods in real world; 2) **RS**: subjective evaluation methods in real world; 3) **VO**: objective evaluation methods in virtual world; 4) **VS**: subjective evaluation methods in virtual world.

The comparison of the evaluation methods is presented in Table 2.1. Subjective assessment has been the most frequently used due to the ease of use (Li and Buckle, 1999), and less time is required for post analysis. However, subjective methods are prone to many influences with the exception of the

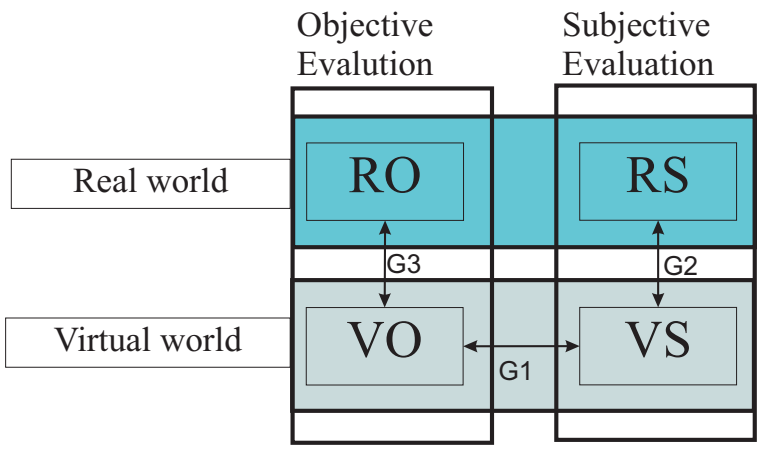

Figure 2.1: Schematic representation of evaluations in virtual reality

task or workplace, and therefore result in low validity and reliability. In conventional pen-paper based observational objective methods, some risk factors cannot be considered in the assessment process, and no agreement for the weighting of different measures has been found in the literature.

As discussed in Chapter 1, conventional posture analysis methods locate in RO or RS. In comparison to simulation-based methods, it requires more resources and more time in real working environment, especially for the high cost physical mock up. Meanwhile, many different factors can be processed at the same time in virtual environment, and the analysis can reach to more detailed results. Furthermore the efficiency is enhanced in comparison to objective methods in real working environment. However, the real work environment provides 100% fidelity which is difficult to be achieved in virtual reality.

After the comparison, it is believed that the most efficient way is to carry out the work analysis using subjective evaluation methods in a virtual environment, and the most expensive methods might be evaluations with objective methods under real conditions. However, the precision and the fidelity are decreasing controversially. Meanwhile it should be noticed that the human's performance can be affected by the virtual environment, either improved (Seymour et al., 2002) or degraded (Arthur, 2000), therefore, the consistency between the different evaluation results might be interesting for the application of virtual environment.

Depending on the fidelity of a virtual system, two approaches have been applied to evaluate the work. One approach is to transfer directly the evaluation methods in real world to virtual world. Once the simulated virtual environment can provide the same information as in real world, conventional methods can be taken into virtual environment for work evaluation, such as RULA in Jayaram et al. (2006). Since there are mismatchings between real world and virtual world and there might be extra information available for virtual world (for instance, the human motion data, the force feedback, etc.), another approach is to create new methods to evaluate operations in virtual world.

Table 2.1: Comparison of different evaluation methods in real and virtual environment

	RO	RS	VO	VS
Digital mock up			✓	✓
Physical mock up	✓	✓		
Consumed time			✓	✓
Reliability	✓		✓	
Fidelity	✓	✓		
Precision	✓		✓	

The aim of computer aided ergonomics is to evaluate manual handling operations in simulation based methods, therefore it is necessary to verify the feasibility of the evaluation methods in virtual environment, which means that the evaluation results from VS or VO should keep consistency with the results from RO or RS. Once the consistency is validated, it is promising that the evaluation in virtual environment can be used to guide the ergonomic oriented design.

The specific focus of our research is on developing a new method for objective evaluation of fatigue in virtual environment. In our case, we are trying to find a method to evaluate the physical fatigue objectively in simulation-based method, and the evaluated result should be validated in objective evaluation method in real working environment.

2.2 Structure of the framework

As stated in Section 1.2, the computer aided virtual human simulation tools have mainly two functions: posture analysis and posture prediction (motion simulation). Our framework is designed to realize the two functions as well. Both functions are explained as below.

Posture analysis: to evaluate human work and predict potential human MSD risks, especially physical fatigue; **Posture prediction:** to predict the human posture under different physical conditions. In this thesis, we are mainly focusing on fatigue evaluation and its effect on posture.

The function structure of the framework is shown in Fig. 2.2. There are two branches in the framework corresponding to posture analysis and posture prediction, respectively. The first branch is the path in solid arrows, and the second branch is the path of the close loop in solid arrows and dashed arrows.

The posture analysis function of our framework aims to evaluate the difficulty of human mechanical work including fatigue, comfort and other aspects, field-independently. This function is mainly realized by the objective work evaluation system (OWES) in the center of the framework. OWES

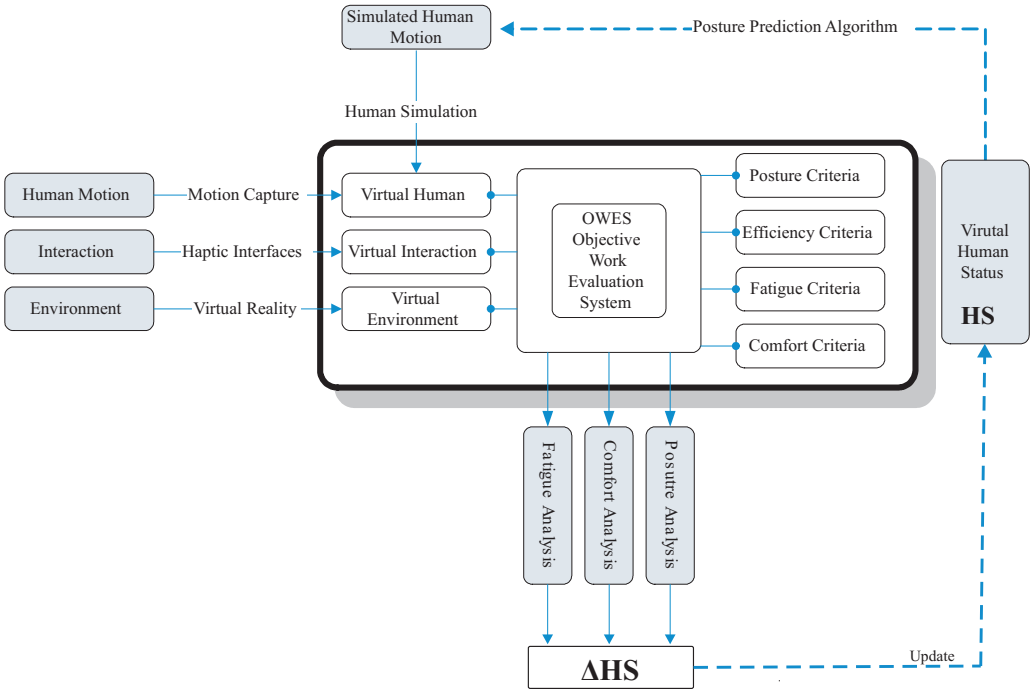

Figure 2.2: Framework of Objective Work Evaluation System

processes all the necessary input information to assess the effect of the operation. Different aspects of the human work can be assessed by using different ergonomic criteria defined in OWES, such as posture, efficiency, fatigue,comfort, etc.

The necessary input information includes: virtual environment, human motion, and the interaction between human and workspace. In order to avoid field-dependent work evaluation, virtual environment techniques are used. Immersive work simulation system should be constructed to provide a virtual working environment for the work simulation and meanwhile all the dimensional information of the workspace. Virtual human should be modeled as well. It is driven by human motion data to map the real working procedure into the virtual environment. In this case, the real operation can be carried out under virtual environment. Human motion can be either captured by motion capture systems or simulated by virtual human simulation. The interaction between the virtual human and the workspace is obtained either via haptic interfaces under motion capture conditions or modeled in the virtual human simulation case.

Posture prediction is to generate the posture or motion automatically for a given task in the simulation tools by taking account of the workspace, human strength, anthropometrical data, etc. In general, the trajectory of the movement can be defined by several important points in the path. The virtual human can complete the operation along the trajectory generated either by inverse kinematics or by some optimization methods.

The posture prediction function in our framework is different from the simulation tools mentioned

in Section 1.2. In the previous simulation tools, the posture or the motion is simulated based on invariable initial physical conditions. Under our framework, the physical conditions are variable according to the work history, therefore the change of the human physical conditions are taken as feedbacks to update the virtual human status in order to regenerate the simulated human motion. The update of the human physical conditions is realized by the dashed arrows.

2.3 Virtual human status

Definition 4 Human Status

It is a state, or a situation in which the human possesses different capacities for an industrial operation. It can be further classified into mental status and physical status. Human status can be described as an aggregation of a set of human abilities, such as visibility, physical capacity (joint strength, muscle strength), and mental capacity.

A new conception called the **human status** is proposed for this framework to generalize the discussion. Virtual human status can be mathematically noted as $\mathbf{HS} = \{\mathbf{V}_1, \mathbf{V}_2, \ldots, \mathbf{V}_n\}$. Each $\mathbf{V}_i$ represents one specific aspect of human abilities, and this state vector can be further detailed by a vector $\mathbf{V}_i = \{v_{i1}, v_{i2}, \ldots, v_{im_i}\}$. The change of the human status is defined as $\Delta\mathbf{HS} = \mathbf{HS}(t+\delta t) - \mathbf{HS}(t) = \{\Delta\mathbf{V}_1, \Delta\mathbf{V}_2, \ldots, \Delta\mathbf{V}_n\}$. For example, one aspect of the physical status (joint strengths) can be noted as $\mathbf{HS} = [S_1, S_2, \ldots, S_n]$, where S_i represents the physical joint strength of the ith joint of the virtual human.

In order to make the simulation as realistic as in real world, it is necessary to know how the human generates a movement. The bidirectional communication between human and the real world in an operation decides the action to accomplish a physical task: worker's mental and physical status can be influenced by the history of operation, while the worker chooses his or her suitable movement according to his or her current mental and physical statuses. Hence the framework is designed to evaluate the change of human status before and after an operation, and furthermore to predict the human motion according to the changed human status.

The human is often simplified for posture control as a sensory-motor system in which there are enormous external sensors covering the human body and internal sensors in the human body capturing different signals, and the central nervous system (CNS) transfer the signals into decision making system (Cerebrum and Spinal cord); the decision making system generates output commands to generate forces in muscles and then drives the motion and posture responding to the external stimulus.

Normally, most of the external input information is directly measurable, such as temperature, external load, moisture, etc. However, how to achieve all the information for such a great number of

sensors all over the human body is a challenging task. In addition, the internal perception of human body, which plays also an important role in motor sensor coordination, is much more difficult to be quantified. The most difficult issue is to know how the brain handles all the input and output signals while performing a manual operation.

In previous simulation tools, the external input information has been already provided and handled. Visual feedback, audio feedback, and haptic feedback are often employed as input channel for a virtual human simulation. One limitation of the existing methods is that the internal sensation is not considered enough. Physical fatigue is going to be modeled and integrated into the framework to predict the perceived strength reduction and the reactions of the human body to the fatigue, which provides a closed-loop for the human simulation. As illustrated in Fig. 2.2 and 2.3, human status is always updated during the simulation in our framework to regenerate the motion.

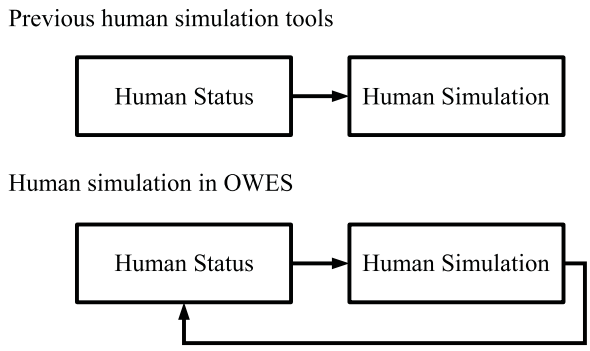

Figure 2.3: Human status in human simulation tools

2.4 Input modules and their technical specifications

For any ergonomic analysis, data collection is the very first important step. All the necessary information has to be collected for further processing. In general, necessary information for evaluating manual handling jobs consists of human motion (posture in static cases), forces, interaction information, and personal factors.

2.4.1 Human motion input module

Human motion concerns the movements without regard to the force production in the motion, and it includes all the displacement, translation, and rotatory movements of human body. In static cases, it can be represented by the static posture of human body. Human motion can be either achieved by motion capture system or by digital human simulation (posture prediction).

Motion tracking module

Tracking module is used to trace the worker's operation in real time and prepare the motion data for further processing.

Motion capture techniques have been applied frequently to obtain the dynamic and natural motion information in current human simulation tools (VSR Research Group, 2004). There are several kinds of tracking techniques available, such as mechanical motion tracking, acoustic tracking, magnetic tracking, optical motion tracking, and inertial motion tracking (Foxlin and Inc, 2002; Welch and Foxlin, 2002). Each tracking technique has its advantages and drawbacks for capturing the human motion. Hybrid motion tracking techniques can be taken to compensate the disadvantages and achieve the best motion data.

In general, the technical requirements for the trackers are: tiny, self-contained, complete, accurate, fast, immune to occlusion, robust, tenacious, wireless and cheap. These are the requirements for the ideal tracker, but actually, every tracker available today falls short on at least seven of these 10 characteristics (Foxlin and Inc, 2002). The performance requirements and purposes of the application are the decisive factors to select the suitable tracker.

In our framework, worker's operation needs to be tracked and digitalized for biomechanical analysis, so the positions and the orientations of the worker's limbs should be known and as well the detailed motions, such as finger movements. The position of the worker's limbs determines the global posture, and the motion of fingers represents the handling situations of the hands. In this case, several basic requirements should be fulfilled for this application.

Tracking speed: Tracking worker's operation is easier than tracking athlete's performance, because normally there's no running or jumping in work. The tracker should satisfy tracking general movements of human body, and data update rate should be at least 24/25 Hz in order to realize real time visualization.

Robustness: Worker's motion is tracked during performing certain tasks. During the working, the tracking should be stable and prevent influences from noises and other factors.

Completeness: No tracker is suitable for tracking full-body motion and finger motion at the same time, and therefore integration of different trackers is necessary in order to capture all necessary motion information.

Absolute accuracy: In general, applications demand accuracy with resolution 1mm in position and 0.1 degree in orientation. For full-body motion tracking, the demands are reduced in applications like character animation and biometrics. In this framework, the demand for accuracy depends on the types of the job. For general moves, the demands for accuracy are not very critical, but for some actions, like using tools or controlling switches, with interactions with virtual objects, the accuracy

should be as high as possible.

Data transferring: Transferring the data from tracking module to the other modules is another problem. Generally, there are real-time and no-real-time modes. In the latter manner, tracking data can be saved for off-line application. In real time manner, it is necessary to transfer the data to the simulation module as quickly as possible to ensure the real-time simulation.

Prototype of an optical tracking system

An optical motion tracking system has been developed in Virtual Reality and Human Interaction Technology Laboratory (VRHIT) in Tsinghua University (Wang et al., 2006). This system is used to capture the whole body motion for posture analysis under this framework. Other possible solutions can be used to fulfill the motion capture task.

The hardware structure of the motion capture system is shown in Fig. 2.4. In this system, optical motion tracking system is employed to capture human motion, while 5DT^{TM} data glove is used to track hand motion. Both of them are transferred via Network to simulation computer to provide real time visualization of human motion. The visual feedback can be provided via head mounted display (HMD). Haptic feedback is realized through clothes-embedded micro vibration motors. Projection-based wide screen display is also used for supervisor or other third party to monitor the tracking procedure.

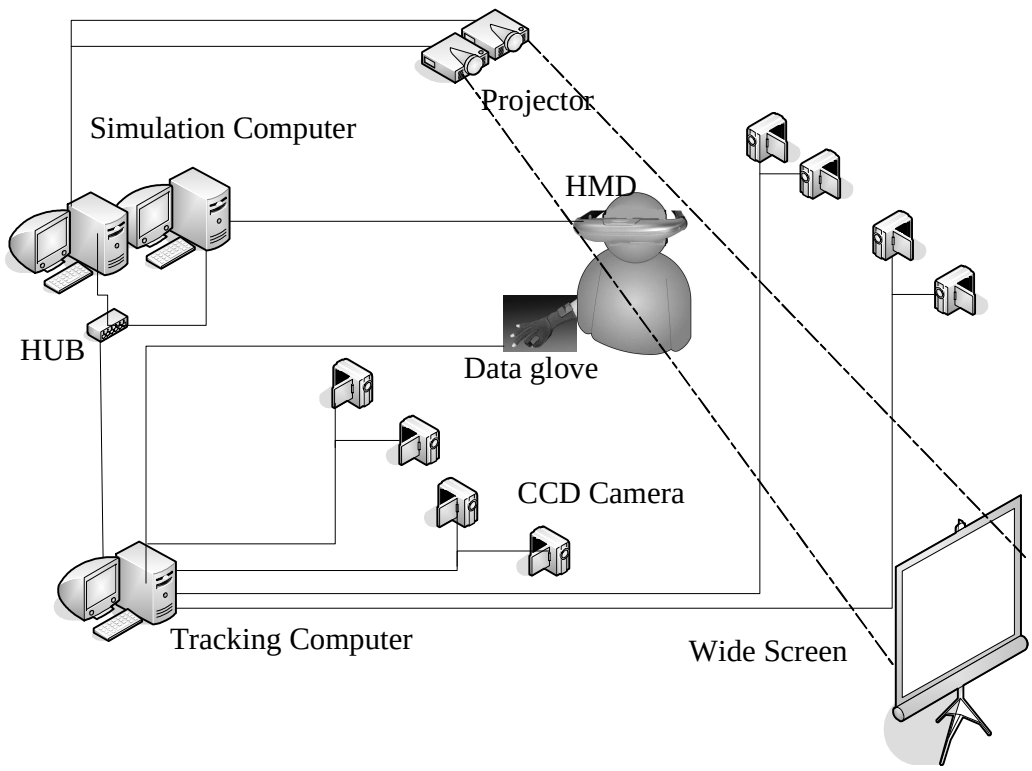

Figure 2.4: Schematic structure of the motion capture system

This capture system is equipped by eight CCD cameras around the work space. The overall capture system works at 25 *Hz*, which satisfies the minimum requirement to provide sufficient update rate of the simulation image, especially for quasi-static postures, and it provides sufficient detailed analysis of the human body motion. In the frequency 25 Hz, the capture system is not suitable for fast motion, but applicable for manual handling operation, since there are rare very fast motions in these operations. The precision of the capture system depends on the hardware system and the algorithms in the capture module. The absolute precision is relative low, with a position error around 5 *cm*. The repeat precision is around 2-3 *mm* which ensures the analysis of human motion. In this case, after calibration, the motion capture system is able to be used to capture confidential motion data. The most important issue in optical motion tracking is to avoid occlusion of optical markers and to identify the marker attached to human body correspondingly. Although certain algorithms have been developed in the capture module to avoid tracking mistakes, the robustness of the motion tracking system is still a challenging task for the system.

The comparison between two real postures and simulated postures based on the tracking data of the real postures is shown in Fig. 2.5. The figure shows that the motion capture system is able to provide accurate motion data for further processing.

Figure 2.5: Posture comparison between real postures and postures in simulation

Motion simulation module

Another method to achieve the human motion is digital human simulation (posture prediction) under a given task. As discussed in Section 1.2, inverse kinematics and posture prediction with optimization have been frequently engaged in digital human models to predict and simulate the human motion.

When a physical task is given, the user has to locate the virtual human in the virtual working

system in simulation tools, and then define the posture or the trajectory manually. When the start point and end point are well defined, the virtual human can act based on the simulation algorithms to generate the simulated trajectory. The aim of posture prediction is to achieve the simulated human motion as real as possible under a computation speed as quick as possible.

In contrast to motion capture system, this method cannot get the motion as real as that in a capture system; and it is also time consuming to locate the virtual human and define the posture; furthermore, it requires efficient computation algorithms to simulate the human motion, and there might be a trade off between the computation efficiency and the reality of the simulation. However, it avoids the engagement of the worker and the installation of the motion capture system, and it can be used to assess the work design in advance of the physical construction without worker. Therefore, both methods are necessary to complete the motion input module in our framework.

2.4.2 Visualization of human simulation

In our framework, the simulation module is to simulate the worker's operation in the virtual working environment, to provide visualization of the simulation to the worker performing the task, and to display the interactions between worker and virtual objects. It includes three parts: visualization of virtual environment, visualization of virtual human, and feedbacks between virtual simulation and worker.

Visualization aims to provide a method for understanding much better the human motion and its interaction with virtual environment. A basic requirement for virtual reality simulation is that the visual content of the simulation should be updated in real time manner under motion capture to supply visual feedback to the worker.

Visualization of virtual environment: Virtual working environment should be prepared from CAD system, so that the operator can at least have the similar spatial feelings as working in a field area. The virtual environment can be the copy of a real field environment or redesigned for new work environment validation. In the virtual environment there are fixed and movable virtual objects. Fixed objects can be work station, machine tools, working plats which remain stationary no matter how the user interacts with them; movable virtual objects can be for example some parts, bolts and boxes which can be moved in the simulation when the user moves them, changeable objects like buttons, switches which changes its state while the user interacts with them.

Visualization of virtual human: Besides virtual working environment, virtual human should be modeled to present the worker's operation virtually. The virtual representation of the human is mapped into the virtual environment by the motion tracking data and can assist the worker working in the virtual environment and can give the observer the overview of the worker's operation. The virtual

human should at least have the similar dimension and appearance as the real human. This objective can be achieved by modeling human from anthropometrical database.

Digital modeling of virtual human: For fatigue evaluation, it requires that loads of each joint and even the forces of each muscle need to determined in virtual human. It demands that the skeleton structure of human should be modeled to determine the linkage relation between muscles and bones as well. After skeleton and muscle modeling, it is possible to compute the load of each individual muscle and joint during the operation. Therefore, biomechanical database should be established to complete the virtual human modeling. Kinematic modeling of the human can represent the human geometrically; dynamic modeling of the virtual human can provide necessary information for determining the loads of each joint; biomechanical modeling in muscles and tendons allows us to calculate the force of each individual muscle.

2.4.3 Force and interaction information

Force information: In order to determine the forces and torques of the virtual human, it is important to measure the force exerted on the human body. External loads can be classified into different groups according the difficulty of measurement. For instance of a lifting job, the gravity of a heavy box is easy to be modeled and calculated. However, if the weight of the box is too large, it is not realizable via force feedback devices. However, it could still be simulated by a real heavy box. In contrast, the reaction force between the human and the floor is calculatable unless when all the dynamic parameters were obtained. In this case, the reaction force between human and the floor can be measured by force plates. In case of complex interaction with workplace, for example, assembly while kneeing on the ground, the external load on the human body is very difficult to be obtained precisely and completely.

Interaction between the user and the virtual objects: In real-time simulation, interactive feedbacks should be provided in order to create immersive working feelings. The interactive feedbacks include visual feedback, haptic feedback, and acoustic feedback and so on. The simulation module should have at least one view based on the viewpoint of the worker, so that correct visual feedback can be supplied to the worker.

Interaction information can be recorded by haptic interfaces. Haptic interface is the channel via which the user can communicate with virtual objects through haptic interactions, and the interaction data between the worker and the virtual environment are also significant for evaluating other ergonomic aspects. Haptic feedback can give the user correct feelings of touching virtual objects, grasping or moving them. It enhances the presence of being in real world, and improves the performance in virtual reality system.

To ensure the fidelity of the haptic feedback, there is one critical requirement for the haptic feedback interfaces: high update rate (300Hz -1000Hz) (Payandeh et al., 2007). In order to provide the right feedback, the interaction between worker and virtual objects should be detected and analyzed in a real time manner. The coupling between the worker and the virtual objects should be simulated, for example, lifting a box. Besides that, feedback forces should be calculated with correct and efficient models to ensure the high update rate.

2.4.4 Personal factors

In order to evaluate the work correctly and confidentially, work related personal factors should also be measured. For fatigue evaluation, individual fatigability is an important term to determine the fatigue evaluation result.

2.5 Output modules

The framework performs mainly two functions: posture analysis and posture prediction (human simulation). Each function can give different outputs: in posture analysis, different aspects of the human work can be evaluated; in posture prediction, the motion strategy of human can be predicted and simulated.

2.5.1 Posture analysis

This part plays the role as ergonomists to evaluate the working process objectively. The evaluation criteria should be applied or designed into this framework to assess the work.Different ergonomic aspects of human work can be analyzed in posture analysis under different evaluation criteria. Although there are several motion analysis techniques available for ergonomic and biomechanical analysis, these techniques should be re-designed suitable for computer analysis in our framework, since instead of providing an index to evaluate the work, the change of the human status is the output of our framework.

The posture analysis focuses on assessing the difficulty of the manual operation in our framework. The difficulty of the work is assessed by the change of human status before and after the operation in our framework, especially the physical status. Physical fatigue is one of the physical aspects, and this aspect is evaluated by the decrease of the strength in joints. Mathematically, the analysis result is $\Delta\mathbf{HS} = \Delta\mathbf{HS}_{physical} = \{\Delta S_1, \Delta S_2, \ldots, \Delta S_n\}$.

Kinematic analysis

With motion data, it is feasible to carry out the kinematic analysis. For the overall human, position, speed, and acceleration of each limb can be calculated. In general, once the configuration of the static posture is determined, conventional ergonomic posture analysis methods can be carried out automatically by the OWES.

Biomechanical analysis

In combination with kinematic information and dynamic parameters, forces and torques at each joint can be calculated out by inverse dynamics. Based on the load analysis of each joint, the biomechanical influence can be easily evaluated.

In our framework, the decrease of the physical strength is our focus. It is observable that there is physical fatigue resulting from repetitive manual handling operation in industry, and in our research we want to find a suitable method to predict the reduction of the physical strengths in those operations. Our method is to find a suitable model which can represent the influence on the physical fatigue from the temporal parameters and the external load. This model is mathematically described and simple for integration into posture analysis.

2.5.2 Posture prediction

The function of posture prediction is to simulate the human motion based on the current virtual human status. Our special interest is to take the fatigue effect to predict the posture.

Physical fatigue resulting from repetitive movements in manufacturing and assembly line work influences neuromuscular pathways, postural stability, and global reorganization of posture (Fuller et al., 2008). The fatigue effect was also found in Chen (2000) that the movement strategy in industrial activities involving combined manual handling jobs, such as lifting, depends significantly on the fatigue state of muscle. The change in movement strategies in the activities directly affects the posture of the operation which results in different loads in muscles and joints.

A more realistic posture prediction can gain clearer understanding of human movement performance, and it is always a tempting goal for biomechanics and ergonomics researchers (Zhang and Chaffin, 2000). The predictive capacity, or the reality is provided by a model in computerized form, and these quantitative models should be able to predict realistically how people move and interact with systems. Physical fatigue, which can be experienced by everyone in the world, changes the human's behavior significantly for manual handling operations, especially for those under high physical demands in a long duration. Therefore, it is necessary to integrate the feature of fatigue into posture

prediction to predict the possible change of posture under fatigue conditions.

In conventional methods, the human status is assumed as constant. For example, the physical strengths keep constant under this mathematical description: $\mathbf{HS}_{t_i} = \mathbf{HS}_{t_j}$ (where $t_i \neq t_j$). The fatigue effect along time is not considered while predicting the posture under joint strength guided strategies. In our research, the fatigue is modeled and integrated into virtual human simulation tools.

2.6 Summary

In this chapter, the framework under which our research is carried out is presented. The framework handles all the necessary information and performs posture analysis and posture prediction functions as the previous commercialized tools. A new conception, so called human status, is proposed to generalize discussions in human simulation.

Different from the existing tools, the special contribution of this framework is that fatigue analysis in posture analysis is assessed based on a simple mathematical muscle fatigue model which includes the temporal and physical parameters. The changed physical status is provided as output for the posture analysis, but not an abstract index. The changed physical strength from fatigue is taken as a feedback to the virtual human simulation to update the posture prediction result.

Chapter 3

Muscle fatigue model and its theoretical validation

Contents

3.1 Introduction 37
3.2 Muscle fatigue model and its explanation 39
3.3 Validation in comparison to MET models 42
3.4 Validation in comparison to other dynamic models 49
3.5 Fatigability of different muscle groups 53
3.6 Summary 65

3.1 Introduction

Although physical fatigue can be described and modeled based on the complex physiological process in CNS and musculoskeletal system, it is originally provoked by different external aspects in manual handling operations: magnitude of the load, duration of the operation, frequency, and personal factors. For ergonomics application, it is necessary to take account of these external factors macroscopically to assess the fatigue, since it is possible to observe or measure these external factors directly in comparison to measuring physiological parameters which takes more time and more effort.

In ergonomics and virtual human tools, one approach to assess the fatigue quantitatively is to integrate fatigue models to predict the fatigue process. The models engaged in fatigue assessment can be constructed based on different principles.

As discussed in Section 1.3, some of the fatigue models (Wexler's model, Giat's pH model, etc)on the basis of muscle physiological principle have been integrated into virtual human tools. In these models, the physiological fatigue process or phenomena is to be modeled to reproduce the fatigue

process, and these models succeed in predicting the fatigue of an individual muscle under certain conditions. They are not suitable for ergonomics applications, since they are either too complex resulting from their complex physiological background, or not relating to external physical factors of the manual operation.

Another major effort has been done to assess fatigue quantitatively in traditional ergonomic methods is the maximum endurance time (MET) model. MET is an assessment of fatigue based on the maximal duration of an exerted force at a present level, and it indicates the relationship between the relative load and the endurance duration under static postures. Since 1960s, lots of effort has been contributed to establish MET models under different work conditions for different muscle groups (Rohmert, 1960, 1973; Rohmert et al., 1986; Bishu et al., 1995; Kanemura et al., 1999; Mathiassen and Ahsberg, 1999; Garg et al., 2002), and the MET was often formulated in function of the relative load in comparison to maximum voluntary contraction MVC, $MET = T(f_{relative}) = T(f_{load}/MVC)$.

The majority of these models have been summarized and compared in El ahrache et al. (2006), and all these models which are formulated in different mathematical functions have some points in common: in mathematics, they are in negative exponential functions with two asymptotic tendencies; they have similar graphical appearances in Force-Time diagrams. These models are often utilized to assess the fatigue by comparing the actual holding time with the maximum endurance time.

Although there are already several MET models available in the literature, there are still some limits for the application of these models.

1. These models are mainly based on empirical regression from experiment results and they are modeled mainly by negative exponential functions. However, the physical relationship in these models cannot be interpreted by muscle physiology, and there is no universality among these models.

2. Each MET model was established based on experimental results under a static specific job design, therefore this approach lacks the ability to be generalized to adapt for more complex tasks.

3. Even for the same muscle group in the same operation, there are still differences in the empirical models, no matter for the different body parts. The variety cannot be explained using different empirical MET models. Since it is observable that the MET models have similar curves indicating the same trend of fatigue, they should be able to be interpreted by a general fatigue rule.

As discussed before, it is necessary to develop a new fatigue model in order to avoid the complexity of the conventional methods and to evaluate the fatigue from external physical factors during the

manual operation, and furthermore this model should be interpretable based on muscle physiology. In this case, based on muscle motor unit recruitment mechanism, we propose a new simple fatigue model in function of external physical and personal parameters.

In this chapter, our fatigue model is going to be firstly presented and explained based on muscle physiological mechanism, from both macroscopic view and from microscopic view. In this model, external physical factors and personal factors (MVC, fatigue resistance) are taken into consideration. The theoretical analysis is the main content of the chapter to demonstrate the consistency of our model to the other existing models in the validation sections. At last, one important personal factor: fatigue resistance, is regressed from MET models in the literature to show the possibility in generalizing our fatigue model to assess the fatigue of different muscle groups for a certain population.

3.2 Muscle fatigue model and its explanation

3.2.1 Muscle fatigue model

In order to construct the new fatigue model and fatigue index, as in the fore mentioned ergonomics methods for physical exposures, external load of the muscle with time and the strength capacity of the muscle are involved in our model. These factors can represent the physical risk factors mentioned before: the external load exposed to the muscle with time can include data related to intensity (or magnitude), repetitiveness, and duration of force. Also the muscle strength capacity can be determined individually and can be treated as personal factor. Thus, the muscle force history (external factor) and maximum voluntary contraction (MVC) (internal factor) are taken into account to construct our muscle fatigue model. MVC is defined as "the force generated with feedback and encouragement, when the subject believes it is a maximal effort" (Vøllestad, 1997). The effect of MVC on endurance time is often used in ergonomic applications to define the worker capabilities or to decide the work-rest regimens (Garg et al., 2002). In our model, MVC describes the maximum force generation capacity of an individual muscle without fatigue.

Our new objective fatigue index attempts to evaluate muscle fatigue by describing the human's perception of muscle fatigue. In general, the fatigue evaluation result is an increasing function with external load. In the same period, the larger the external load, the more fatigue people can feel. The same concept is also applied to posture analysis methods with a higher risk level for a heavier external load. Meanwhile, fatigue is a growth function with the reciprocal of muscle force capacity. The smaller the capacity, the quicker the muscle becomes fatigued. Furthermore, fatigue is a growth function with time. The longer a load is applied, the more fatigue people can feel. This is represented in conventional methods as frequency and duration of physical task. If the fatigue is expressed in a

differential equation, the influence of time can be excluded. The fatigue index is proposed in Eq. 3.1. The parameters used in the equations are listed and described in Table 3.1.

$$\frac{\mathrm{d}U(t)}{\mathrm{d}t} = \frac{MVC}{F_{cem}(t)} \frac{F_{load}(t)}{F_{cem}(t)} \tag{3.1}$$

Table 3.1: Parameters in Dynamic Fatigue model

Item	Unit	Description
MVC	N	Maximum voluntary contraction, maximum capacity of muscle, F_{max}
$F_{cem}(t)$	N	Current exertable maximum force, current capacity of muscle
$F_{load}(t)$	N	External load of muscle, the force which the muscle needs to generate
	min^{-1}	Constant value, rate of fatigue, here $k = 1$
$\%MVC$		Percentage of the voluntary maximum contraction
f_{MVC}		$\%MVC/100$, $f_{MVC} = \frac{F_{load}}{MVC}$.

Meanwhile, the capacity of muscle (current muscle force capacity) $F_{cem}(t)$ is changing with time due to the external muscle load. The larger the external load, the faster $F_{cem}(t)$ decreases. The differential equation for F_{cem} is proposed in Eq. 3.2 which is the basic function of the new dynamic fatigue model.

$$\frac{\mathrm{d}F_{cem}(t)}{\mathrm{d}t} = -k\frac{F_{cem}(t)}{MVC}F_{load}(t) \tag{3.2}$$

The integration result of Eq. 3.2 is Eq. 3.3, if $F_{cem}(0) = MVC$.

$$F_{cem}(t) = MVC\, e^{\int_0^t -k\frac{F_{load}(u)}{MVC}du} \tag{3.3}$$

Assume that $F(t)$ is:

$$F(t) = \int_0^t \frac{F_{load}(u)}{MVC}du \tag{3.4}$$

MVC is a constant value of a muscle or a muscle group for an individual person during a certain period, so we can change Eq. 3.3 into Eq. 3.5. If the external load F_{load} is constant, assign $C = F_{load}/MVC$, then $F(t) = Ct$, and Equation 3.3 can be further simplified into Eq. 3.5. This constant case can occur during static posture and static load.

$$\frac{F_{cem}(t)}{MVC} = e^{-kF(t)} = e^{-kCt} \tag{3.5}$$

The subjective perception is a function below, which is closely related to MVC and $F_{load}(t)$. MVC can represent the personal factors (Chaffin et al., 1999), and $F_{load}(t)$ is the force exerted on the muscle

along time and it reflects the influences of external loads. From Eq. 3.1, and 3.5, the fatigue index can be expressed in Eq. 3.6.

$$U(t) = \frac{1}{2k}e^{2kF(t)} - \frac{1}{2k}e^{2kF(0)} \tag{3.6}$$

3.2.2 Explanation of the fatigue model

Explanation from macroscopic view

Equation 3.1 can be explained as follows:

- F_{cem} describes the capacity of the muscle during the contraction process at a time instant t. It falls down during the contraction process because the muscle becomes fatigued in a continuous contraction.
- $F_{load}(t)/F_{cem}(t)$ is the relative load at a time instant t which describes the current muscle force normalized the capacity of the muscle at a time instant t. This term describes the relation of the fatigue index with normalized relative load.
- $MVC/F_{cem}(t)$ is the reciprocal of muscle force capacity and represents the inverse percentage capacity of the tester at a time instant t relative to the initial MVC. With the development of time, this term gets larger while the $F_{cem}(t)$ falls lower, and accordingly the increase of the fatigue index becomes faster.

Explanation in motor-untis pattern

Equation 3.2 can be explained by the motor unit activation pattern of muscle. Muscle is made of muscle fibers. Force and movement of muscle are produced by contraction of muscle fibers controlled by nervous-system command (Liu et al., 2002; Vøllestad, 1997). The basic functional unit of muscle is motor unit, which consists of a motoneuron and the muscle fibers that it innervates. The motoneurons supply the control signals from the central nervous-system (CNS) to the muscle fibers. A muscle consists of many motor units, and the number of which varies depending on the size and function of the muscle. Each motor unit has different force generation capability, and different fatigue and recovery properties. Generally, they can be divided into three types: type I (S, SO) is slow-twitch motor units with small force generation capability and slow conduction velocity, but a very high fatigue resistance; type IIb (FF, FG) is of fast-twitch speed, high force capacity, but fast fatigability; type IIa (FR, FOG),between type I and type IIb, has a moderate force capacity and moderate fatigue resistance. The sequence of recruitment is in the order of: I → IIa → IIb (Vøllestad, 1997). For a

specified muscle, larger F_{load} means more type II motor units are involved into the force generation. As a result, the muscle becomes fatigued more rapidly, as expressed in Eq. 3.2. F_{cem} represents the non-fatigue motor units of the muscle. In the process of force generation, the number of non-fatigue type II motor units gets smaller and smaller due to fatigue, while the number of the type I motor units remains almost the same due to their high fatigue resistance, and the decrease of F_{cem} with time becomes slower, as expressed in Eq. 3.2 by term $F_{cem}(t)/MVC$.

In this model, personal factors and external load history are considered in evaluating the muscle fatigue. It can be easily used and integrated into simulation software for real time evaluation especially for dynamic working processes. This model needs to be mathematically validated and ergonomic experimentally validated.

3.3 Validation in comparison to MET models

3.3.1 Mathematical principle of the validation

The proposed dynamic muscle fatigue model is based on the hypothesis of the reduction of the maximum exertable force capacity of muscle. It should be able to describe the most singularly important condition: static situations. In static posture analysis, there is no model to describe the reduction of the muscle capacity related to muscle force, but there are several models that consider maximum endurance time (MET) which is a measurement related to static muscular work. MET represents the maximum time during which a static load can be maintained (El ahrache et al., 2006). The MET is most often calculated in relation to the percentage of the voluntary maximum contraction ($\%MVC$) or to the relative force ($f_{MVC} = \%MVC/100$) required by the task. These models, cited from (El ahrache et al., 2006), are listed in Table 3.2.

MET models can be used to predict the endurance time of a muscle contraction under static posture. A general MET model can be extended by supposing that $F_{load}(t)$ is constant in static situation. MET is the duration in which F_{cem} falls down to the current F_{load}. Thus, MET can be determined in Eq. 3.7 and Eq. 3.8.

$$F_{cem}(t) = MVC\, e^{\int_0^t -k\frac{F_{load}(u)}{MVC}du} = F_{load}(t) \tag{3.7}$$

$$t = MET = -\frac{ln\frac{F_{load}(t)}{MVC}}{k\frac{F_{load}(t)}{MVC}} = -\frac{ln(f_{MVC})}{k\, f_{MVC}} \tag{3.8}$$

In order to analyze the relationship between MET obtained from our dynamic model and the other models, two correlation coefficients are calculated. One is Pearson's correlation r in Eq. 3.9 and the other one is intraclass correlation ICC in Eq. 3.10. The linear relationship between two random variables is indicated by r and ICC represents the similarity between two random variables. The closer r is to 1, the more the two models are linearly related. The closer ICC is to 1, the more similar the models are. $MS_{between}$ (the mean-square estimate of between pair variance) is the mean square between different MET values at different f_{MVC} levels, MS_{within} (the mean-square estimate of within-pair variance) is the mean square within MET values in different models at the same f_{MVC} level. p is the number of models in the comparison. In our case, we compare the other models, one by one, with our dynamic model, thus p equals to 2. The calculation results are shown in Table 3.2 and Fig. 3.1 to 3.8.

$$r = \frac{\sum_n (A_n - \bar{A})(B_n - \bar{B})}{\sqrt{\sum_n (A_n - A)^2 \sum_n (B_n - B)^2}} \tag{3.9}$$

$$ICC = \frac{MS_{between} - MS_{within}}{MS_{between} + (p-1)MS_{within}} \tag{3.10}$$

Since Huijgens' general model was developed using data from Rohmert's general, only Rohmert's general model is drawn in Fig. 3.1 and Fig. 3.2. Also since Sjogaard's general model was constructed using data from Hagberg's elbow model and Rohmert's general model, Sjogaard's model is excluded from Fig. 3.1 and from Fig. 3.2.

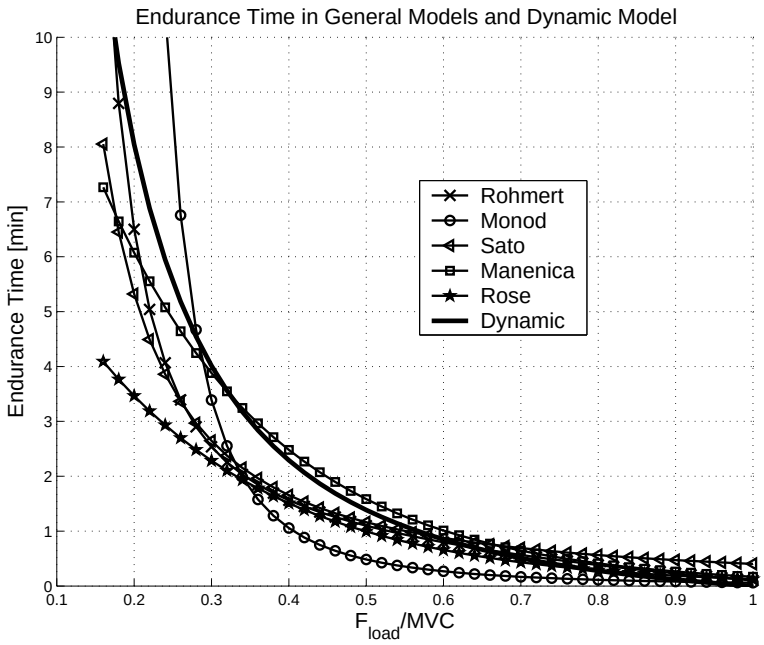

Figure 3.1: Endurance time in general models and dynamic model

Table 3.2: Static validation results r and ICC between Eq. 3.8 and the other existing MET models in the literature (El ahrache et al., 2006)

Model	Equations in the literature	r	ICC
General models			
Rohmert	$MET = -1.5 + \frac{2.1}{f_{MVC}} - \frac{0.6}{f_{MVC}^2} + \frac{0.1}{f_{MVC}^3}$	0.9937	0.8820
Monod and Scherrer	$MET = 0.4167\,(f_{MVC} - 0.14)^{-2.4}$	0.8529	0.6474
Huijgens	$MET = 0.865\left[\frac{1-f_{MVC}}{f_{MVC}-0.15}\right]^{-2.4}$	0.9964	0.8800
Sato et al.	$MET = 0.3802\,(f_{MVC} - 0.04)^{-1.44}$	0.9992	0.8512
Manenica	$MET = 14.88\ \exp(-4.48\,f_{MVC})$	0.9927	0.9796
Sjogaard	$MET = 0.2997\ f_{MVC}^{-2.14}$	0.9935	0.9917
Rose et al.	$MET = 7.96\ \exp(-4.16\,f_{MVC})$	0.9897	0.7080
Upper limbs models			
Shoulder			
Sato et al.	$MET = 0.398\ f_{MVC}^{-1.29}$	0.9997	0.7188
Rohmert et al.	$MET = 0.2955\ f_{MVC}^{-1.658}$	0.9987	0.5626
Mathiassen and Ahsberg	$MET = 40.6092\ \exp(-9.7\,f_{MVC})$	0.9783	0.7737
Garg	$MET = 0.5618\ f_{MVC}^{-1.7551}$	0.9981	0.9029
Elbow			
Hagberg	$MET = 0.298\ f_{MVC}^{-2.14}$	0.9935	0.9921
Manenica	$MET = 20.6972\ \exp(-4.5\,f_{MVC})$	0.9929	0.9271
Sato et al.	$MET = 0.195\ f_{MVC}^{-2.52}$	0.9838	0.9712
Rohmert et al.	$MET = 0.2285\ f_{MVC}^{-1.391}$	0.9997	0.7189
Rose et al.2000	$MET = 20.6\ \exp(-6.04\,f_{MVC})$	0.9986	0.9594
Rose et al.1992	$MET = 10.23\ \exp(-4.69\,f_{MVC})$	0.9943	0.7843
Hand			
Manenica	$MET = 16.6099\ \exp(-4.5\,f_{MVC})$	0.9929	0.9840
Back/hip models			
Manenica (body pull)	$MET = 27.6604\ \exp(-4.2\,f_{MVC})$	0.9901	0.6585
Manenica (body torque)	$MET = 12.4286\ \exp(-4.3\,f_{MVC})$	0.9911	0.9447
Manenica (back muscles)	$MET = 32.7859\ \exp(-4.9\,f_{MVC})$	0.9957	0.7306
Rohmert (posture 3)	$MET = 0.3001\ f_{MVC}^{-2.803}$	0.9745	0.5353
Rohmert (posture 4)	$MET = 1.2301\ f_{MVC}^{-1.308}$	0.9989	0.7041
Rohmert (posture 5)	$MET = 3.2613\ f_{MVC}^{-1.256}$	0.9984	-0.057

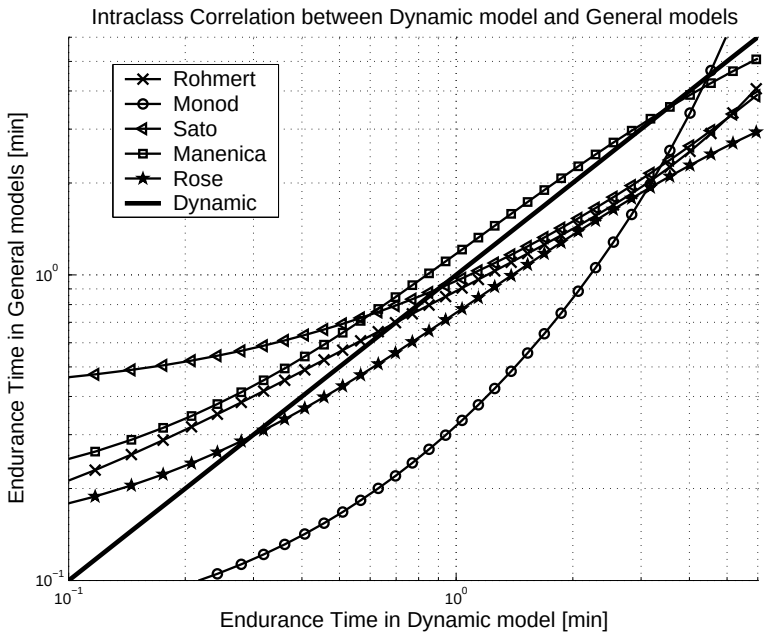

Figure 3.2: *ICC* of general models

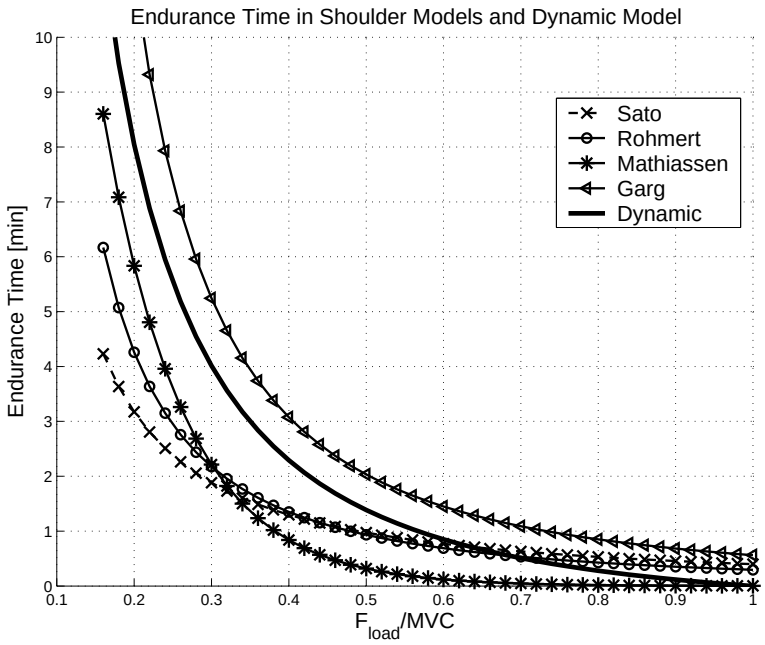

Figure 3.3: Endurance time in shoulder endurance models and dynamic model

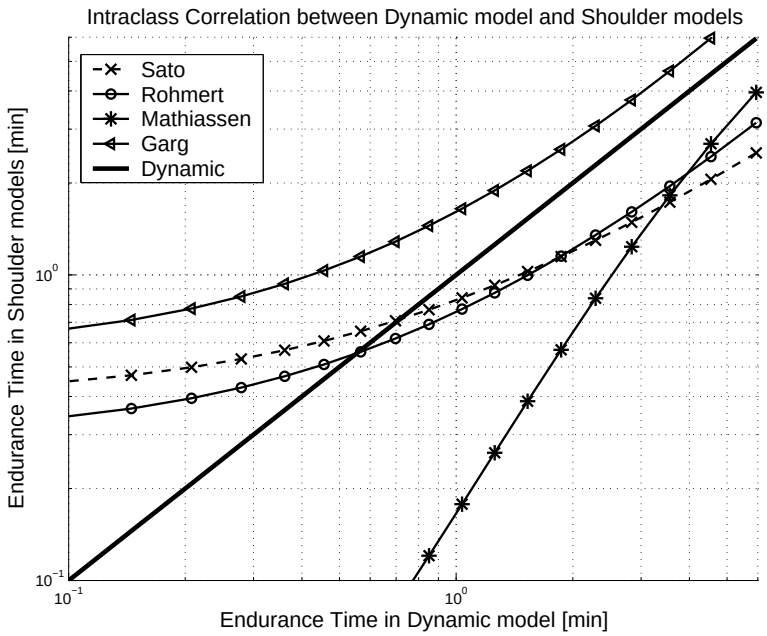

Figure 3.4: *ICC* of shoulder endurance models

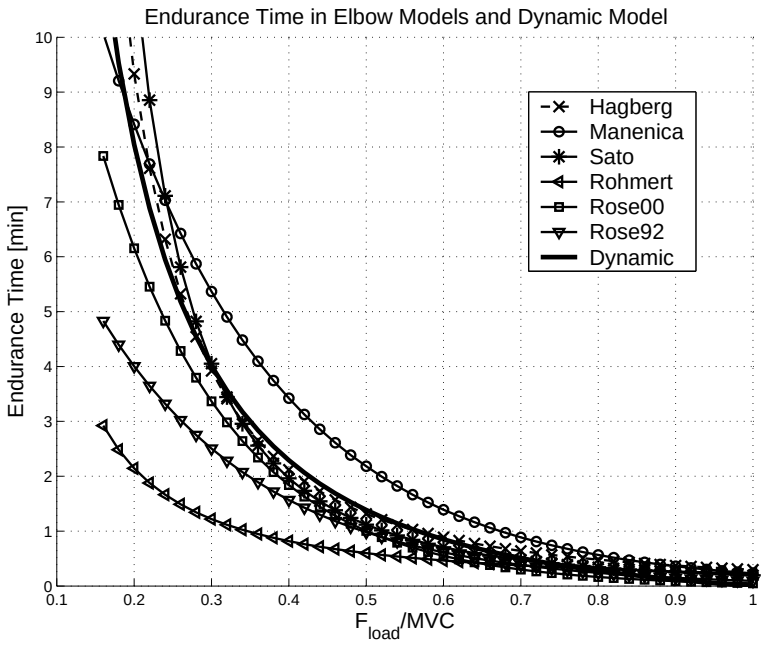

Figure 3.5: Endurance time in elbow endurance models and dynamic model

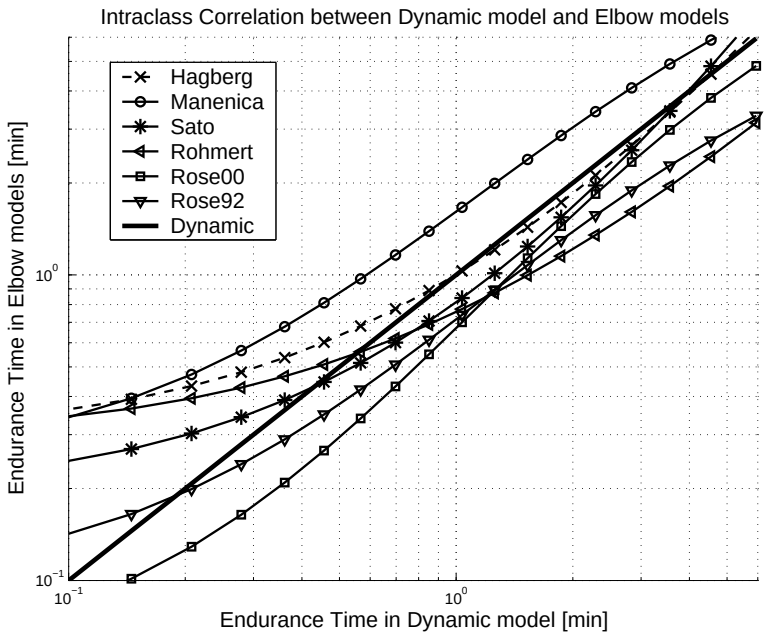

Figure 3.6: *ICC* of elbow endurance models

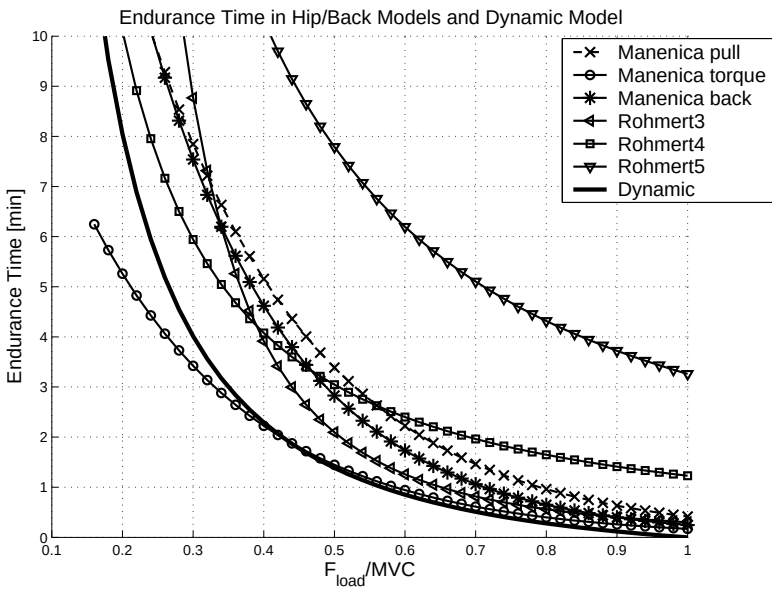

Figure 3.7: Endurance time in hip and back models and dynamic model

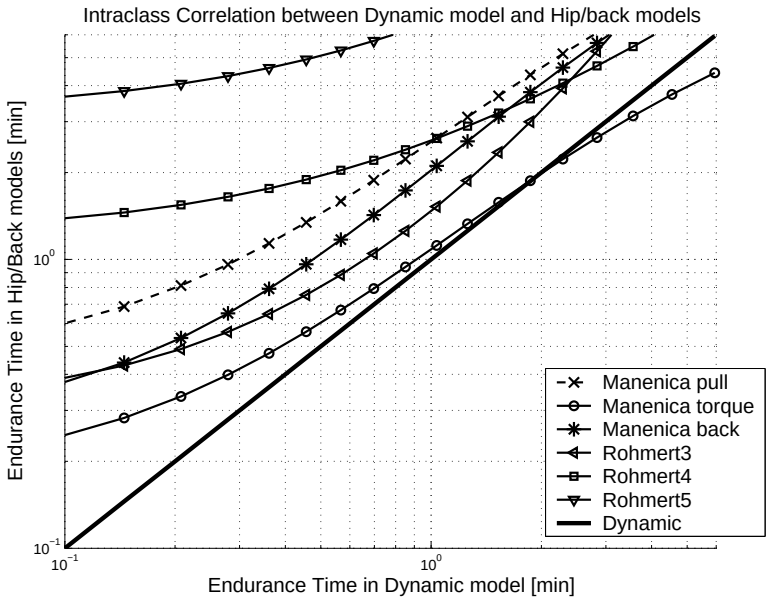

Figure 3.8: *ICC* of hip/back models

3.3.2 Results and discussion

From the comparison results of the static validation, it is obvious that the MET model derived from our dynamic model has an excellent linear correlation with the other experimental static endurance models, and almost all the Pearson's correlation r are above 0.97. Despite the high linear correlation, there are still large differences between the dynamic model and other MET models. These differences mainly include the following influencing factors:

- Experiment methods and model construction: In order to measure the MET, several tools, such as subjective scales and EMG, are involved. The subjective scales and the variability of participants can bring significant differences into the MET result (El ahrache et al., 2006). Furthermore, the MET models are constructed using different mathematical models, mainly power function and negative exponential function. However, the negative exponential function can not describe the two asymptotic tendencies: a tendency towards infinity for low $\%MVC$ and a tendency towards zero for values bordering on $100\%MVC$. In fact, all the parameters of the other MET models are fitted from experimental data, and due to the limitations of sampling amount, the MET models can be quite different, especially for the two extreme $\%MVC$s.

- Muscle group and posture variability: MET models for different muscle groups are different, and the statistical results showed that there is a significant difference between the MET values for the back/hip and the MET values for the upper limbs, for the same $\%MVC$ value (El ahrache et al., 2006). In addition, the MET models are mathematically different even for the same mus-

cle group under different postures. Different muscle groups have different anatomical structure and different complexity. In the same muscle group, the involvement of muscle elements can be changed significantly, which can also explain the signficance between different postures. In the literature (Garg et al., 2002), the influences of shoulder postures were discussed. It indicated that different posture would produce different moments and loads on the same muscle group, thus it would cause different MET curves.

- Interindividual variability: from the figures, it is obvious that the differences of MET values are greater for low $\%MVC$ than those for high $\%MVC$. The significant interindividual differences in MET (El ahrache et al., 2006) can cause the differences.

In ICC column in Table 3.2, it shows high similarity between the dynamic model and several MET models: for elbow and hand models, 5 out of 7 are higher than 0.90; for general models, 3 out of 5 (Huijgens' and Sjogaard's model are not counted) ICC values are higher than 0.85. But it also shows moderate or low similarity with the other MET models, for example, with the back/hip models, ICC varies from -0.057 to 0.9447. The explanation is: ICC correlation is significantly influenced by the complexity of the anatomical structure. In the shoulder and back/hip of the human body, the anatomical structure is in a much more complex way than in the elbows and hands. For this reason, in these experimental models, the measurement of MVC and MET is an overall performance of the complex muscle group, but not MET of an individual muscle or simple muscle group. Meanwhile, even for one muscle group, in Fig. 3.7, the differences between the experimental models for hip/back are greater than the MET models for other muscle groups, e.g. in elbow models (Fig. 3.5). It can also be explained by the complexity of the anatomical structure. In different working conditions (for example, different postures), the engagement of the muscles in the task in the hip/back of the human body plus the contraction of muscles are different as well, which can further influence the experimental result.

In conclusion, the dynamic model was validated by comparing with 24 static MET models. The validated results show high similarity with many of the static MET models, while moderate similarity with a few static MET models, possibly due to complex muscle structure, mathematical function limitation, and measurement condition.

3.4 Validation in comparison to other dynamic models

Validation results in comparison to MET models have shown promising explanations for general static load and even for some specific body parts. However, static procedures are still quite different from dynamic situations, thus our dynamic model needs to be examined alongside the other dynamic

models. To accomplish this objective, we set out to verify our dynamic model through comparison with some existing muscle fatigue models, quantitatively or qualitatively. The results of our effort are as follows.

3.4.1 Comparison with Freund's model

In Freund and Takala (2001), a muscle fatigue model was proposed and integrated into a dynamic model of forearm. In this model, the muscle was treated somewhat like reservoir, and force production capacity S^0 reduces with the time that the muscle is contracted. As shown in Eq. 3.11, S^0 varies between 0 and the upper limits of the muscle force S^l. In this model, the recovery and decay rates depend on $(S^l - S^0)$ and muscle force S. The constants α and β were obtained by fitting the solution using experimental results from static endurance time test. In this model, muscle force is taken into consideration as a factor causing muscle fatigue, and furthermore, muscle force production capacity S^0 was proposed the same as in our dynamic model F_{cem} to describe the capacity of the muscle after performing a certain task. Although in this model, the force production capacity and the muscle force are decoupled with each other, which is different in our model, the same concept was employed to describe the fatigue mechanism of muscle.

$$\frac{\mathrm{d}S^0}{\mathrm{d}t} = \alpha(S^l - S^0) - \beta S \tag{3.11}$$

3.4.2 Comparison with Wexler's model

Wexler's dynamic muscle fatigue model based on Ca^{2+} cross-bridge mechanism can also verify our dynamic model qualitatively. The electrical stimulation to activate skeletal muscle to perform functional movements, and this model can be used to predict the muscle force fatigue under different stimulation frequencies, and the details have been presented in Section 1.3.

The frequency of functional electrical stimulation is to simulate the control commands of CNS for muscle contraction. The higher stimulation frequency, the more muscle motors are activated to generate contraction force, so it represents higher muscle load. From Fig. 3.9, it is clear that the higher the stimulation frequency is, the larger the force can be generated by the muscle. The larger the peak force (higher frequency) is, the faster the curve declines and the quicker the muscle becomes fatigued. This trend is similarly represented in our dynamic model by Eq. 3.2. Figure 3.9 also shows that in the force-time curve with stimulation frequency of 10 Hz, there are oscillations of the force. This has been explained that it is because the force generation capacity is recovered during the interval of the stimulation (Ding et al., 2000a).

Though qualitatively verified, it is impossible to verify our dynamic model with Wexler's model quantitatively due to the way in which Wexler's model was obtained. Wexler's model is experimentally validated in stimulation trials, and all the parameters were calculated from an external stimulation experiment. However, when the muscle is stimulated in an external manner, the motor recruitment mechanism could be different from that controlled by CNS. Using the external manner, all the motor units of the muscle are stimulated simultaneously, creating a larger force than voluntary contraction and fatigue of the muscle happens more rapidly (Vignes, 2004).

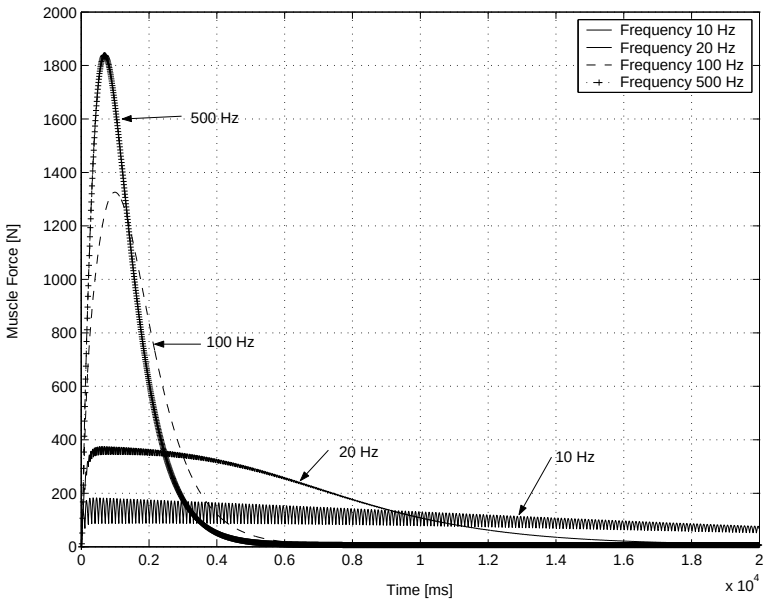

Figure 3.9: Maximum exertable force and time relationship in Wexler's Model. Frequency: simulation frequency

3.4.3 Comparison with Liu's model

In Liu et al. (2002), the dynamic model of muscle activation, fatigue and recovery was proposed. This model is based on biophysical mechanisms: motor units pattern, and the details have been presented in Section 1.3.

When $t = 0$ under the initial conditions of $M_A = 0$, $M_F = 0$, $M_{uc} = M_0$, we can have Eq. 3.12 and Eq. 3.13.

$$\begin{aligned}\frac{M_A(t)}{M_0} &= \frac{\gamma}{1+\gamma} + \frac{\beta}{(1+\gamma)(\beta-1-\gamma)}e^{-(1+\gamma)Ft} \\ &\quad - \frac{\beta-\gamma}{\beta-1-\gamma}e^{-\beta Ft}\end{aligned} \tag{3.12}$$

$$\frac{M_{uc}(t)}{M_0} = e^{-\beta Ft} \tag{3.13}$$

In the new dynamic fatigue model, we assume that there is no recovery during physical work, and the workers are trying their best to finish the task which means the brain effort is infinitely high. In this assumption, we set γ=0 and $\beta \rightarrow \infty$, then Equation 3.14 represents the motor units which are not fatigued in the muscle. The activated motor units $M_A(t)/M_0$ and the motor units at rest $M_{uc}(t)/M_0$ represent the relative muscle force capacity. We can simplify the sum of Eq. 3.12 and 3.13 to Eq. 3.14 which do have the same form as our dynamic model Eq. 3.5.

$$\begin{aligned}\frac{M_A(t)}{M_0} + \frac{M_{uc}(t)}{M_0} &= \frac{\gamma}{1+\gamma} + \frac{\beta}{(1+\gamma)(\beta-1-\gamma)} e^{-(1+\gamma)Ft} \\ &+ \frac{1}{\beta-1-\gamma} e^{-\beta Ft} = e^{-Ft}\end{aligned} \tag{3.14}$$

This fatigue model has been experimentally verified in Liu et al. (2002). In the experiment, each subject performed an MVC of the right hand by gripping a hand grip device for 3 min. It was found that the fitting curve from the experimental result has almost the same curve as our model in MVC condition (Fig. 3.10). In this model, F and R are assumed to be constant for an individual under MVC working conditions. There is no experimental result for F and R under the other load situations, thus this muscle fatigue model can only verify our model in the MVC condition.

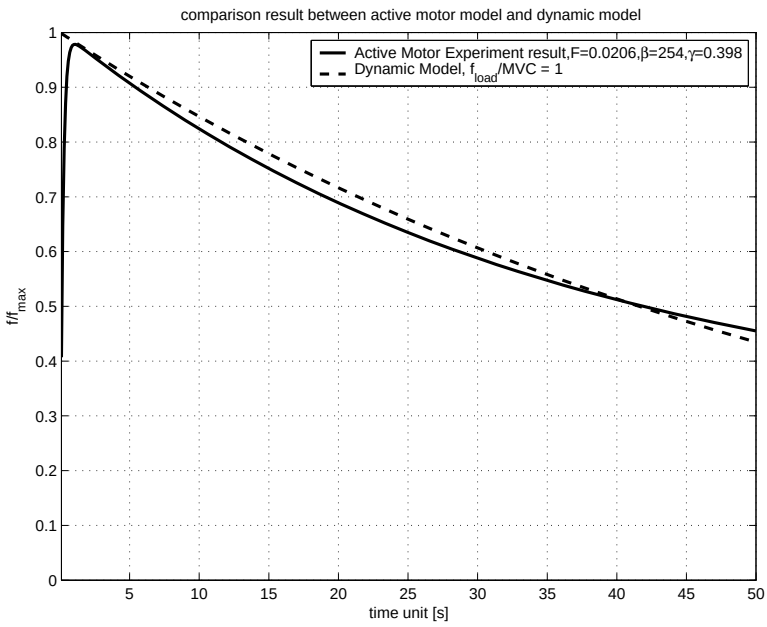

Figure 3.10: Comparison between the experimental result of the active motor model and dynamic model in the maximum effort

3.4.4 Discussion

Through the comparison, our dynamic model is either qualitatively or quantitatively verified with the other three existing muscle fatigue models. The fatigue model for the forearm used the same concept as in our fatigue model: the muscle force capacity is related to muscle force with time. Wexler's model based on Ca^{2+} cross-bridge shows the reduction of the muscle force with time under different stimulation frequencies and the reduction of the muscle capacity shows the same trend as in our muscle fatigue model. In comparison to the active motor model, the muscle force can be expressed in the same form under extreme situation. Yet in the active motor model, only parameters are available for a MVC case. The active motor model does not supply further validation for other load situations, therefore experimental validation is necessary to confirm the applicability of our fatigue model.

3.5 Fatigability of different muscle groups

In the theoretical analysis, external load F_{load}, time t, and personal strength factors MVC have been used to construct the fatigue model. In our model, another important factor is individual fatigability k. This parameter describes the susceptibility to fatigue or the tendency to get tired or lose strength. In order to assess the physical fatigue, personal strength and personal fatigability are two determinant parameters for ergonomic application.

3.5.1 Regression for determining the fatigability

In Section 3.3, ICC and r were calculated and listed under the condition where the rate of fatigue $k = 1\ min^{-1}$. ICC are noted as ICC_1 in Table 3.3 in order to facilitate the comparison. There are still large differences from 1 in ICC_1 column, which means that the dynamic model cannot fit perfectly the MET models for different muscle groups, so it is necessary to determine the parameter k in order to extend the availability of the dynamic model for different muscle groups.

From Table 3.2, it is observed that almost all the static MET models have high linear relationship with the dynamic model (for most models, $r > 0.95$), which means that each static model can be described mathematically by a linear equation (Eq. 3.15). In Eq. 3.15, x is used to replace f_{MVC} and $p(x)$ represents the dynamic MET model in Eq. 3.8. m and n are constants describing the linear relationship between an existing MET model and the dynamic model, and they are needed to be determined in linear regression. It should be noticed that $m = 1/k$ indicates the fatigue resistance of the static model, and k is fatigue ratio or fatigability of different static model.

$$f(x) = m\,p(x) + n \tag{3.15}$$

Due to the asymptotic tendencies of the MET models mentioned in El ahrache et al. (2006), when $x \rightarrow 1$ ($\%MVC \rightarrow 100$), $f(x) \rightarrow 0$ and $p(x) \rightarrow 0$ ($MET \rightarrow 0$), therefore, we can assume that $n = 0$. For this reason, only one parameter m needs to be determined. Since some MET models are not available for $\%MVC$ under 15%, the regression was carried out in the interval from $x = 0.16$ to $x = 0.99$. With a space 0.01, $N = 84$ MET values were calculated to determine the parameter m by minimizing the function in Eq. 3.16.

$$M(x) = \sum_{i=1}^{N} (f(x_i) - m\,p(x_i))^2 = a\,m^2 + b\,m + c \tag{3.16}$$

In Eq. 3.16, $a = \sum_{i=1}^{N} p(x_i)^2$ is always greater than 0, and $b = -2\sum_{i=1}^{N} p(x_i) f(x_i)$ is always less than 0, therefore m can be calculated by Eq. 3.17.

$$m = \frac{-b}{2a} = \frac{\sum_{i=1}^{N} p(x_i) f(x_i)}{\sum_{i=1}^{N} p(x_i)^2} > 0 \tag{3.17}$$

After regression for each MET model, new ICC values were calculated by comparing $f(x)/m$ and $p(x)$, and they are listed in the column ICC_2 of Table 3.3. It should be mentioned that the regression does not change the r correlation, and the explanation can be found in Eq. 3.18. For this reason, only ICC is recalculated.

$$r_{regress} = \frac{\sum_n (A_n - \bar{A})(mB_n - m\bar{B})}{\sqrt{\sum_n (A_n - A)^2 \sum_n (mB_n - mB)^2}} = r \tag{3.18}$$

3.5.2 Results and discussion

Regression results

Both of the correlations before regression ICC_1 and after regression ICC_2 are shown in Table 3.3. It should be noticed that the results ICC_1 before regression in Table 3.2 were a little different from the results presented in Section 3.3, because the range of f_{MVC} varies from 0.15 to 0.99 in this section while it varied from 0.20 to 0.99 in Section 3.3 in order to validate the dynamic fatigue model. Some models were sensitive for such a change, e.g. Monod's model. However, the little change of the validation result does not change the conclusion in Section 3.3.

Almost all the ICC_2 are greater than 0.89, and only one is an exception (Monond and Scherrer, 0.4736). This exception is because of its relative worse linear correlation r with the dynamic MET model, while almost all the other ones have r over 0.96, and the Monod's model has only 0.6241. For the Monod's model, the linear error occurs mainly when the f_{MVC} approaches to 0.15. This error is

mainly caused by the way in which the Monod's model is formulated. This exception was eliminated in the following analysis and discussion.

The *ICC* results are also graphically presented in log-log diagram from Fig. 3.11 to 3.18. The straight solid line is the comparison result between the dynamic model and itself. For the other models, the one which is more approach to the straight line has a higher *ICC*. There are larger differences between the dynamic model and the existing MET models, especially when the f_{MVC} approaches to 0.15. Those differences can be explained by the interindividual difference in MET, and these differences are greater for the low %MVC (El ahrache et al., 2006). From the graphical representation, it can be noticed that the MET errors are mainly decreased in the range from 10^0 *min* to 10^1 *min*, which means the dynamic model after regression can predict MET with less error than before regression.

The greatest improvement of the fitness between the dynamic model and the MET models is the Hip/Back model (Fig. 3.17 and 3.18). This approves that the dynamic model with a suitable fatigue ratio can adapt itself well to the most complex part of human body. The same improvement can be found for shoulder models and most of the elbow models. It should be noticed not all the MET models have been improved after the regression. Little fall can be found for the MET models (hand model) with *ICC* over 0.98 in the ICC_1 column. The possible reason is that it has already high *ICC* correlation, and the regression does not improve its fitness. However, those models after regression still have high *ICC* (> 0.95). As a summary, the regression approach achieves high *ICC* and improves the similarity between the dynamic model and the existing models. This proves that the dynamic model can be adapted to fit different body parts, and the dynamic model can predict the MET for static cases.

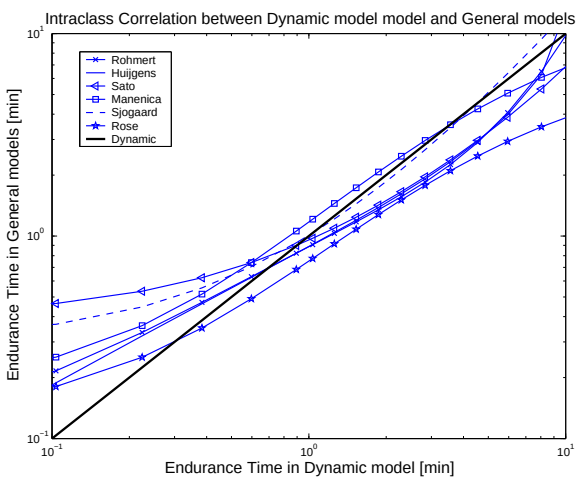

Figure 3.11: ICC diagram for MET general models before regression

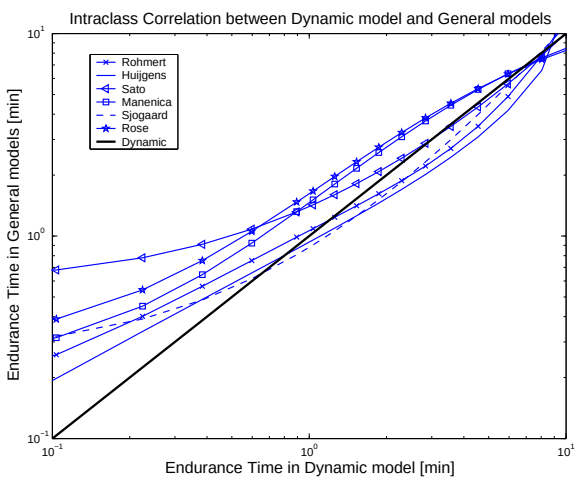

Figure 3.12: ICC diagram for MET general models after regression

Table 3.3: Static validation results r and ICC between the new model and the other existing MET models in the literature (El ahrache et al., 2006)

Model	MET equations (in minutes)	r	ICC_1	ICC_2
General models				
Rohmert	$MET = -1.5 + \frac{2.1}{f_{MVC}} - \frac{0.6}{f_{MVC}^2} + \frac{0.1}{f_{MVC}^3}$	0.9717	0..9505	0.9707
Monod and Scherrer	$MET = 0.4167\,(f_{MVC} - 0.14)^{-2.4}$	0.6241	0.0465	0.4736
Huijgens	$MET = 0.865\left[\frac{1-f_{MVC}}{f_{MVC}-0.15}\right]^{1/1.4}$	0.9036	0.8947	0.8916
Sato et al.	$MET = 0.3802\,(f_{MVC} - 0.04)^{-1.44}$	0.9973	0.8765	0.9864
Manenica	$MET = 14.88\ \exp(-4.48\,f_{MVC})$	0.9829	0.9357	0.9701
Sjogaard	$MET = 0.2997\ f_{MVC}^{-2.14}$	0.9902	0.9739	0.9898
Rose et al.	$MET = 7.96\ \exp(-4.16\,f_{MVC})$	0.9783	0.6100	0.9573
Upper limbs models				
Shoulder				
Sato et al.	$MET = 0.398\ f_{MVC}^{-1.29}$	0.9988	0.5317	0.9349
Rohmert et al.	$MET = 0.2955\ f_{MVC}^{-1.658}$	0.9993	0.7358	0.8982
Mathiassen and Ahsberg	$MET = 40.6092\ \exp(-9.7\,f_{MVC})$	0.9881	0.8673	0.9711
Garg	$MET = 0.5618\ f_{MVC}^{-1.7551}$	0.9968	0.9064	0.9947
Elbow				
Hagberg	$MET = 0.298\ f_{MVC}^{-2.14}$	0.9902	0.9751	0.9898
Manenica	$MET = 20.6972\ \exp(-4.5\,f_{MVC})$	0.9832	0.9582	0.9708
Sato et al.	$MET = 0.195\ f_{MVC}^{-2.52}$	0.9838	0.9008	0.9688
Rohmert et al.	$MET = 0.2285\ f_{MVC}^{-1.391}$	0.9997	0.2942	0.9570
Rose et al.2000	$MET = 20.6\ \exp(-6.04\,f_{MVC})$	0.9958	0.9627	0.9708
Rose et al.1992	$MET = 10.23\ \exp(-4.69\,f_{MVC})$	0.9855	0.7053	0.9766
Hand				
Manenica	$MET = 16.6099\ \exp(-4.5\,f_{MVC})$	0.9832	0.9840	0.9646
Back/hip models				
Manenica (body pull)	$MET = 27.6604\ \exp(-4.2\,f_{MVC})$	0.9789	0.7672	0.9591
Manenica (body torque)	$MET = 12.4286\ \exp(-4.3\,f_{MVC})$	0.9804	0.8736	0.9634
Manenica (back muscles)	$MET = 32.7859\ \exp(-4.9\,f_{MVC})$	0.9878	0.8091	0.9819
Rohmert (posture 3)	$MET = 0.3001\ f_{MVC}^{-2.803}$	09655	0.4056	0.9482
Rohmert (posture 4)	$MET = 1.2301\ f_{MVC}^{-1.308}$	0.9990	0.8356	0.9396
Rohmert (posture 5)	$MET = 3.2613\ f_{MVC}^{-1.256}$	0.9984	0.1253	0.9263

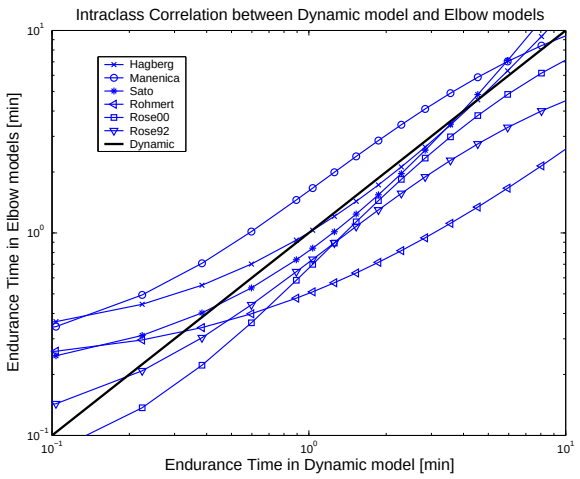

Figure 3.13: ICC diagram for MET elbow models before regression

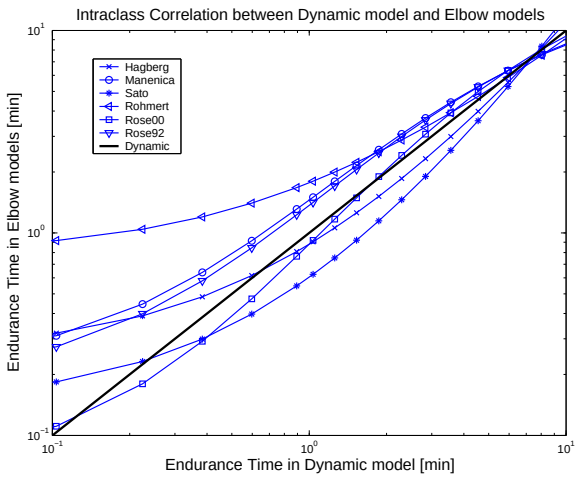

Figure 3.14: ICC diagram for MET elbow models after regression

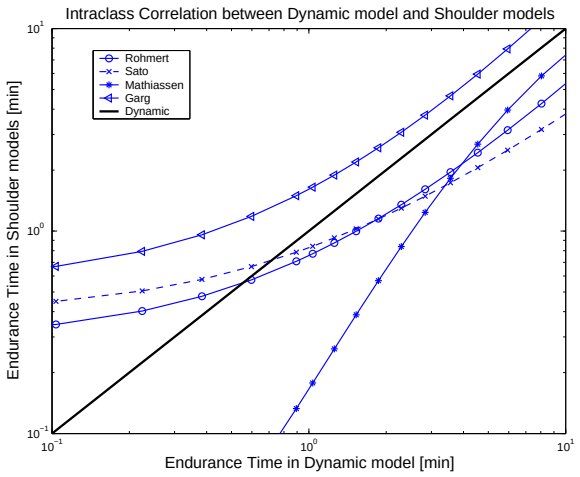

Figure 3.15: ICC diagram for MET shoulder models before regression

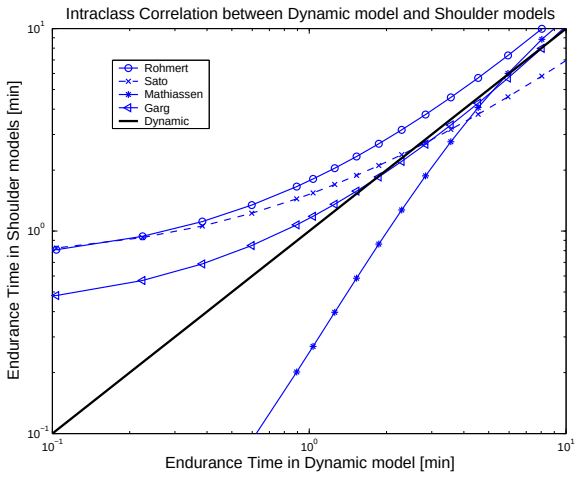

Figure 3.16: ICC diagram for MET shoulder models after regression

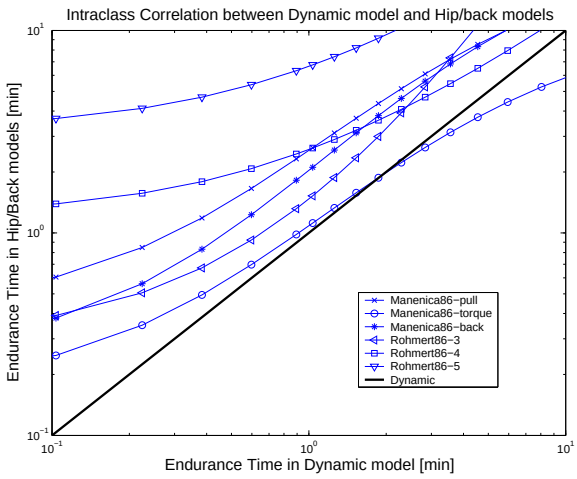

Figure 3.17: ICC diagram for hip/back shoulder models before regression

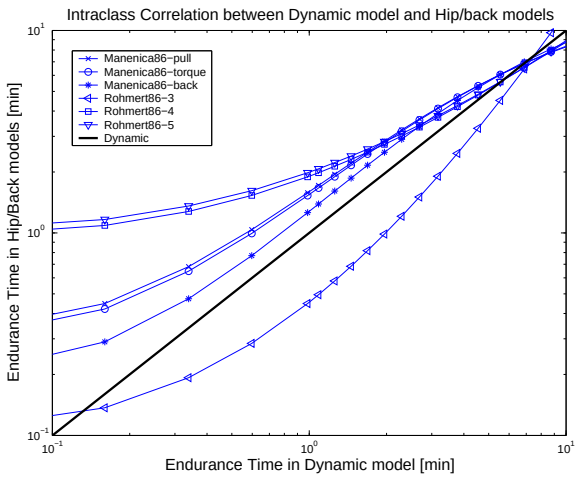

Figure 3.18: ICC diagram for hip/back shoulder models after regression

Fatigue resistance results

The regression results (m) for each MET model are listed in Table 3.4. The mean value $\bar{m}$ and the standard deviation σ_m were calculated for different muscle groups as well. The Monod's general model is eliminated from the calculation due to its poor ICC value. The intergroup differences are represented by the mean value of each muscle group. The Hip/back models have a higher mean value $\bar{m} = 1.9701$, while the other human body segments and the general models have relative lower fatigue resistances ranging from 0.76 to 0.90, without big differences. The fluctuation in each muscle group, namely the intra muscle group difference, is presented by σ_m. The stability in the general group is the best, and the hip/back model has the largest variation. There is no big difference between elbow and shoulder models.

The regression result of the fatigue resistance of different muscle groups were tested with normplot function in Matlab in order to graphically assess whether the fatigue resistances could come from a normal distribution, since the characteristic of the fatigue resistance might be very important for evaluating the fatigue of a given population. The test result shows fatigue resistances for general models and elbow models scatter near the diagonal line in Fig. 3.19 and Fig. 3.20. Due to limitation of sample numbers in shoulder models and the large variance in hip/back models, the distribution test did not achieve satisfying result. Once there are enough sample models, it can be extrapolated that the fatigue resistances for different muscle groups for the overall population distributes in normal probability, therefore, the mean value locates in $\bar{m} \pm \sigma$ could predict the fatigue property of 50% percentile of a given population.

Table 3.4: Fatigue resistance m of different MET models

Segment	m_1	m_2	m_3	m_4	m_5	m_6	m_7	$\bar{m}$	σ_m
General	Rohm.	Mono.	Hijg.	Sato.	Mane.	Sjog.	Rose		
	0.8328	-	0.9514	0.6836	0.8019	1.1468	0.4647	0.8135	0.2320
Shoulder	Sato.	Rohme.	Math.	Garg					
	0.4274	0.545	0.698	1.3926				0.7562	0.4347
Elbow	Hagb.	Mane.	Sato.	Rohm.	Rose00	Rose92			
	1.1403	1.1099	1.3461	0.2842	0.7616	0.5234		0.8609	0.4079
Hand	Mane.								
	0.8907							0.8907	-
Hip	pull	torq.	back	pos3	pos4	pos5			
	1.5986	0.7005	1.5931	3.2379	1.356	3.3345		1.9701	1.1476

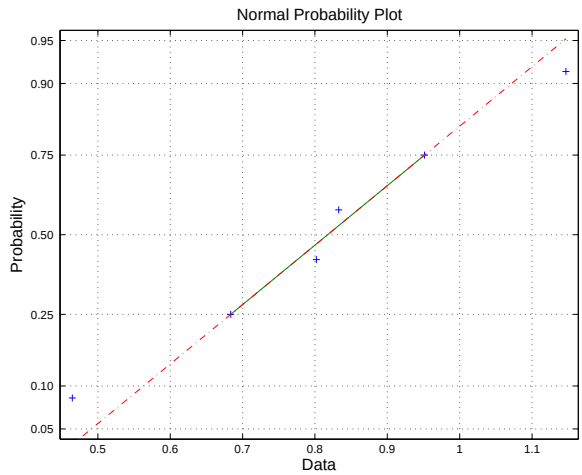

Figure 3.19: Normal distribution test for the general model

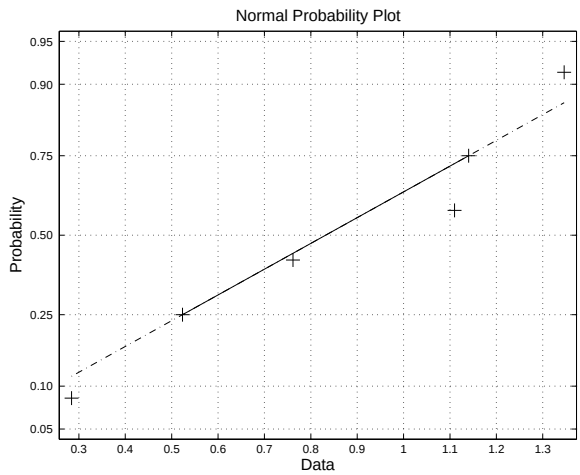

Figure 3.20: Normal distribution test for the elbow model

Therefore, the mean value of $\bar{m}$ and its standard deviation σ_m are used to redraw the relation between MET and f_{MVC}, and they are presented from Fig. 3.21 to 3.24. The black bold solid line is the dynamic model adjusted by $\bar{m}$ and it locates in the range constrained by two slim solid lines adjusted by $\bar{m} \pm \sigma_m$. After adjusting our fatigue model with $\bar{m} \pm \sigma_m$, the dynamic fatigue model can cover most of the existing MET models from 15% MVC to 80% MVC. Although there is an exception in Hip/back model due to the relative large variability in hip muscle groups, it should also be admitted that the adjustment makes the dynamic model suitable for most of the static cases. In another word, the adjustment by mean and deviation makes the dynamic model suitable for evaluating the fatigue for the overall population.

The prediction by the dynamic model cannot cover the models for the %MVC over 80 as well as the interval under 80%. However in the industrial cases, it is very rare that the force demande can cross that limit. Meanwhile, the prediction error is smaller than one minute in such range, normally less than 1 minute.

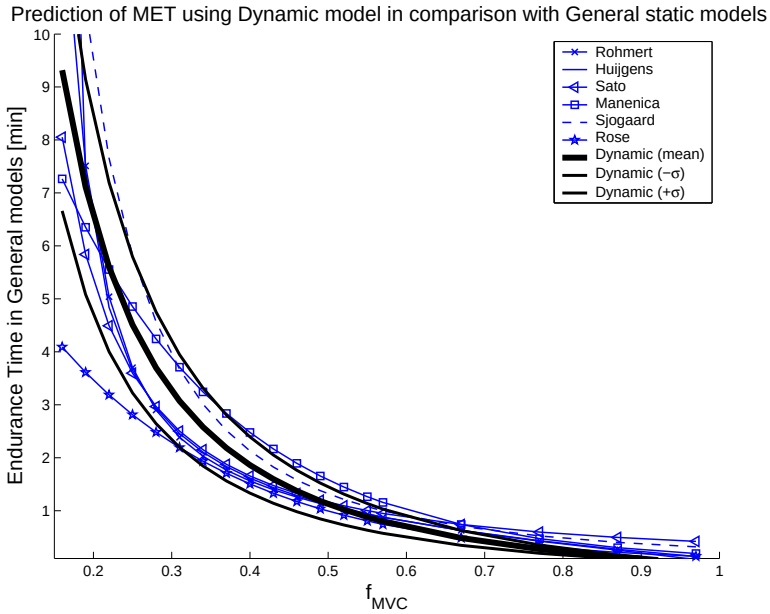

Figure 3.21: MET prediction using Dynamic model in comparison with general static models

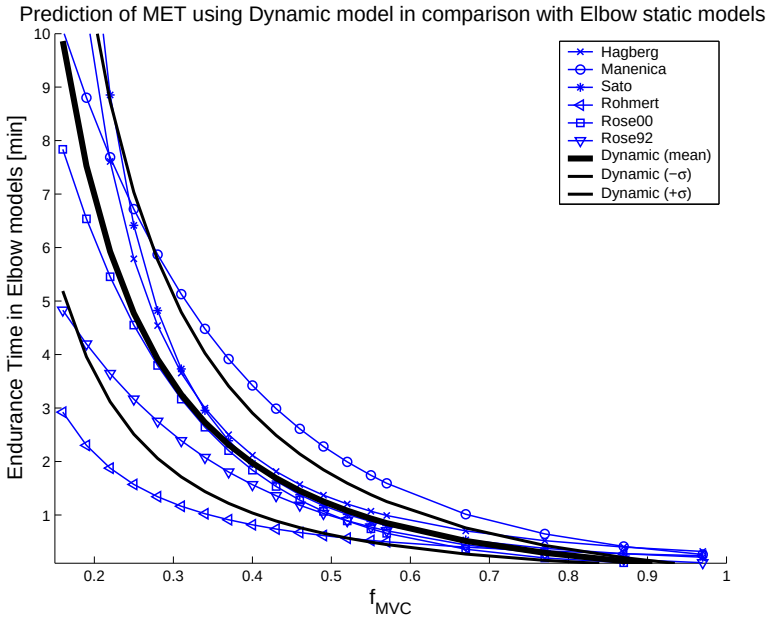

Figure 3.22: MET prediction using Dynamic model in comparison with elbow static models

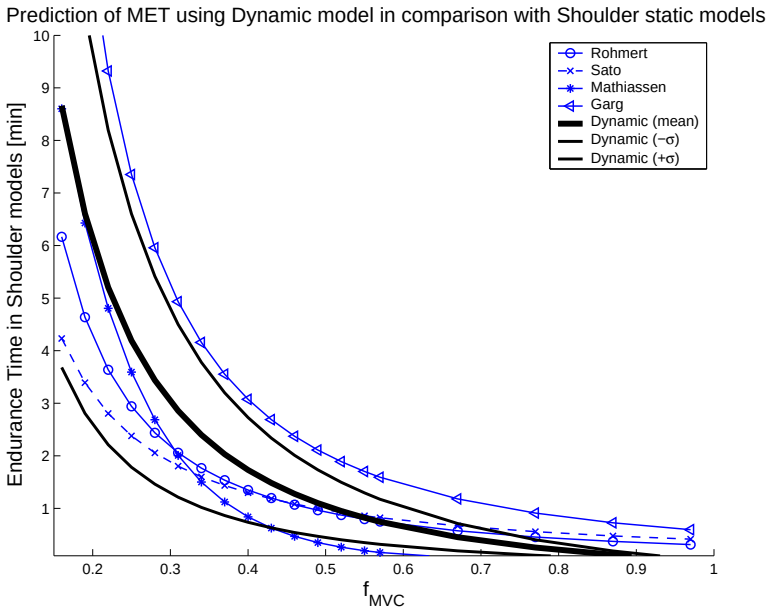

Figure 3.23: MET prediction using Dynamic model in comparison with shoulder static models

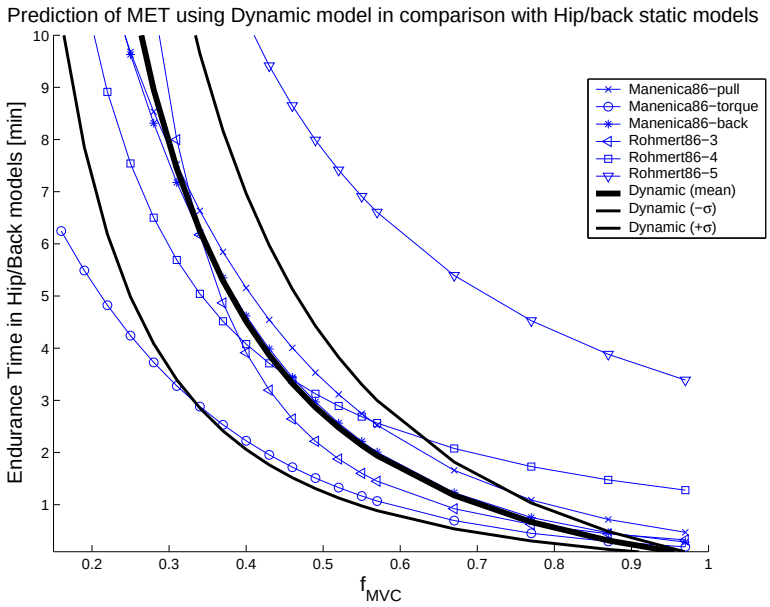

Figure 3.24: MET prediction using Dynamic model in comparison with hip/back static models

3.5.3 Discussion on fatigue resistance

Although the MET models fitted from experiment data were formulated in different forms, the m can still provide some useful information for the fatigue resistance, especially for different muscle groups. The differences in fatigue resistance result is possible to be concluded by the mean value and the deviation, but it is still interesting to know why and how the fatigue resistance is different in different muscle groups, in the same muscle group, and even in the same person at different period.

There is no doubt that there are several factors influencing the fatigue resistance of a muscle group, and it should be very useful if the fatigue resistance of different muscle groups can be mathematically modeled. In this section, the fatigue resistance and its variability are going to be discussed in details based on the fatigue resistance results from Table 3.4 and the previous literature about fatigability. Different influencing factors are going to be discussed and classified in this section.

All the differences inter muscle groups and intra muscle groups in MET models can be classified into four types: 1) Systematic bias, 2) Fatigue resistance inter individual for constructing a MET model, 3) Fatigue resistance intra muscle group: fatigue resistance differences for the same muscle group, and 4) Fatigue resistance inter muscle groups: fatigue resistance differences for different muscle groups. Those differences can be attributed to different physiological mechanisms involved in different tasks, and influencing variables are subject motivation, central command, intensity and duration of the activity, speed and type of contraction, and intermittent or sustained activities (Enoka, 1995; Elfving and Dedering, 2007). In those MET models, all the contractions were exerted under static conditions until exhaustion of muscle groups, therefore, several task related influencing factors can be neglected in the discussion, e.g., speed and duration of contraction. The other influencing factors might contribute to the fatigue resistance difference in MET models.

Systematic bias : all the MET models were regressed or reanalyzed based on experiment results. Due to the experimental background, there were several sources for systematic error. One possible source of the systematic bias comes from experimental methods and model construction (El ahrache et al., 2006), especially for the methods with subjective scales to measure MET. The subjective feelings significantly influenced the result. Furthermore, the construction of the MET model might cause system differences for MET model, even in the models which were constructed from the same experiment data (e.g. Huijgens' model and Sjogaard's model in General models). The estimation error was different while using different mathematic models, and it generates systematic bias in the result analysis.

Fatigue resistance inter individual : besides the systematic error, another possible source for the endurance difference is from individual characteristic. However, the individual characteristic is too complex to be analyzed, and furthermore, the individual characteristic is impossible to be separated from existing MET models, since the MET models already represent the overall performance of the sample participants. In addition, in ergonomic application, the overall performance of a population is often concerned. Therefore, individual fatigue resistance is not discussed in this part separately, but the differences in population in fatigue resistance are going to be discussed and presented in the following part.

Fatigue resistance intra muscle group : the inter individual variability contributes to the errors

in constructing MET models and the errors between MET models for the same muscle group. The influencing factors on the fatigue resistance can be mainly classified into sample population characteristic (gender, age, and job), personal muscle fiber composition, and posture.

The influences on fatigability from gender and age were observed in the literature. In the research for gender influence, women were found with more fatigue resistance than men. Based on muscle physiological principle, four families of factors were adopted to explain the fatigability difference in gender in Hicks et al. (2001). They are: 1) muscle strength (muscle mass) and associated vascular occlusion, 2) substrate utilization, 3) muscle composition and 4) neuromuscular activation patterns. It concluded that although the muscle composition differences between men and women is relatively small (Staron et al., 2000), the muscle fiber type area is probably one reason for fatigability difference in gender, since the muscle fiber type I occupied significantly larger area in women than in men (Larivière et al., 2006). In spite of muscle fiber composition, the motor unit recruitment pattern acts influences on the fatigability as well. The gender difference in neuromuscular activation pattern was found and discussed in Larivière et al. (2006), and it was observed significantly that females showed more alternating activity between homolateral and contralateral muscles than males.

Meanwhile, in Mademli and Arampatzis (2008), older men were found with more endurance time then young men in certain fatigue test tasks charging with the same relative load. One of the most common explanations is changes in muscle fiber composition for fatigability change while aging. The shift towards a higher proportion of muscle fiber type I leads old adults having a higher fatigue resistance but smaller MVC. Gender and age were also already taken into a regression model to predict shoulder flexion endurance (Mathiassen and Ahsberg, 1999).

Besides those two reasons, the muscle fiber composition of muscle varies individually in the population, even in a same age range and in the same gender (Staron et al., 2000), and this could cause different performances in endurance tasks. Different physical work history might change the endurance performance. For example, it appeared that athletes with different fiber composition had different advantages in different sports: more type I muscle fiber, better in prolonged endurance events (Wilmore et al., 2008). Meanwhile, the physical training could also cause shift between different muscle fibers (Costill et al., 1979). As a result, individual fatigue is very difficult to be determined using MET measurement (Vøllestad, 1997), and the individual variability might contribute to the differences among MET models for the same muscle group due to selection of subjects.

Back to the existing MET models, the sample population was composed of either a single gender or mixed. At the same time, the number of the subjects was sometimes relative small. For example, only 5 female students (age range 21–33) were measured (Garg et al., 2002), while 40 (20 males, age range 22–48 and 20 females, age range 20–55) were tested in shoulder MET model (Mathiassen and

Ahsberg, 1999). Meanwhile, the characteristics of population (e.g., students, experiences workers) could cause some differences in MET studies. Due to different population selection method, different gender composition, and different sample number of participant, fatigue resistance for the same muscle group exists in different experiment results and finally caused different MET models under the similar postures.

In Hip/back models, even with the same sample participants, difference existed also in MET models for different postures. The variation is possibly caused by the different MU recruitment strategies and load sharing mechanism under different postures. Kasprisin and Grabiner (2000) observed that the activation of biceps brachii was significantly affected by joint angle, and furthermore confirmed that joint angle and contraction type contributed to the distinction between the activation of synergistic elbow flexor muscles. The moment arm of each individual muscle changes along different postures which results in different intensity of load for each muscle and then causes different fatigue process for different posture. Meanwhile, the contraction type of each individual muscle might be changed under different posture. Both contraction type change and lever differences contribute to generate different fatigue resistance globally. In addition, the activation difference was also found in antagonist and agonist (Karst and Hasan, 1987; Mottram et al., 2005) muscles as well, and it is implied that in different posture, the engagement of muscles in the action causes different muscle activation strategy, and as a result the same muscle group could have different performances. With these reasons, it is much difficult to indicate the contribution of posture in fatigue resistance because it refers to the sensory-motor mechanism of human, and how the human coordinates the muscles remains not clear enough until now.

Fatigue resistance inter muscle groups: As stated before, the three different muscle fiber types have different fatigue resistances, and different muscle is composed of types of muscles with composition determining the function of each muscle (Chaffin et al., 1999). The different fatigue resistance can be explained by the muscle fiber composition in different human muscle groups.

In the literature, muscle fiber composition was measured by two terms: muscle fiber type percentages and percentage fiber type area (CSA: cross section area). Both terms contribute to the fatigue resistance of the muscle groups. Type I fibers occupied 74% of muscle fibers in the thoracic muscles, and they amounted 63% in the deep muscles in lumbar region (Sirca and Kostevc, 1985). On average type I muscle fibers ranged from 23 to 56% for the muscles crossing the human shoulder and 12 of the 14 muscles had average SO proportions ranging from 35 to 50% (Dahmane et al., 2005). In Staron et al. (2000) and Shepstone et al. (2005), the muscle fiber composition shows the similar composition for the muscle around elbow and vastus lateralis muscle and the type I muscle fibers have a proportion from 35 - 50% in average. Although we cannot determine the relationship between the muscle type

composition and the fatigue resistance directly and theoretically, the composition distribution among different muscle groups can explain the MET differences between general, elbow models and back truck models. In addition, the fatigue resistance of older adults greater than young ones could also be explained by a shift towards a higher proportion of type I fiber composition with aging. These evidences meet the physiological principle of the dynamic muscle fatigue model.

Another possible reason is the loading sharing mechanism of muscles. Hip and back muscle group has the maximum joint moment strength (Chaffin et al., 1999) among the important muscle groups. For example, the back extensors are composed of numerous muscle slips having different moment arms and show a particularly high resistance to fatigue relative to other muscle groups (Jorgensen, 1997). This is partly attributed to favorable muscle composition, and the variable loading sharing within back muscle synergists might also contribute significantly to delay muscle fatigue.

In summary, individual characteristics, population characteristics, and posture are external appearance of influencing factors for the fatigue resistance. Muscle fiber composition, muscle fiber area, and sensory motor coordination mechanism are the determinant factors inside the human body deciding the fatigue resistance of muscle group. Therefore, how to construct a bridge to connect the external factors and internal factors is the most important way for modeling the fatigue resistance for different muscle groups. How to combine those factors to model the fatigue resistance remains a challenging work. Despite the difficulty of modeling the fatigue resistance, it is still applicable to find the fatigue resistance for a specified population by MET experiments in regression with the dynamic static MET model due to its simplicity and universal availability.

3.5.4 Limitations

In the previous discussion, the fatigue resistance of the existing MET models were quantified using m from regression. The possible reasons for the different fatigue resistance were analyzed and discussed. However, how to quantify the influence from different factors on the fatigue resistance remains unknown due to the complexity of muscle physiology and the correlation among different factors.

The availability of the dynamic MET model in the interval under 15% MVC is not validated. The fatigue resistance is only accounted from the 15% to 99% MVC due to the unavailability of some MET models under 15% MVC. For the relative low load, the individual variability under 15% could be much larger than that over 15%. The recovery effect might play a much more significant role within such a range.

3.6 Summary

In this chapter, a simple muscle fatigue model has been presented taking account of external physical factors and personal factors. This model can be well explained in muscle physiology and it is validated in both static case in comparison with the MET models and in dynamic case in comparison with dynamic models.

This model is further generalized to determine the fatigue resistance of different muscle groups. They were calculated by linear regression from the new fatigue model and the existing MET static models. Higher *ICC* has been obtained by regression which proves that our fatigue model can be generalized to predict MET for different muscle groups. Mean and standard deviation in fatigue resistance for different muscle groups were calculated, and it is possible to use both together to predict the MET for a certain population. The possible reasons responsible for the variability of fatigue resistance were discussed based on the muscle physiology.

Our fatigue model is relative simple and computationally efficient. With the dynamic model it is possible to carry out the fatigue evaluation in virtual human modeling and ergonomic application, especially for static and quasi-static cases. The fatigue effect of different muscle groups can be evaluated by fitting k from several simple static experiments for certain population.

Chapter 4

Muscle fatigue model: experimental validation

Contents

4.1 Introduction 67
4.2 Material and methods 69
4.3 The fatigue model and regression 74
4.4 Results 77
4.5 Discussion 84
4.6 Summary 86

4.1 Introduction

Human intervention is often engaged in most occupational activities, especially in assembly and maintenance tasks. In such cases, muscular strengths are necessary to exert enough forces and torques to operate equipments and sustain external loads. The physical capacity to perform mechanical tasks is determined by the individual ability to exert muscular strength. Insufficient strength can lead to overexertion of the muscle skeleton system and consequent injury (Mital and Kumar, 1998). Insufficient strength can result from physical fatigue in a continuous working process.

A decrease of maximal physical output is observed in the operation with a submaximal force, either in a continuous way or in an intermittent work (Wood et al., 1997; Mital and Kumar, 1998). The decrease in maximum force output is caused by muscle fatigue, which has been defined as “any exercise-induced reduction in the capacity to generate force or power output ” (Vøllestad, 1997) in Section 1.3 . Muscle fatigue leads to the decrease of the force output, generates more risks of overexertion, and furthermore results in musculoskeletal disorders (MSDs).

In general, two approaches have been used to assess fatigue quantitatively and schedule the work-rest allowance.

One approach is the maximum endurance time (MET) and work-rest allowance model approach. MET assesses the fatigue based on the maximal duration of an exerted force at a present level. Hereafter work-rest allowances can be further determined according to the actual holding time and the predicted recovery time in work-rest allowance models on the basis of MET models. El ahrache and Imbeau (2009) reported four work-rest allowance tools. Substantial differences for designing the rest period have been found among these models. The differences in work-rest allowance tools result from different approaches in building up the models, such as different subject groups, different fatigue measurement methods, etc. In comparison with the differences in MET models, the work-rest allowance tools lack accordance with each other. In other words, the recovery model is not well established in work-rest allowance tools. Furthermore, although the MET models can predict the endurance time for a given force level in static postures, the decrease of the physical capacity is not predictable in these models.

The other approach is trying to model the decrease of the physical strength in successive work cycles. Effort has been done in recent studies (Wood et al., 1997; Roman-Liu et al., 2004, 2005; Iridiastadi and Nussbaum, 2006a,b). Cycle time, submaximal force level, and duty cycle, these task parameters were taken into consideration in these studies aiming at the development of a muscle fatigue model. In these models, the fatigue caused by the external load and the recovery after the duty cycle are mixed together to predict the overall decrease of the muscle strength. Exponential decreases in force capability were indicated by the measured data. Although different prediction models have been established, the universal applicability is limited to job specific tasks (Iridiastadi and Nussbaum, 2006a), and it is difficult to generalize these models for different industrial operations. In addition, the mixture of the duty cycle and the rest cycle leads to the mixture of fatigue and recovery, and consequently this modeling process cannot decouple them to evaluate the fatigue effect or the recovery procedure separately.

It should be noted that in the studies mentioned above, static strengths were often taken as measurement to evaluate the fatigue process, and participants' postures were strictly constrained in the experiment. For this reason, the design of tasks in a fixed posture based on static strengths has lost its relevance in most industrial processes, and job simulated strength should be used to provide better strength guide for the operation design (Mital and Kumar, 1998).

Because of the limitations of the two approaches mentioned above, we proposed a new simple fatigue model based on muscle motor unit recruitment mechanism in Chapter 3. Different from MET models, the decrease of the muscle strength is predictable in this model for static operations by taking account of the submaximal force and the duration of the force. The model was validated in comparison with 24 existing MET models and three theoretical fatigue models. The observed strong correlations

suggest that the model is suitable for static posture or slow operation. Another approach was also proposed in Chapter 3 to predict fatigue resistances of different muscle groups by generalizing the fatigue model, and higher interclass correlations *ICC* indicate that the model is capable of assessing the fatigue process for different muscle groups in a general approach.

In this chapter, the aims of the experimental validation were firstly to quantify the fatigue of the upper limb and secondly to check the adaptability of the fatigue model. A simulated drilling operation in an airplane assembly line was carried out under laboratory conditions. The external loads were predefined to simulate the physical workload in real work environment. Simulated job static strengths were measured, the shoulder joint torques were estimated at different time instants in the operation to assess the physical fatigue, and then the strength results were regressed to check the goodness of fit of the general fatigue model. Posture changes in the operation were observed and interpreted as well.

4.2 Material and methods

4.2.1 EADS drilling case and its simplification

In our research project, the application case is the assembly of two fuselage sections with rivets. One part of the job consists of drilling holes all around the aircraft cross section. The number of the holes could be up to 2,000 on an orbital fuselage junction of an airplane. The drilling machine has a weight around 5 *kg*, and even up to 7 *kg* in the worst condition with consideration of the pipe weight. The drilling force applied to the drilling machine is around 49 *N*. In general, it takes 30 seconds to drill a hole. The drilling operation is graphically shown in Fig. 4.1.

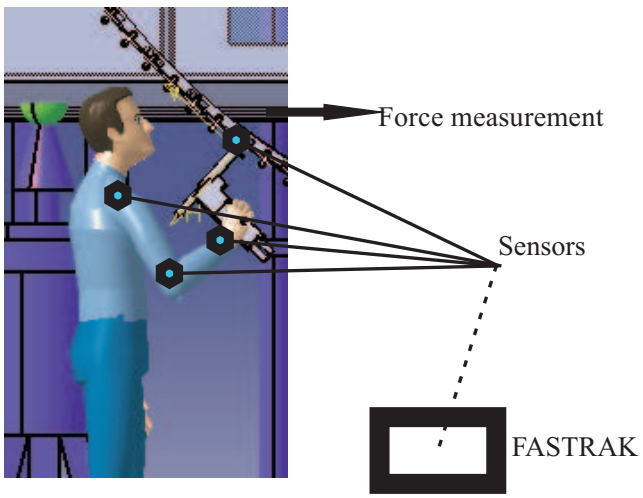

Figure 4.1: Schematic layout of experiment design

There are some ergonomics issues in this drilling operation. First, the heavy external load demands

great physical capacity to sustain the machine and maintain the operation, and the physical fatigue happens rapidly in the upper limb and the lower back. The MSD risks can be augmented by the overexertion of forces and the long lasting vibration while drilling. In order to avoid muscle fatigue, two main factors are considered to simulate the task under laboratory conditions: the magnitude of the external load and the duration of the external load. The vibration and the frequency of the operation are out of consideration in this study in order to precise the muscle fatigue process. Only half of the external load is taken into account in order to simplify the load sharing problem between two hands: 25 N drilling force and 2.5 kg weight of the drilling machine.

4.2.2 Experiment design

The aims of the experiment design were to evaluate the physical fatigue by measuring the decreasing maximal strength and to verify the usability of the fatigue model (see Section 3.2.1) in predicting the decrease of the physical capacity.

A schematic example of muscle fatigue is given in Fig. 4.2. In a continuous static operation, the external load F_{load} normalized by the maximal strength is constant (dashed line), and the physical strength decreases in function of the curve under this normalized load. The curve can be obtained in the experiment by measuring the strength F_{t_i} at time instant t_i. In our case, F_{t_i} is the simulated job static strength measurement, the maximum force output in the drilling direction. Force measurement is used to measure the fatigue, since it is "one of the most direct assessments of fatigue in response to a maximal voluntary effort" (Vøllestad, 1997).

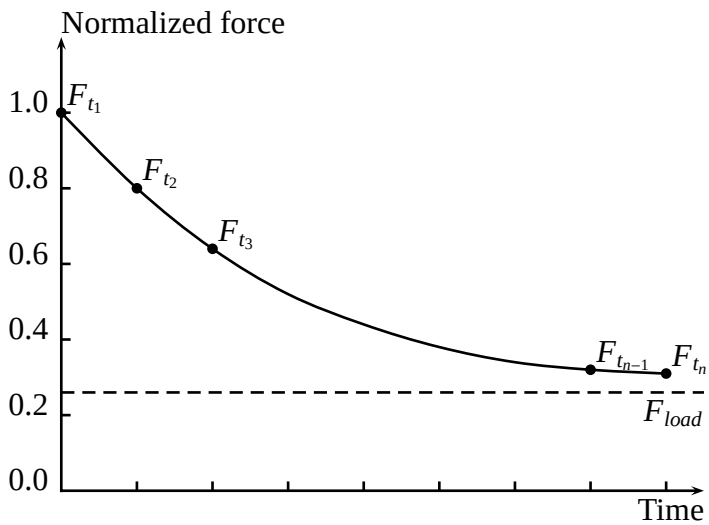

Figure 4.2: Schema of the decrease of the physical capacity in a continuous operation

Roman-Liu and Tokarski (2005) and Anderson et al. (2007) reported large posture related variabilities in joint strengths, and in a real drilling operation, the force perpendicular to the drilling direction can be shared by the holes, while the force in the drilling direction remains the one which

has to be charged by the operator. Therefore the force produced in the drilling direction is taken as the measurement. Due to simulated drilling conditions, the measurement results are also the job specific static strengths in this special drilling case.

After holding the constant external load for a duration t_i, F_{t_i} can be measured by exerting the maximal voluntary strength with a force peak from four to six seconds. However, the continuous work procedure is broken after each measurement of the remained maximum voluntary strength, since it is obvious that the force decreases in maximum voluntary contraction in a different way from that holding a submaximal load. Hence, the participant has to take some break in order to recover his/her physical capacity and then to repeat the operation from the very beginning. Therefore, a continuous operation has to be simulated by several procedures with different working durations.

A continuous operation with a maximum duration t_n can be substituted by several shorter exertions as below:

1. Perform the static operation from $t = 0$ to $t = t_i$;
2. Measure the remained maximum capacity F_{t_i} at time instant t_i;
3. Take a break until total recovery;
4. Repeat steps from 1 to 3 until $i = n$.

With this method, we assume that the decrease capacity can be reproduced as in one continuous exertion.

4.2.3 Subjects

A total of 40 right-handed male industrial workers participated in the experiment. Age, stature, and body mass were recorded or measured at the arrival in the laboratory. Upper limb related anthropometry data were obtained. Related data are listed in Table 4.1. Participation was limited to those with no reported previous history of upper limb problems. Participation was not compulsory and those who participated provided written informed consent.

Table 4.1: Participant characteristics

Characteristic	Mean	Standard Deviation (SD)	Maximum	Minimum
Age [year]	41.2	11.4	58	19
Height [cm]	171.2	5.1	183	160
Weight [kg]	70.2	10.4	95	50

Figure 4.3: Participant in the experiment

4.2.4 Material

Magnetic motion capture device FASTRAK® (Fig. 4.4) from POLHEMUS Inc. was used to capture the upper limb posture in the experiment. As shown in Fig. 4.1, four sensors were attached to the key joints of the human upper limb and the drilling machine. The Cartesian coordinates of shoulder, elbow, wrist, and the contact point between the drilling machine and the workpiece were captured. The tracking device runs at 30 Hz per sensor with a static position accuracy 1 mm. The recorded coordinates of each tracker were used to reconstruct the posture of the worker in post-experiment analysis. The optical tracking system developed by Tsinghua University was not used in the experiment validation, since it has a lower static precision than the magnetic one and it was not robust enough for practical application.

The force measurement device (see Fig. 4.6) was developed by Tsinghua University, and it can measure the press force perpendicular to the surface of the device with a precision of 1 N. Force measurement device was located behind the drilling contact point with the surface perpendicular to the drilling direction to measure the force output.

The two external loads in the drilling case were provided by a wooden beam and a special drilling machine. Wooden material (see Fig. 4.6) was used in order to avoid magnetic distortion caused by ferrous material. The wooden beam had a weight 10 kg, and it was suspended by three straight wires. In the simulated drilling operation, the subject had to push the beam to the force measurement device and hold it for a given duration. In this situation, there was an inclination angle between the beam and the horizontal line around 14.5°. According to the force analysis of pendulum, a tangential force around 25 N was applied to the upper limb. Before each operation, this external load was calibrated

Figure 4.4: Complete FASTRAK System

to ensure that there was a 25 N force load in the drilling direction. The gravity of the drilling machine was simply provided by a drilling tool filled with concrete weighted around 2.5 kg.

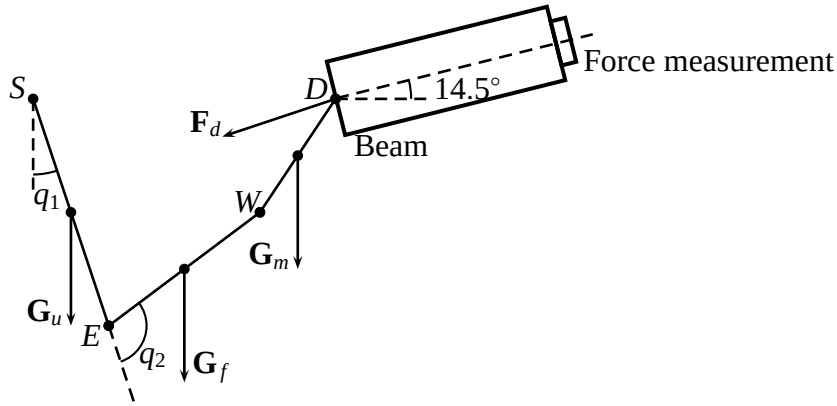

Figure 4.5: Force schema in the drilling operation

4.2.5 Experiment procedure

The subject was seated upright, and the right shoulder was fixed to a shoulder support against the wall in order to constrain the movement of the shoulder and decrease the engagement of the lower back. The left upper limb was set free, and the right upper limb was limited in the sagittal plane by position constraints. The position constraints provided only posture references to the subject to order keep the initial posture as well as possible, but provided no force support to the upper limb.

Before starting the experiment, maximum voluntary contraction (MVC) was determined as the greatest exerted pushing force in the drilling direction during three trials. In each trial, the subject was verbally encouraged and had to maintain the maximum force peak for five seconds. The measured

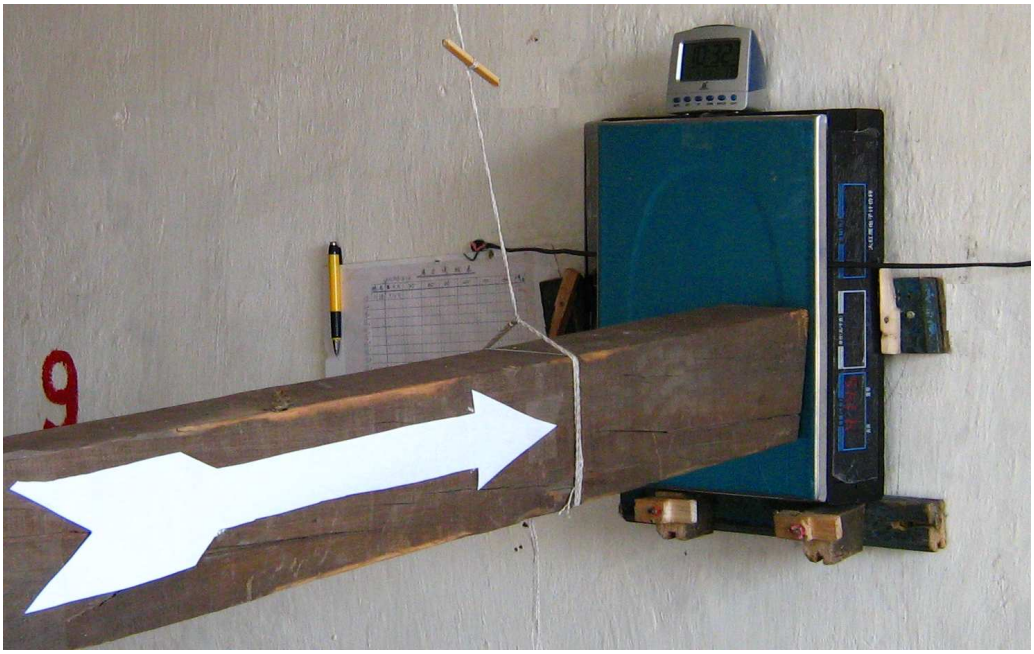

Figure 4.6: Experiment layout in VRHIT laboratory Tsinghua University

MVC was also noted as F_0 to represent subject's initial maximum capacity at the very beginning of the operation.

For a continuous drilling operation with a length of 180 seconds, physical capacities at 9 time instants were measured after holding the external load for different durations: 15, 30, 45, 60, 75, 90, 120, 150, 180 seconds, respectively. The physical capacities were also measured in the same way as MVC but only with one trial, and the measurement results were recorded as F_t, where t represents the corresponding duration. After each measurement, subjects took a rest for at least three minutes or even longer until self-reported total recovery. Once the subject reported that he could not sustain the operation within 180 seconds, the experiment was stopped immediately to avoid injuries to the subject.

4.3 The fatigue model and regression

4.3.1 The fatigue model

The fatigue model (Ma et al., 2009) has been proposed in Chapter 3 on the basis of a differential Equation (Eq. 3.2). Related parameters and their descriptions are given in Table 3.1. This model describes the muscle fatigue mechanism from a macro aspect based on the muscle motor unit recruitment principle.

In static or quasi-static muscular work, F_{load} keeps constant and the reduction of the physical

capacity can be predicted by Eq. 4.1. This equation indicates the theoretical decrease procedure of the maximal force along time in a static operation.

$$\frac{F_{cem}}{F_{max}} = e^{-k\, f_{MVC}\, t} \tag{4.1}$$

Theoretically, three parameters (F_{max}, F_{load}, and k) need to be determined to predict the fatigue process for a static operation. F_{load} can be measured and calculated by force analysis of the external loads, and F_{max} needs to be measured in simulated job conditions. The rate of fatigue k, which describes the individual fatigability and which is influenced by several factors (e.g., muscle strength, muscle fiber type composition, etc.), needs to be determined in mathematical regression.

Rates of fatigue for different muscle groups have also been theoretically analyzed in Chapter 3. Higher interclass correlations ICC have been found with adjusted rates of fatigue which were fitted from the fatigue model to previous MET models. The results suggest that the rate of fatigue is a parameter in normal distribution for a given population and it can be used to evaluate the individual fatigue resistance in an effective manner.

4.3.2 Regression analysis

The aim of the regression analysis was to find the relationship between the measured results and the theoretical model (Eq. 4.1).

The participants were numbered from 1 to 40, noted as j. There were ten measurements from the very beginning to the end of three minutes: one initial capacity and 9 measurements in the working operation. These measurements were noted as $F^j_{t_i}$ indicating the F_{cem} at time instant t_i for the jth subject.

At the beginning of the experiment, subject was considered without any physical fatigue. Therefore, the $F^j_{t_0}$ was treated as the maximum exertion capacity without fatigue. This value was also noted as MVC^j. Equation 4.1 can be further transformed to Eq. 4.2.

$$\ln(\frac{F^j_{t_i}}{MVC^j}) = -k_j\, f^j_{MVC}\, t_i \tag{4.2}$$

In a static operation, theoretically, f^j_{MVC} is constant. Suppose that $k_j\, f^j_{MVC} = a_j$, and then Eq. 4.2 can be simplified to Eq. 4.3.

$$\ln(\frac{F^j_{t_i}}{MVC^j}) = -a_j\, t_i \tag{4.3}$$

With linear regression method, a_j can be calculated. In the drilling operation, f^j_{load} can be estimated by the force analysis in the experiment, and f^j_{MVC} can be calculated from data analysis by

normalizing the f^j_{load} with the MVC^j. In this case, since only the force output in the drilling direction could be measured, only the load in the drilling force direction was taken as f^j_{load}. Once the f^j_{MVC} is determined, then the individual rate of fatigue k_j can be further figured out. After the regression, Pearson's correlation r between the measured result and the theoretical predicted results was calculated for each subject. The closer the correlation approaches to 1, the higher predictability the model has.

4.3.3 Torque estimation

In ergonomics, strengths can be either defined as the maximal force output or by the joint moment strength (Mital and Kumar, 1998). The fatigue model in Eq. 3.2 can be extended to Eq. 4.4 by replacing all the force terms by moment terms.

$$\frac{d\Gamma_{cem}(t)}{dt} = -k\frac{\Gamma_{cem}(t)}{\Gamma_{max}}\Gamma_{load}(t) \tag{4.4}$$

We assumed that the measured force output was mainly determined by joint moment strengths in the right upper limb. The shoulder joint and the elbow joint have similar strength profiles according to the joint moment strength models in Chaffin et al. (1999), and both joints have similar fatigability in MET models (El ahrache et al., 2006), and furthermore it was obvious that the shoulder was charged with much larger torque load than the elbow joint in our drilling case, so we assumed that the bottleneck for the output strength was the shoulder joint. In other words, the shoulder joint moment strength can be estimated with the maximum force output and the related posture information. The torque about the shoulder joint was calculated to check the extensibility of the fatigue model.

In the drilling operation, mainly four external forces contribute to the shoulder torque load. They are the gravity of upper arm $\mathbf{G}_u$, the gravity of forearm $\mathbf{G}_f$, the gravity of the drilling machine $\mathbf{G}_m$, and the drilling force at the contact point $\mathbf{F}_d$. The torque load about the shoulder joint can be approximately estimated by Eq. 4.5.

$$\begin{aligned}\mathbf{\Gamma}_{load} = &\left(\frac{\mathbf{s}-\mathbf{e}}{2}\right)\times\mathbf{G}_u + \left(\frac{\mathbf{w}+\mathbf{e}}{2}-\mathbf{s}\right)\times\mathbf{G}_f \\ &+\left(\frac{\mathbf{d}+\mathbf{w}}{2}-\mathbf{s}\right)\times\mathbf{G}_m + (\mathbf{d}-\mathbf{s})\times\mathbf{F}_d\end{aligned} \tag{4.5}$$

where $\mathbf{s}$, $\mathbf{e}$, $\mathbf{w}$ and $\mathbf{d}$ represent the coordinates of the markers attached to shoulder (S), elbow (E), wrist (W), and drilling contact point (D), respectively.

In this estimation, each segment was assumed having a uniform density distribution, and the gravity center was simplified as the geometrical center of the limb segment. The gravity of each body

segment was estimated proportional to the overall weight of human from anthropometry database (Chaffin et al., 1999).

4.3.4 Interface in Matlab

A graphical interface for experiment analysis has been designed in Matlab (see Fig. 4.7). With this interface, we were able to input all the measurement results, load the motion data for posture analysis, estimate the joint torques, and at last carry out the mathematical regression.

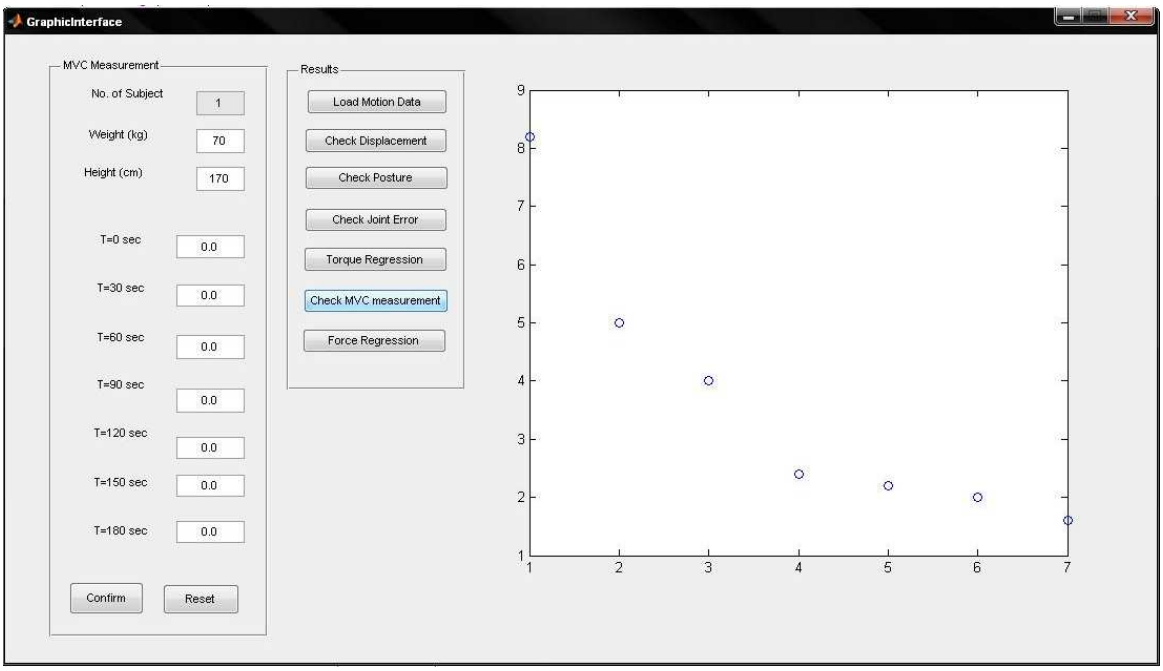

Figure 4.7: Matlab interface for experiment analysis

4.4 Results

4.4.1 General descriptive findings

The strength measurement results were graphically shown in Fig. 4.8. The measured force at each time instant for each subject was represented by the symbol "+". The mean values of the measurements at each time instant were calculated and shown by circles with rectangles indicating the standard deviations. Original data can be found in Appendix D.

From the observation of the measured data, it can be stated in general:

1. There was substantial variability in *MVC* measurements. The average muscle strength at the beginning of the exercise was 104.1 N (SD=21.7). The majority of the measurement results fell

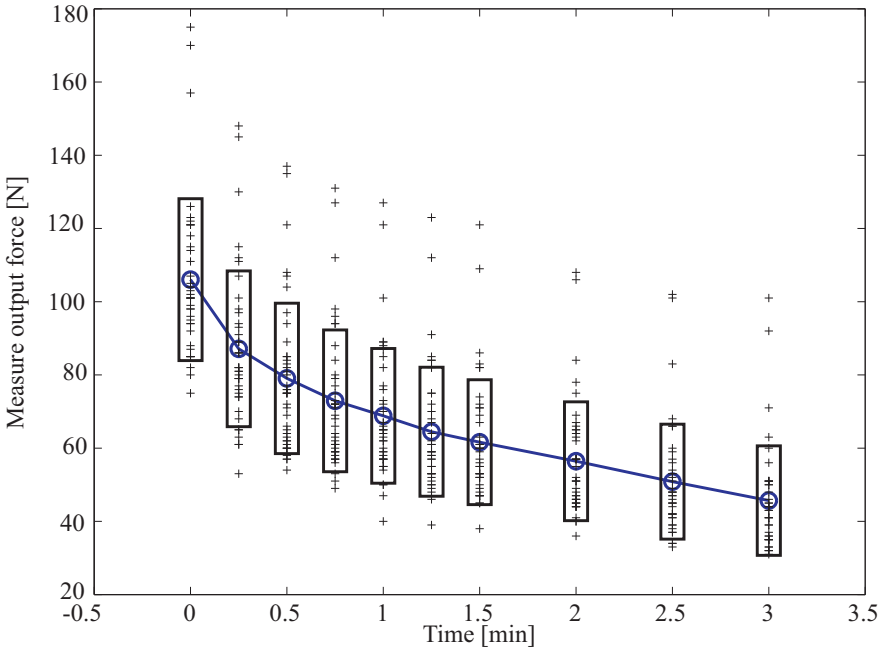

Figure 4.8: Force measurement results and the mean values and standard deviations at each time instant

in the interval limited by the standard deviation.

2. The decrease of the physical capacity was observable in a continuous working process. Reductions in output strength ranged from 36% to 74% across subjects (Mean=58%, SD=8.8%), while the relative external load in the drilling direction varied from 14% to 33% (Mean=24.3%, SD=4.4%).

3. The trend of the fatigue indicated that the longer the operation was maintained, the more fatigue could be found by larger reduction of the maximum force capacity. The decrease rate was more rapid at the beginning period, and the rate decreased along with time. All the characteristics of the reduction curve could be formulated to a negative exponential function.

The mean force measurement values were regressed and shown in Fig. 4.9. The high Pearson's correlation $r = 0.9680$ suggested that the regressed general model could predict the general decrease precisely. Using *ttest* in Matlab, the general rate of fatigue $k_{force} = 1.353$ which had no difference with the mean value of the rates of fatigue k_{MET} regressed from general MET models in El ahrache et al. (2006) (see Table 4.3).

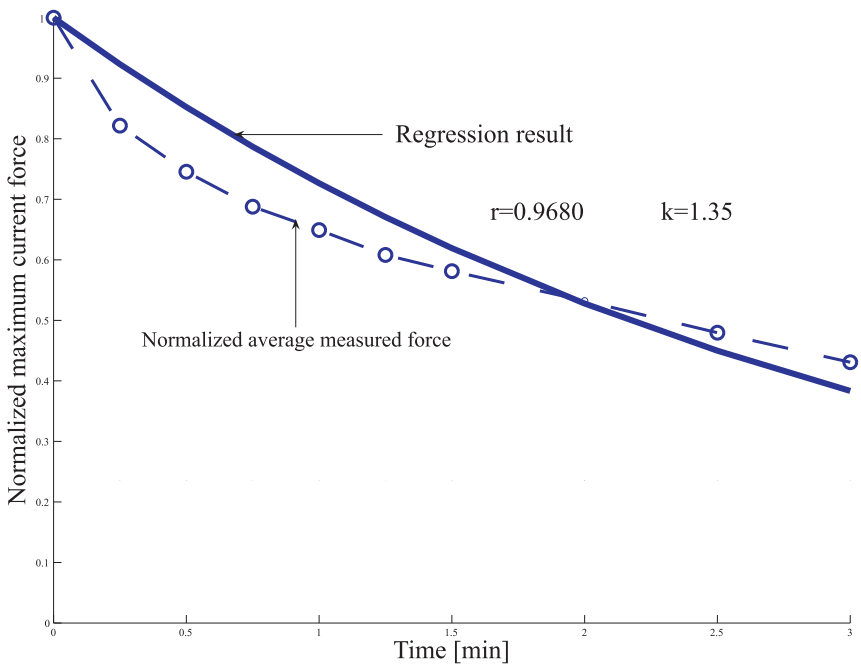

Figure 4.9: General regression result of the decrease of the measured forces

4.4.2 Individual force and torque analysis

In order to validate the availability of the fatigue model, individual force measurements and torques were regressed and analyzed. Pearson's correlations between the regression results and the measured results were also calculated and listed individually in Table 4.2.

Table 4.2: Pearson's correlation r and rate of fatigue in force output and joint torque estimation

Subject	r_{torque}	k_{torque}	r_{force}	k_{force}	Subject	r_{torque}	k_{torque}	r_{force}	k_{force}
1	**0.9493**	0.92	**0.9454**	1.69	21	**0.9297**	0.36	**0.9179**	1.12
2	**0.9879**	0.66	**0.9845**	1.06	22	0.4783	0.33	**0.9038**	1.13
3	**0.9381**	0.36	0.8984	1.29	23	**0.9696**	0.77	**0.9046**	1.17
4	**0.9940**	0.89	**0.9762**	1.94	24	**0.9872**	1.55	**0.9734**	1.68
5	**0.9880**	0.52	0.8989	1.09	25	**0.9888**	0.42	**0.9631**	0.60
6	**0.9656**	0.70	**0.9569**	1.58	26	**0.9219**	0.88	**0.9510**	1.92
7	0.7940	0.92	0.8685	1.32	27	**0.9158**	0.62	**0.9247**	0.93
8	0.8701	2.11	**0.9676**	0.87	28	0.8494	0.93	0.8674	1.62
9	**0.9396**	0.94	**0.9126**	1.71	29	**0.9811**	0.85	**0.9926**	1.29
10	**0.9631**	0.87	**0.9435**	1.71	30	**0.9690**	0.85	**0.9027**	1.86

Continued on Next Page...

Subject	r_{torque}	k_{torque}	r_{force}	k_{force}	Subject	r_{torque}	k_{torque}	r_{force}	k_{force}
11	0.8957	0.63	**0.9014**	1.43	31	**0.9406**	1.32	**0.9561**	1.99
12	**0.9227**	1.33	**0.9500**	1.93	32	**0.9432**	0.58	**0.9595**	0.95
13	**0.9718**	1.14	**0.9968**	1.55	33	**0.9398**	1.12	**0.9671**	1.13
14	0.8976	0.35	**0.9862**	1.27	34	**0.9516**	0.95	**0.9562**	1.41
15	**0.9782**	1.00	**0.9955**	1.49	35	**0.9803**	1.57	**0.9881**	1.28
16	0.8651	1.02	0.8516	1.76	36	0.8615	1.98	**0.9077**	1.34
17	**0.9760**	0.92	**0.9724**	1.52	37	**0.9587**	0.84	**0.9712**	1.14
18	**0.9729**	0.92	**0.9439**	1.45	38	0.6930	1.61	**0.9328**	0.67
19	**0.9380**	1.19	0.8743	1.47	39	**0.9728**	0.70	**0.9856**	1.78
20	**0.9712**	0.71	**0.9544**	1.00	40	**0.9269**	0.66	**0.9460**	0.70

A total of 34 in the 40 subjects had a correlation r_{force} over 0.9. Individual rate of fatigue k_{force} was also calculated, and the mean value and the standard deviation of the rates of fatigue were calculated and listed in Table 4.3. For torque regression, 31 among 40 subjects had a correlation r_{torque} over 0.9. Individual rate of fatigue k_{torque} was also calculated, and the mean value and the standard deviation of the rate of fatigue were also calculated and listed in Table 4.3.

Representative examples were given to show the decrease of the output force strength and the shoulder joint moment strength in the simulated operation in Fig. 4.10 and Fig. 4.11, respectively. The symbol "+" presents the external load (force or torque) at each working duration, and the circle represents the measured or calculated strength data.

Lilliefors test (Conover, 1980) was used to test the goodness of fit of rates of fatigue to a normal distribution with a significant level 5%. Rates of fatigue in forces and torques, both of them showed goodness of fit to a normal distribution.

In Chapter 3, the rates of fatigue for different sample groups were calculated based on the fatigue model and the general MET models in the literature. Parts of the results were also listed in Table 4.3. Kolmogorov-Smirnov test was used to compare the distribution of k_{force} and k_{MET} in general models[1]. Tested result showed that both obey the same normal distribution with a significance level 10%.

The average individual fatigue resistance in torque regression was smaller than that of force regression and less than the average of the shoulder fatigue resistance from the literature (Mean=1.58) (see Table 4.4). The substantial difference might be explained by the selected subjects in the experi-

[1]Rohmert's MET model: 1.20, Huijgens' MET model: 1.05, Stato's MET model: 1.46, Manenica's MET model:1.25, Sjogaard's model: 0.87, Rose's model: 2.15.

Table 4.3: Statistical analysis of rate of fatigue k

Item	Mean	SD	Minimum	Maximum
k_{force}	1.36	0.39	0.61	1.99
k_{torque}	0.88	0.31	0.36	1.57
k_{MET}	1.33	0.45	0.87	2.15

ment: they were industrial workers handling high physical demands. The work trained them suitable for fatiguing physical work. However, since sufficient information could not be obtained from the literature, it was difficult for us to make further judgments about the shoulder resistance analysis. The possible conclusion in torque regression is that the normal distribution characteristic of the given industrial worker population might be recommended by this experiment.

Table 4.4: Fatigue resistances of shoulder MET models

Model	Subjects	k
Sato et al. (1984)	5 male	2.34
Rohmert et al. (1986)	6 male and 1 female students	1.83
Mathiassen and Ahsberg (1999)	20 male and 20 female municipal employees	1.43
Garg et al. (2002)	12 female college subjects	0.72

4.4.3 Posture change in the work

The posture of upper limb in the work duration was calculated from the motion data. Since the arm was limited in sagittal plane, only the flexion angles of the shoulder joint and the elbow joint were calculated to represent the arm posture to eliminate the influences from different limb lengths, and the results were shown in Table 4.5. The posture change in the working process was observable either in regression result (Fig. 4.12) or in graphical posture representation (Fig. 4.13). The changes of the posture followed the same trend: the more the fatigue was, the closer the upper limb was to the trunk. The moment produced by the mass of the upper limb about the shoulder joint could be reduced in this way.

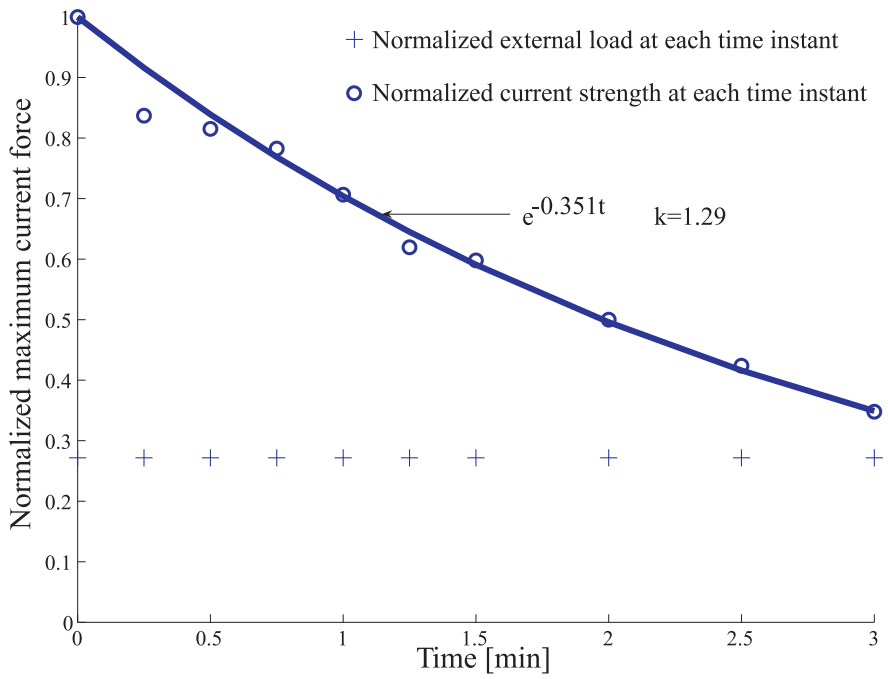

Figure 4.10: Force regression analysis from representative subject data (r_{force} = 0.9926)

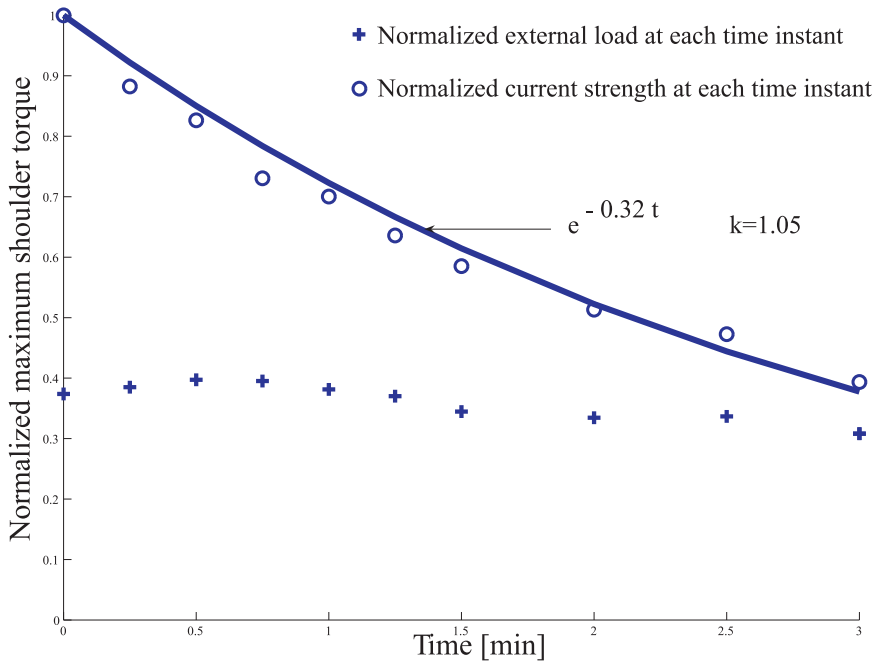

Figure 4.11: Torque regression analysis from representative subject data (r_{torque} = 0.9940)

Table 4.5: Posture change in the experiment [deg]

Time [sec]	0	15	30	45	60	75	90	120	150	180
Elbow q_2										
Mean	50.1	53.1	55.1	55.1	57.5	59.9	59.9	64.2	66.7	75.5
SD	16.1	15.4	15.0	15.7	16.4	19.0	19.2	19.9	21.3	21.9
Shoulder q_1										
Mean	46.4	44.5	43.6	44.2	42.8	42.1	41.9	39.7	37.5	30.5
SD	16.2	15.0	14.6	15.2	14.7	16.6	17.0	16.6	17.9	17.3

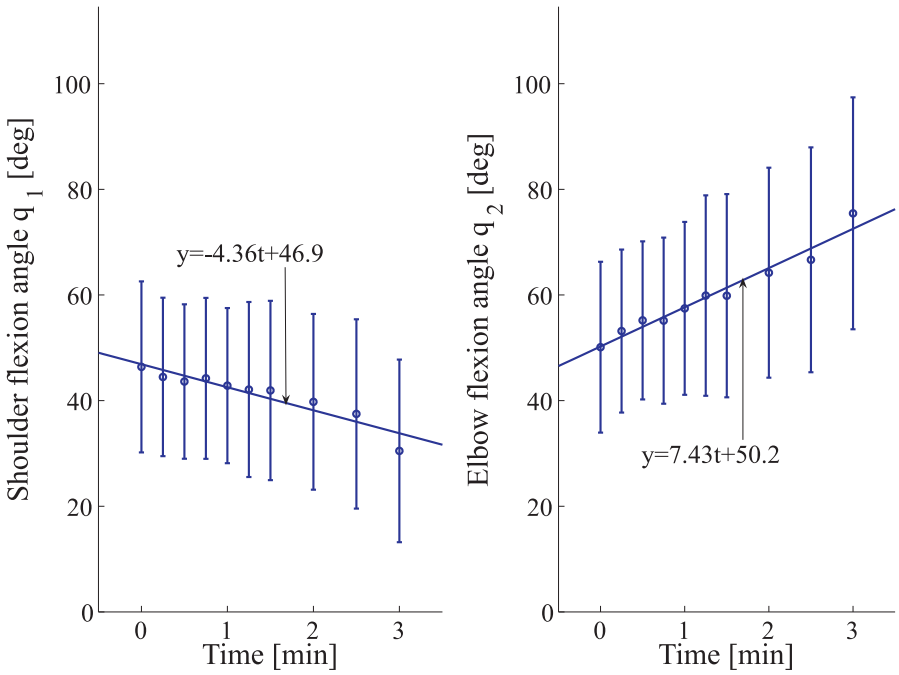

Figure 4.12: Joint flexion angles in different work steps

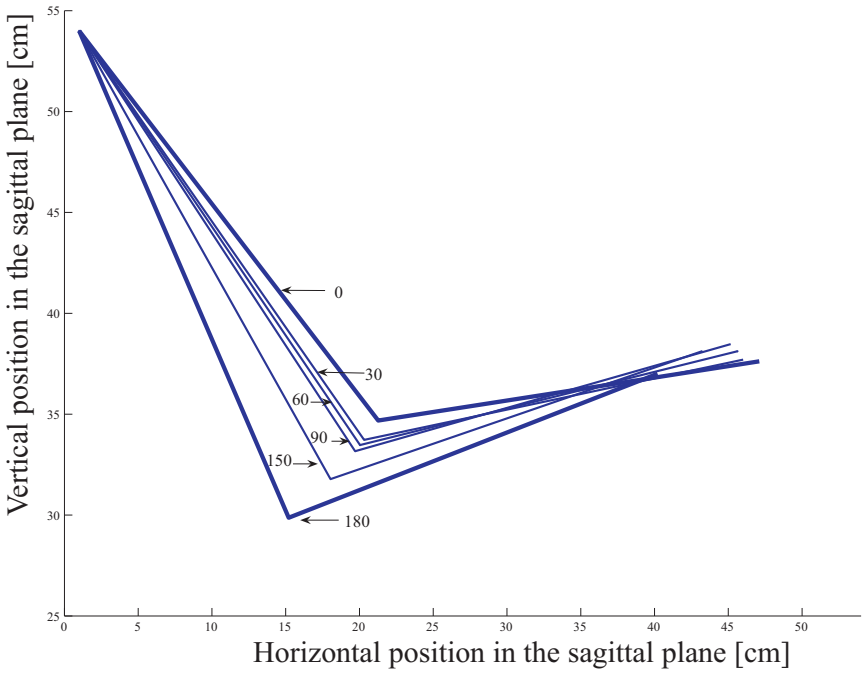

Figure 4.13: Posture change in the drilling operation

4.5 Discussion

4.5.1 Experiment design

Muscle fatigue and its prediction is a long time issue in ergonomics and biomechanics, and many efforts have been contributed either in MET and work-rest allowance methods or in successive work cycle methods. Although fatigue and recovery effects have been considered in both methods, the mixtures of both effects were different. The former approach evaluates the fatigue in MET models, and work-rest allowance models are used separately based on MET models and the actual holding time (El ahrache and Imbeau, 2009), while both effects were mixed and considered in different duty cycle ratios simultaneously in the latter approach. Strong agreement has been found in MET models (El ahrache et al., 2006), while substantial differences were found in work-rest allowance model (El ahrache and Imbeau, 2009). Meanwhile task parameters were closely related to work cycle approach (Iridiastadi and Nussbaum, 2006b), and the models in this approach cannot be easily generalized.

In order to overcome the limitations above, we focus only on the fatigue effect in static and quasi-static industrial operations in a continuous working process, and no recovery is taken into consideration in the experiment design. In this way, most of the recovery effect is separated from the manual handling operation. Although it seems like an old-fashioned method as those for constructing MET

models and pure static muscular efforts are rarely found in the workplace, it simplifies the problem and it is possible to assess the physical fatigue generally and theoretically.

There were several sources of errors in the experiment. In force measurement, only the force in the drilling direction was taken into consideration. Other possible external forces might occur during the experiment and produce torques about the shoulder joint, and those forces were out of consideration in the analysis. Furthermore, the estimation of the joint torque was also influenced by the simplification in the weight and the gravity center of the upper limb. Therefore, fairly good correlations in force measurement suggest that the fatigue model is useful for simulated job strength prediction, while the result in torque analysis cannot provide the same confidential level as in force analysis. Further improvement in experiment design should be necessary to obtain more precise analysis in torque analysis.

4.5.2 Fatigue model and rates of fatigue

From the experiment result analysis, the fatigue model was able to predict the muscle fatigue in force output and joint torque for the majority of the subjects. Differences in fatigue processes have been found from the strength measurement and the torque estimation results. Theoretically, there are mainly two factors resulting in the differences: relative load and individual rate of fatigue.

In the experiment, the external load is not adjusted to the same level according to the individual strength but a fixed load for every subject, since normally the external load is already predetermined in the work design and the only determinant variable in the workplace is the subject to perform the physical operation in most industrial applications. For this reason, the relative load for each subject is different (Mean=24.3%, SD=4.4%). The relative force cannot be further grouped into different force levels.

Substantial differences in individual rates of fatigue can be found from the result, and the variability is determined by several factors (e.g., gender, age, posture, sample subjects, muscle fiber composition, physical training, and physical work history, etc) (Hicks et al., 2001). It should be a challenging task to determine or model the individual rate of fatigue theoretically based on the influencing factors. But the finding of the normal distribution characteristic of this parameter is also interesting, which means the analysis for a given population may be possible if more subjects and more experiment results for industrial operations are obtained.

4.5.3 Posture changes

Although posture reference was provided to avoid the mismatches in different test periods, it was still very difficult to keep the posture pure static in the operation. The changes in the posture can be

Table 4.6: Correlation between Pearson's correlations in force and torque and the individual posture changes

Individual SD of Segment	rate of fatigue	Correlation
Elbow	r_{force}	0.07
Elbow	r_{torque}	0.07
Shoulder	r_{force}	0.11
Shoulder	r_{torque}	0.03

explained by a global posture control strategy: decreasing the joint loads in the operation by moving the upper limb closer to the body, and the similar finding has been reported by Fuller et al. (2008).

Small changes happened in the experiment, but the changes did not generate too much variation in the joint strength. In our case, the variation of the joint moment strength is no more than 3% (analysis see Appendix C) relative to the initial posture according to the joint moment strength model (Chaffin et al., 1999). Such disturbances might not generate great differences in the joint strength analysis. In order to confirm this assumption, the dependences between the posture changes and Pearson's correlations in force and torque regression were also evaluated. The change of the posture for each subject was represented by the standard deviations of the elbow flexion and the shoulder flexion in the work process. Correlations across both flexion angles and both Pearson's correlations were calculated and listed in Table 4.6. No strong correlation was found, and it suggested that the regression results were independent of the posture change. Namely, the decrease of the physical strength can be modeled by the fatigue model in a certain range of the postures.

4.5.4 Study limitations

In this study, only the fatigue with the relative force falling from 20% to 30% of the specific job operation was tested, so the obtained result is only available for similar industrial operations. The general fatigue model might be able to predict muscle fatigue in other industrial applications, but it still requires more effort to validate the assumption and generalize the model.

In addition, the recovery model has not been well developed to complete the work-rest schedule design. Although effort has been done in Wood et al. (1997) and Ma et al. (2008) to model the recovery theoretically, the theoretical validation of the recovery model has not yet been verified. The lacking of the recovery model limits the potential application of the fatigue model.

Finally, the present study was only a step toward to predict the fatigue based on a theoretical analysis. More effort is needed to develop, validate, and complete the theoretical approach. That will be one of our main research objectives in the future.

4.6 Summary

In this chapter, the physical fatigue in a simulated drilling operation and its theoretical analysis on the basis of our general fatigue model is presented. Both the measured simulated static strengths and the estimated joint torques in a continuous operation were found following negative exponential functions, and high Pearson's correlations between the measured results and the regressed functions recommended that the general fatigue model could be used to assess the fatigue for industrial manual handling operations. The normal distribution characteristic for the rates of fatigue in both output strengths and joint moment strengths suggests that it is possible to make use of this parameter for evaluating the fatigue resistance individually or for a given population with more empirical data.

Taking the rate of fatigue and the relative force level together, this chapter provides an approach to predict the physical fatigue in industrial operations. Different from the MET approaches and the work cycle methods, this approach may predict the physical fatigue theoretically for a continuous fatigue operation in advance by decoupling the recovery effect. This model could be integrated into virtual human simulation for computer aided ergonomics design.

However, a recovery model is still necessary to be developed to make the prediction completely. Furthermore, the applicability of this model should be tested in more industrial operations. At last, in this case, only a special simulated operation using the arm was carried out under lab conditions, so other conditions and the body parts should be further examined to extend the application field of our model.

Chapter 5

Application cases in computer-aided ergonomics

Contents

5.1 Introduction 89
5.2 Digital human modeling 91
5.3 Physical fatigue assessment in posture analysis 98
5.4 Multi-objective posture prediction 105
5.5 Summary 113

5.1 Introduction

The main functions of our framework are posture analysis and posture prediction. Posture analysis targets to evaluate the physical fatigue based on fatigue model, while posture prediction aims to predict the posture under different criteria.

As stated in the previous chapters, although there are several fatigue assessment tools in ergonomics, they are not suitable for detailed analysis by reason of their intermittent background. The relationship between external loads, duration, frequency, and individual factors is established in a rough estimation method. That is the origin of our motivation to develop a new and suitable model for ergonomic applications. In previous chapters, we have presented the fatigue model and its validation, both in theoretical analysis and in experimental analysis. This fatigue model fulfills the requirements from the framework in ergonomic analysis, since it is relatively simple and well explained based on muscle physiological principle, and it generalizes the MET models. In this chapter, the fatigue model is going to be integrated into digital human simulation. With this suitable fatigue model, the change of human physical status can be evaluated, and furthermore the possible change of the posture can be predicted using multi-objective optimization methods.

Concerning posture prediction, there are different approaches in the literature. The aim of the posture prediction is to generate realistic human posture based on the context of a simulation or study. Mainly there are three approaches to predict posture: classical animation approach, inverse kinematics, and optimization method. The classical animation approach involves empirical-statistical modeling using anthropomertical data. These data are collected from thousands of human subjects (Zhang, 1997; Zhang and Chaffin, 2000). This methods need not be verified in terms of realism by reason of the actual human data, but it involves a time-consuming data collection. Inverse kinematics is an approach to posture prediction in which a set of equations have to be solved to determine parameters for the human model. This approach is restricted to relatively simple models with a few degrees of freedom.

Optimization method has been frequently used in posture prediction and motion simulation, and different optimization methods are trying to simulate strategies to interpret the posture control in different ways, such as minimizing the energy expenditure, minimizing the joint torques, etc. Single objective optimization method has been used in the literature with different objective functions: joint range availability (JRA)(Jung et al., 1995), joint effort (Dysart and Woldstad, 1996), perceived disocmfort (Jung and Choe, 1996), driver discomfort (Sun et al., 2006), joint displacement (Abdel-Malek et al., 2001; Yang et al., 2006b), and visibility (Smith, 2009). However, the single-objective method is limited by reason of its single performance measurement. Yang and his colleagues proposed a multi-objective optimization approach to predict human posture (Yang et al., 2004, 2006a, 2007), and it has been stated that different performance measures (joint displacement, potential energy, and joint discomfort) are aggregated to integrate different disciplines in posture prediction. However, in all those optimization based methods, the fatigue effect along time is not considered enough. Rodríguez and Boulic (2008) proposed a method to predict the time-varying posture based on half-joint endurance model, however, this method is limited due to limitations from its model. Therefore, in this chapter, our fatigue model is integrated into a multi-objective method to predict the posture under fatigue process.

No matter how the motion data can be obtained, either in motion capture or in motion simulation, digital human modeling is necessary to reproduce the real human in the simulation system. The digital human is modeled mainly following four steps: kinematic modeling (geometrical modeling), biomechanical modeling, dynamic modeling, and graphical modeling. Kinematic modeling aims to represent the human structure by a kinematic chain in tree structure. By kinematic modeling, the relative positions of different human joints can be established in a unique way. Biomechanical modeling is to integrate different biomechanical properties into virtual human, from joint strength to musculoskeletal structure. Dynamic modeling aims to obtain all the necessary dynamic parameters

in order to carry out the dynamic analysis. Last but not least, graphical modeling is to reproduce the virtual human with a relative real appearance for visual feedback.

In this chapter, a digital human is modeled in the same method as mentioned before, and the modeling process will be explained in details. After modeling the virtual human, physical aspects of the operation can be assessed in the simulation system. An EADS drilling case is simulated for fatigue evaluation by evaluating the change of the joint strengths. The changed strength can be further used to guide the human motion, therefore the application for posture prediction is also introduced.

5.2 Digital human modeling

5.2.1 Kinematic modeling of virtual human

In this study, the human body is modeled kinematically as a series of revolute joints. The Modified Denavit-Hartenberg (modified DH) notation system (Khalil and Dombre, 2002) is used to describe the movement flexibility of each joint (see Appendix A). According to the joint function, one natural joint can be decomposed into 1 to 3 revolute joints. Each revolute joint has its rotational joint coordinate, labeled as q_i, with joint limits: the upper limit q_i^U and the lower limit q_i^L. A general coordinate $\mathbf{q} = [q_1, q_2, \ldots, q_n]$ is defined to represent the kinematic chain of the skeleton.

The human body is geometrically modeled by $n = 28$ revolute joints to represent the main movement of the human body in Fig. 5.1. The posture, velocity, and acceleration are expressed by the general coordinates $\mathbf{q}$, $\dot{\mathbf{q}}$, and $\ddot{\mathbf{q}}$. It is feasible to carry out the kinematic analysis of the virtual human based on this kinematic model. By implementing inverse kinematic algorithms, it is able to predict the posture and trajectory of the human, particularly for the end effectors (e.g., the hands). All the parameters for modeling the virtual human are listed in Table 5.1. $[X_r, Y_r, Z_r]$ is the Cartesian coordinates of the root point (the geometrical center of the pelvis) in the coordinates defined by $X_0Y_0Z_0$.

The geometrical parameters of the limb are required in order to accomplish the kinematic modeling. Such information can be obtained from anthropometry database in the literature. The dimensional information can also be used for the dynamic model of the virtual human. The lengths of different segments can be calculated as a proportion of body stature H in Table 5.2.

5.2.2 Dynamic modeling of virtual human

Dynamic modeling aims to provide all the necessary parameters for further biomechanical analysis. In order to simplify the analysis problem, the human body is considered to be a system of mechanical links, each of known physical size and form. Necessary dynamic parameters for each

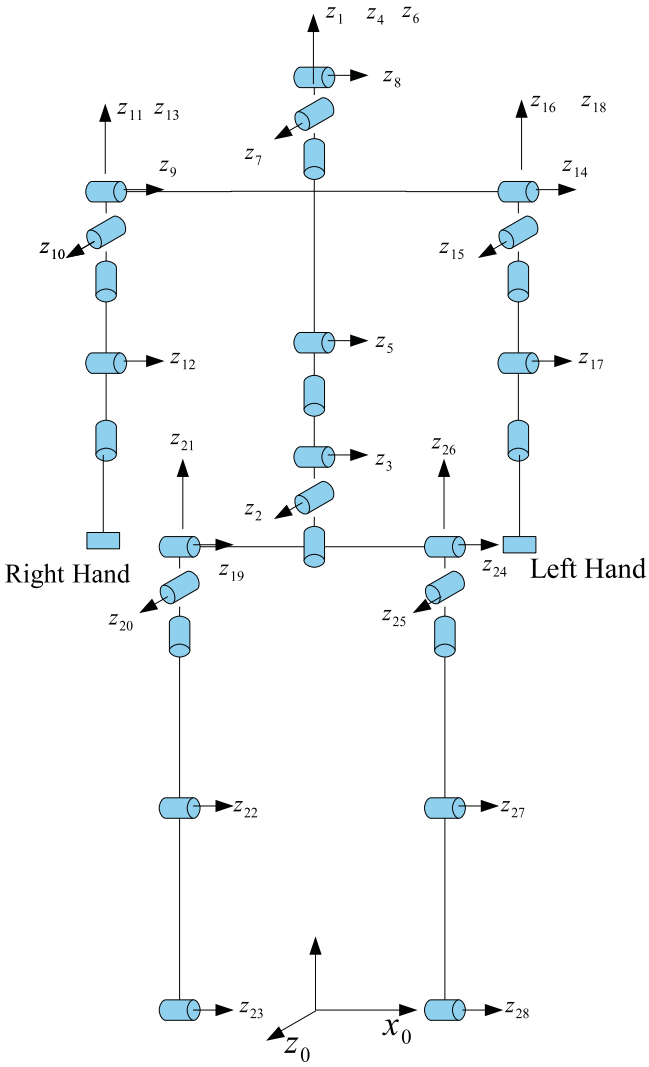

Figure 5.1: Geometrical modeling of virtual human

Table 5.1: Geometric modeling parameters of the overall human body

j	$a(j)$	u_j	σ_j	γ_j	b_j	α_j	d_j	q_j	r_j	q_{ini}
1	0	1	0	0	Z_r	$-\frac{\pi}{2}$	X_r	θ_1	Y_r	0
2	1	0	0	0	0	$\frac{\pi}{2}$	0	θ_2	0	$\frac{\pi}{2}$
3	2	0	0	0	0	$\frac{\pi}{2}$	0	θ_3	0	$\frac{\pi}{2}$
4	3	0	0	0	0	$\frac{\pi}{2}$	0	θ_4	R_{lb}	0
5	4	0	0	0	0	$-\frac{\pi}{2}$	0	θ_5	0	0
6	5	0	0	0	0	$\frac{\pi}{2}$	0	θ_6	R_{ub}	$\frac{\pi}{2}$
7	6	0	0	0	0	$\frac{\pi}{2}$	0	θ_7	0	$\frac{\pi}{2}$
8	7	0	0	0	0	$\frac{\pi}{2}$	0	θ_8	0	0
9	5	1	0	$-\frac{\pi}{2}$	0	0	D_{ub}	θ_9	$-\frac{W_s}{2}$	0
10	9	0	0	0	0	$-\frac{\pi}{2}$	0	θ_{10}	0	$-\frac{\pi}{2}$
11	10	0	0	0	0	$-\frac{\pi}{2}$	0	θ_{11}	$-R_{ua}$	$-\frac{\pi}{2}$
12	10	0	0	0	0	$-\frac{\pi}{2}$	0	θ_{12}	0	0
13	11	0	0	0	0	$\frac{\pi}{2}$	0	θ_{13}	0	0
14	5	1	0	$-\frac{\pi}{2}$	0	0	D_{ub}	θ_{14}	$\frac{W_s}{2}$	0
15	14	0	0	0	0	$-\frac{\pi}{2}$	0	θ_{15}	0	$-\frac{\pi}{2}$
16	15	0	0	0	0	$-\frac{\pi}{2}$	0	θ_{16}	$-R_{ua}$	$-\frac{\pi}{2}$
17	16	0	0	0	0	$-\frac{\pi}{2}$	0	θ_{17}	0	0
18	17	0	0	0	0	$\frac{\pi}{2}$	0	θ_{18}	0	0
19	1	1	0	$-\frac{\pi}{2}$	0	$-\frac{\pi}{2}$	0	θ_{19}	$-\frac{W_w}{2}$	$-\frac{\pi}{2}$
20	19	0	0	0	0	$-\frac{\pi}{2}$	0	θ_{20}	0	$-\frac{\pi}{2}$
21	20	0	0	0	0	$-\frac{\pi}{2}$	0	θ_{21}	$-R_{ul}$	$-\frac{\pi}{2}$
22	21	0	0	0	0	$-\frac{\pi}{2}$	0	θ_{22}	0	$-\frac{\pi}{2}$
23	22	0	0	0	0	0	$-D_{ll}$	θ_{23}	0	0
24	1	1	0	$-\frac{\pi}{2}$	0	$-\frac{\pi}{2}$	0	θ_{24}	$\frac{W_w}{2}$	$-\frac{\pi}{2}$
25	24	0	0	0	0	$-\frac{\pi}{2}$	0	θ_{25}	0	$-\frac{\pi}{2}$
26	25	0	0	0	0	$-\frac{\pi}{2}$	0	θ_{26}	$-R_{ul}$	$-\frac{\pi}{2}$
27	26	0	0	0	0	$-\frac{\pi}{2}$	0	θ_{27}	0	$-\frac{\pi}{2}$
28	27	0	0	0	0	0	$-D_{ll}$	θ_{28}	0	0

Table 5.2: Body segment lengths as a proportion of body stature (Chaffin et al., 1999; Tilley and Dreyfuss, 2002)

Symbol	Segment	Length
R_{ua}	Upper arm	0.186H
R_{la}	Forearm	0.146H
R_h	Hand	0.108H
R_{ul}	Thigh	0.245H
D_{ll}	Shank	0.246H
W_s	Shoulder width	0.204H
W_w	Waist width	0.100H
D_{ub}, L_{ub}	Torso length (L5-L1)	0.198H
R_{ub}	Torso length (L1-T1)	0.090H

body segment include: gravity center, mass, moment of inertia about the gravity center, etc. According to the percentage distribution of total body weight for different segments (Chaffin et al., 1999), the weights of different segments can be calculated using Table 5.3.

It is feasible to calculate other necessary dynamic information with simplification of the segment shape. For limbs, the shape is simplified as a cylinder, head as a ball, and torso as a cube. The moment of inertia can be further determined based on the assumption of uniform density distribution. For the virtual human system, once all the dynamic parameters are known, it is possible to calculate the torques and forces at each joint following Newton-Euler method (Khalil and Dombre, 2002). If further detailed modeling is required, anthropometrical database need be established to fulfill the dynamic modeling functions.

5.2.3 Biomechanical modeling of virtual human

The biomechanical properties of the musculoskeletal system should also be modeled for virtual human simulation. From the physical aspect, the skeleton structure, muscle, and joint are the main biomechanical components in a human. In our study, only the joint moment strengths and joint movement ranges are used for the fatigue evaluation.

As mentioned before, with correct kinematic and dynamic models, it is possible to calculate torques and forces in joints with an acceptable precision. Although biomechanical properties of muscles are reachable and different optimization methods have been developed in the literature, the determination of the individual muscle force is still very complex and not as precise as that of joint torque

Table 5.3: Percentage distribution of total body weight according to different segmentation plans (Chaffin et al., 1999)

Grouped segments, % of total body weight	individual segments % of grouped-segments weight
Head and neck=8.4%	Head=73.8%
	Neck=26.2%
Torso=50%	Thorax=43.8%
	Lumbar=29.4%
	Pelvis=26.8%
Total arm=5.1%	Upper Arm=54.9%
	Forearm=33.3%
	Hand=11.8%
Total leg=15.7%	Thigh=63.7%
	Thigh=63.7%
	Shank=27.4%
	Foot=8.9%

(Xia and Frey Law, 2008). Since there are several muscles attached around a joint, it creates an mathematical underdetermined problem for force calculation in muscle level. In addition, each individual muscle has different muscle fiber compositions, different levers of force, and furthermore different muscle coordination mechanisms, and the complexity of the problem will be increased dramatically in muscle level. Therefore, in our system, only the joint moment strength is taken to demonstrate the fatigue model.

The joint torque capacity is the overall performance of muscles attached around the joint, and it depends on the posture and the rotation speed of joint (Anderson et al., 2007). When a heavy load is handled in a manual operation, the action speed is relatively small, and it is almost equivalent to static cases. The influence from speed can be neglected, so only posture is considered. In this situation, the joint strength can be determined according to strength models in Chaffin et al. (1999). The joint strength is measured in torque and modeled as a function of joint flexion angles. An example of joint strength is given in Fig. 5.2. The shoulder flexion angle and the elbow flexion angle are used to determine the profile of the male adult elbow joint strength. The 3D mesh surfaces represent the elbow joint strengths for 95% population. For the 50th percentile, the elbow joint strength varies from 45 to 75 N according to the joint positions.

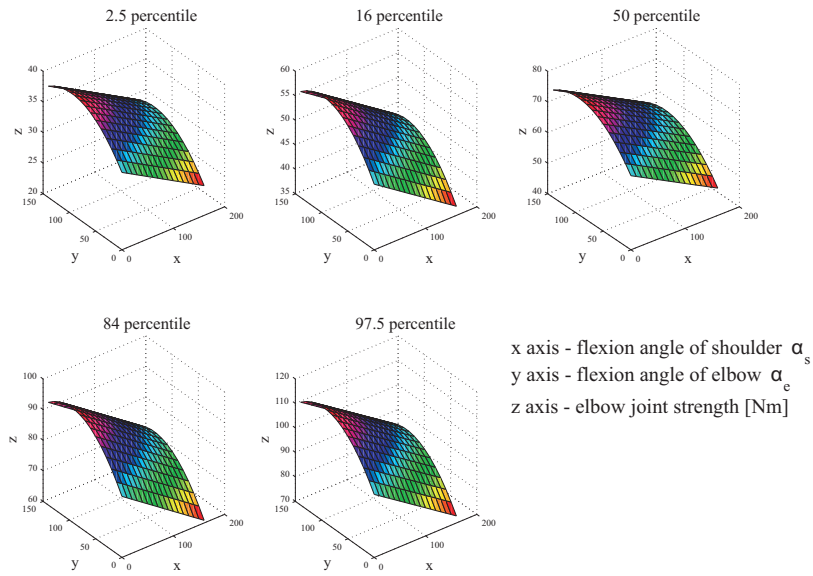

Figure 5.2: Elbow static strength depending on the human elbow and shoulder joint position, α_s, α_e [deg]

5.2.4 Graphical modeling of virtual human

The final step for modeling the virtual human is its graphical representation. The skeleton is divided into 11 segments in our self-developped software: body (1), head and neck (1), upper arms (2), lower arms (2), upper legs (2), lower legs (2), and feet (2). Each segment is modeled in 3ds file (3D Max, Autodesk Inc.) (Fig. 5.3(a)) and is connected via one or more revolute joints with another one to assemble the virtual skeleton (Fig. 5.3(b)). The graphical rendering of the 3D models are realized in C++ and OpenGL. For each segment, an original point and two vectors perpendicular to each other are attached to it to represent the position and the orientation in the simulation, respectively. The position and orientation can be calculated from the kinematic model of the virtual human based on Modified DH method.

5.2.5 Workflow for fatigue analysis

The general process of the posture analysis has been discussed in Section 2.6, and here is the flowchart in Fig. 5.4 to depict all the details in processing all the input information.

First, human motion obtained either from human simulation or from motion capture system is further processed to displacement $\mathbf{q}$, speed $\dot{\mathbf{q}}$, and acceleration $\ddot{\mathbf{q}}$ in general coordinates.

The external forces and torques on the human body are either measured directly by force measurement instruments or estimated in the simulation. The external loads are transformed to Γ_i and F_i in the coordinates attached to q_i in the modified DH method.

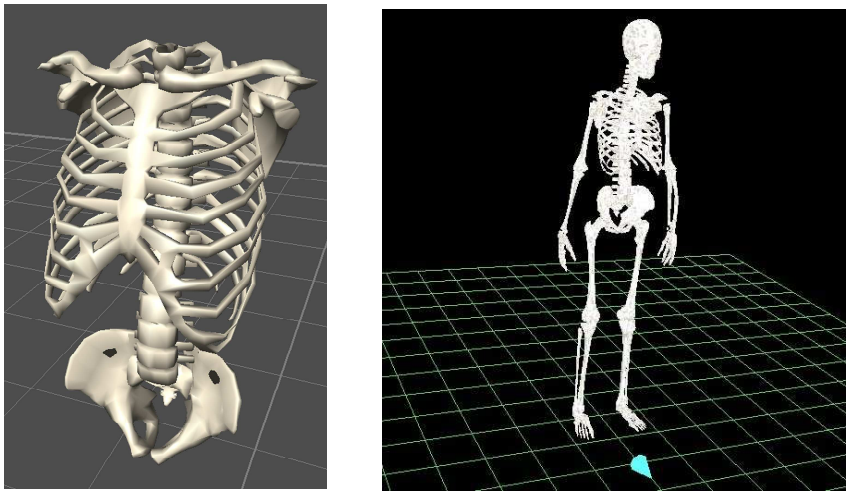

(a) 3DS model (b) virtual skeleton

Figure 5.3: Virtual skeleton composed of 3DS models

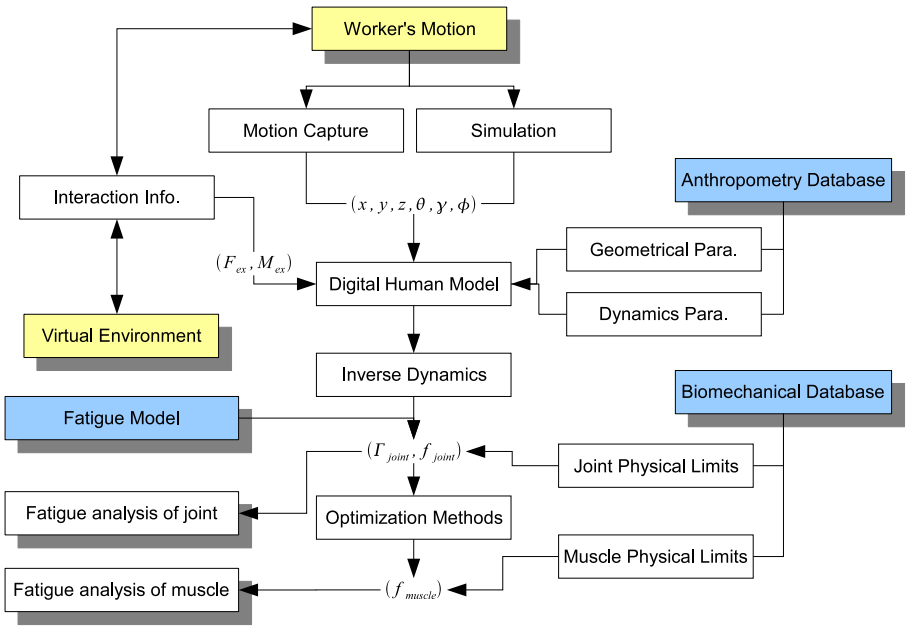

Figure 5.4: Workflow for the fatigue evaluation

Human motion and interaction (forces, torques) are mapped into the digital human model which is geometrically and dynamically modeled from anthropometry database and biomechanical database. Inverse dynamics is used to calculate the torque and force at each general joint. If it goes further, the effort of each individual muscle can be determined using optimization method as well.

Once the loads of the joints are determined, the fatigue of each joint can be analyzed using the fatigue model. The reduction of the physical strength can be evaluated, and finally the difficulty of the operation can be estimated by the change of physical strengths.

5.3 Physical fatigue assessment in posture analysis

5.3.1 Operation description

The application case is the assembly of two fuselage sections with rivets from the assembly line of an airplane in European Aeronautic Defence & Space (EADS) Company. The drilling operation is illustrated in Fig. 5.5 and detailed task description can be found in Section 4.2.1. The fatigue happens often in shoulder, elbow, and lower back because of the heavy load. Only the upper limb is taken into consideration in this demonstration case to decrease the complexity of the analysis. In our research, the dynamic parameters for the arm have already been modeled while the Newton-Euler inverse dynamic method has been used to determine the joint efforts, and the detailed process can be found in Appendix B.

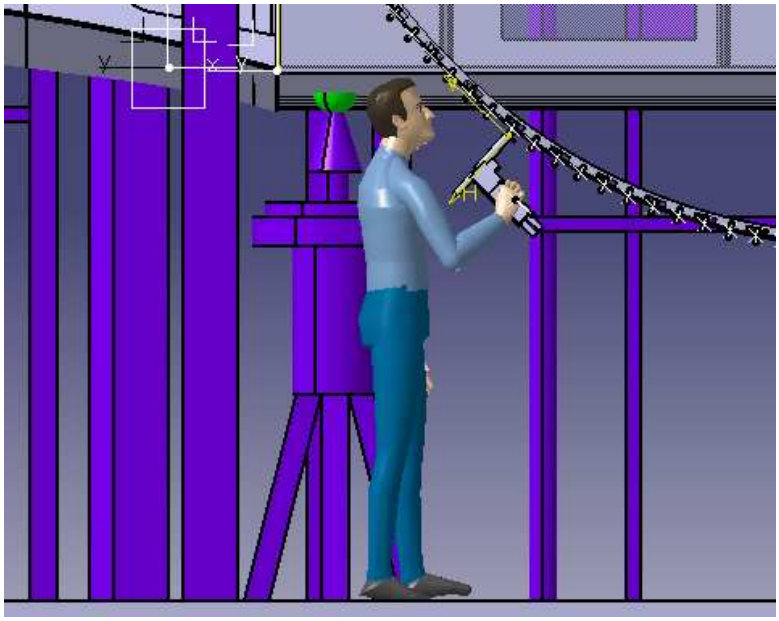

Figure 5.5: Drilling case in CATIA

5.3.2 Endurance time prediction

The drilling machine with a weight 5 *kg* is taken to calculate the maximum endurance time under a static posture with shoulder flexion as 30° and elbow flexion 90° for maintaining the operation in a continuous way. The weight of the drilling machine is divided by two in order to simplify the load sharing problem. The endurance result is shown in Table 5.4 for the population falling in the 95% strength distribution. It is found that the limitation of the work is determined by the shoulder, since the endurance time for the shoulder joint is much shorter than that of the elbow joint.

Table 5.4: Maximum endurance time of shoulder and elbow joints for drilling work. (S: mean joint strength of the male adult population; σ: standard deviation of the joint strength; $\bar{m}$: mean joint fatigue resistance; σ_m: standard deviation of the joint fatigue resistance)

MET [sec]	$S-2\sigma$	$S-\sigma$	S	$S+\sigma$	$S+2\sigma$
Shoulder					
$\bar{m}-\sigma_m$	19	45	75	109	145
$\bar{m}$	45	106	177	256	341
$\bar{m}+\sigma_m$	72	167	279	403	538
Elbow					
$\bar{m}-\sigma_m$	231	424	640	874	1120
$\bar{m}$	438	806	1217	1660	2129
$\bar{m}+\sigma_m$	646	1188	1793	2447	3137

The difference in endurance results has two origins. One is the external load relative to the joint strength. The second comes from the fatigue resistance difference among the population. These differences are graphically presented from Fig. 5.6 to Fig. 5.9. Figure 5.6 and Figure 5.7 show the variable endurance caused by the joint strength distribution in the adult male population with the mean fatigue resistance. Larger strength results in longer endurance time for the same external load. Figure 5.8 and Figure 5.9 present the endurance time for the population with the average joint strength but different fatigue resistances, and it shows that larger fatigue resistance leads to longer endurance time. Combining with the strength distribution and the fatigue resistance variance, the MET can be estimated for a given population.

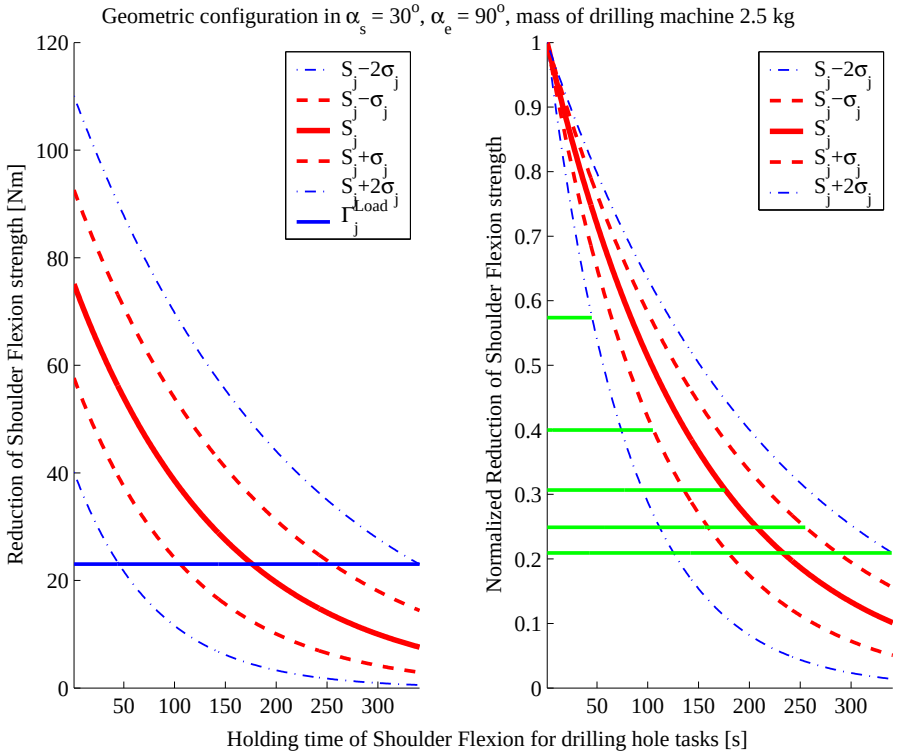

Figure 5.6: Endurance time prediction for shoulder with average fatigue resistance

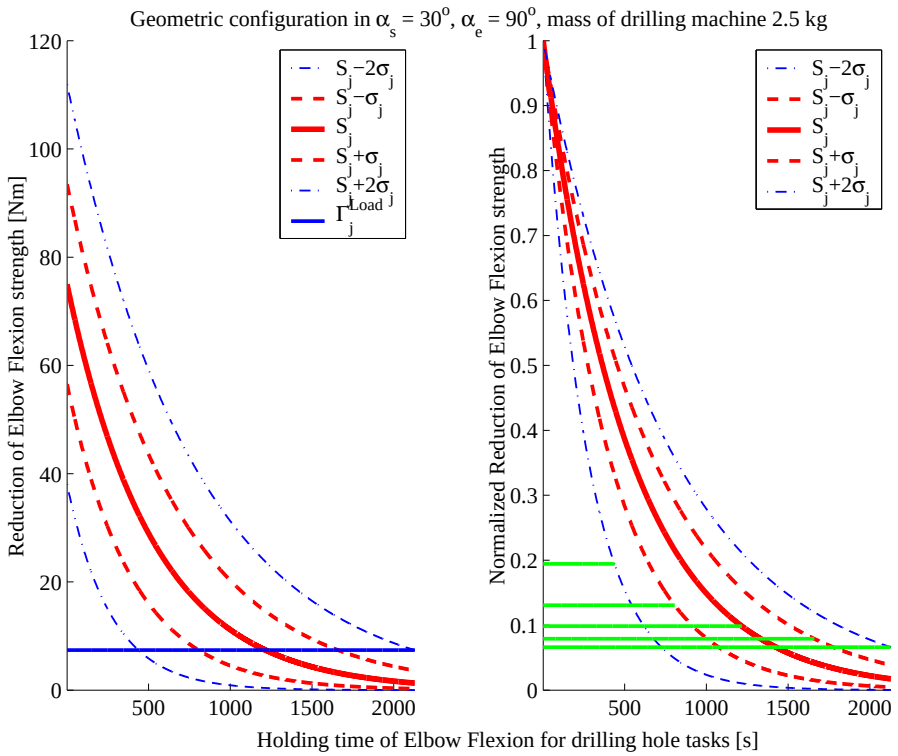

Figure 5.7: Endurance time prediction for the elbow with average fatigue resistance

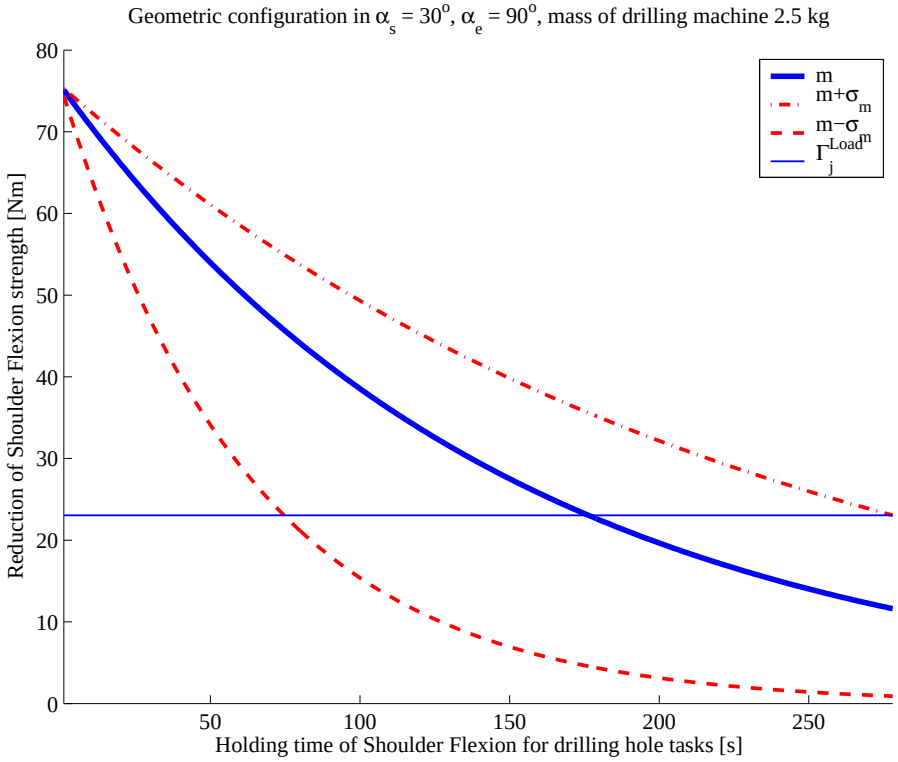

Figure 5.8: Endurance time for the population with average strength for shoulder joint

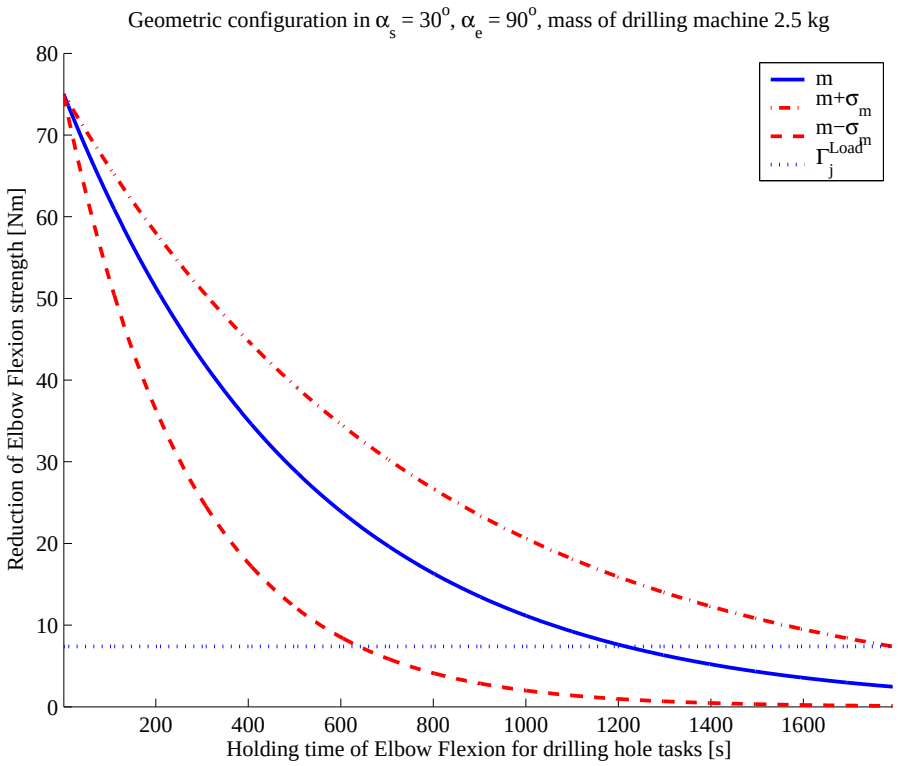

Figure 5.9: Endurance time for the population with average strength for elbow joint

5.3.3 Fatigue evaluation

The fatigue is evaluated by the change of the joint strength in a fatigue operation. The working history can generate influence on the fatigue. Therefore, the fatigue for drilling a hole is evaluated in a continuous working process up to 6 holes. Only the population with the average strength and the average fatigue resistance is analyzed in fatigue evaluation in order to present the effect of the work history. The reduced strength is normalized by dividing the maximum joint strength, and it is shown in Fig. 5.10. It takes 30 seconds to drill a hole, and the joint strength is calculated and normalized every 30 seconds until exhaustion for the shoulder joint.

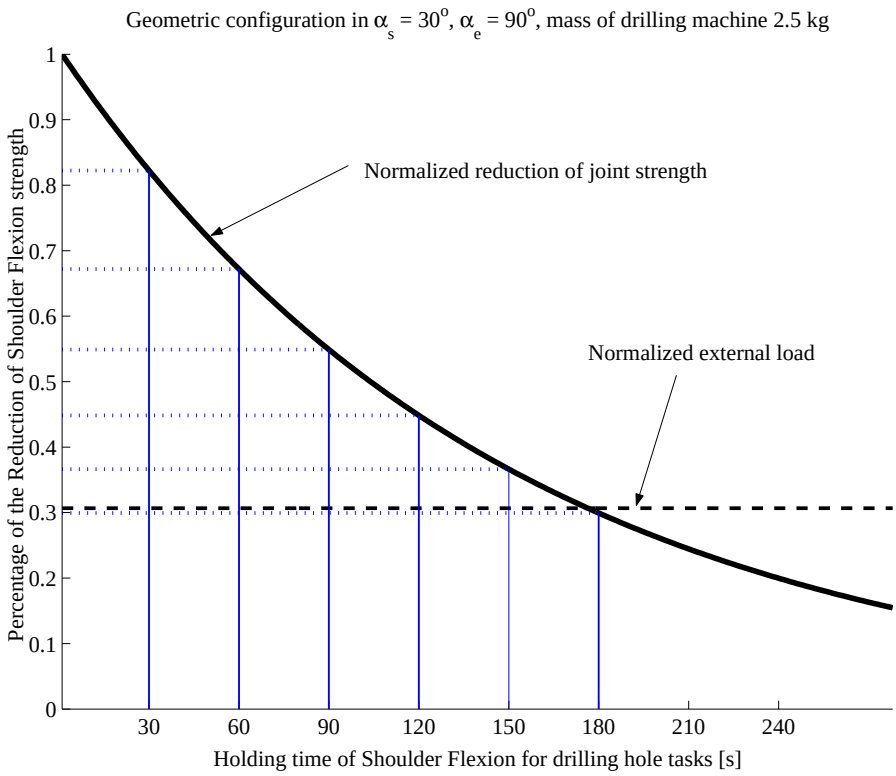

Figure 5.10: Fatigue evaluation after drilling a hole in a continuous drilling process

In our current research, **HS** includes only the joint strength vector. The evaluation of the fatigue is measured by the change of the joint strength for drilling a hole. The result is shown in Table 5.5. Three measurements are given in this table: one is the normalized physical strength every 30 seconds, noted as $\frac{\mathbf{HS}_i}{\mathbf{HS}_{max}}$; one is the difference between the joint strength before and after finishing a hole, noted as $\frac{\mathbf{HS}_i - \mathbf{HS}_{i+1}}{\mathbf{HS}_{max}}$; the last one is the difference between the joint strength and the maximum joint strength, noted as $\frac{\mathbf{HS}_{max} - \mathbf{HS}_i}{\mathbf{HS}_{max}}$. In Table 5.5, only the reduction of the shoulder joint strength is presented, since the relative load in elbow joint is much smaller.

From Fig. 5.10 and Table 5.5, the joint strength keeps the trend of descending in the continuous

Table 5.5: Normalized shoulder joint strength in the drilling operation

Time [s]	0	30	60	90	120	150	180
$\bar{m}$							
$\frac{\mathbf{HS}_i}{\mathbf{HS}_{max}}$	100%	82.2%	67.2%	54.9%	44.8%	36.6%	30.1%
$\frac{\mathbf{HS}_i - \mathbf{HS}_{i+1}}{\mathbf{HS}_{max}}$	0%	17.8%	15.0%	12.3%	10.1%	8.2%	6.5%
$\frac{\mathbf{HS}_{max} - \mathbf{HS}_i}{\mathbf{HS}_{max}}$	0%	17.8%	32.8%	45.1%	55.2%	63.4%	69.9%

work. The rate of the reduction gets smaller in the work progress due to the physiological change in the muscle fiber composition. More time consumed to work leads more reduction in physical strengths. The reduction relative to the maximum strength is able to assess the difficulty of the operations.

5.3.4 Experiment validation

Simulated drilling operations were tested under laboratory conditions in Tsinghua University. A total of 40 male industrial workers were asked to simulate the drilling work in a continuous operation for 180 seconds. Maximum output strengths were measured in the simulated operations at different periods of the operation. Fatigue was indexed by the reduction of the joint strength along time relative to the initial maximum joint strength. Three out of the 40 subjects could not sustain the external load for a duration of 180 seconds, and 34 subjects had a shoulder joint fatigue resistance (Mean=1.32, SD=0.62) greater than the average shoulder joint fatigue resistance in Table 3.4, which means that the sample population has a higher fatigue resistance than the population grouped in the regression.

The physical strength has been measured in simulated job static strengths, and the reduction in the operation varies from 32.0% to 71.1% (Mean=53.7% and SD=9.1%). The reduction falls in the fatigue prediction of the theoretical methods in Table 5.6 (Mean=51.7%, SD=12.1%).

Table 5.6: Normalized torque strength reduction for the population with higher fatigue resistance

$\frac{\mathbf{HS}_{max} - \mathbf{HS}_{180}}{\mathbf{HS}_{max}}$	$S - 2\sigma$	$S - \sigma$	S	$S + \sigma$	$S + 2\sigma$
$\bar{m}$	-	-	69.9%	62.5%	56.3%
$\bar{m} + \sigma_m$	-	63.2%	53.2%	46.4%	40.8%
$\bar{m} + 2\sigma_m$	64.9%	51.9%	43.0%	36.7%	31.9%

5.3.5 Discussion

Under the proposed framework, the conception of the virtual human status is introduced and realized by a virtual human modeling and simulation tool. The virtual human is kinematic modeled based on the modeling method in robotics. Inverse dynamics is used to determine the joint loads. With the integration of a general fatigue model, the physical fatigue in a manual handling operation in EADS is simulated and analyzed. The decrease in human joint strengths can be predicted in the theoretical approach, and it has been validated with experimental data.

Human status is introduced in this framework in order to generalize all the discussion for the human simulation. We concentrate only on the physical aspect of the virtual human, in particular on joint strengths. Physical status can be extended to other aspects, either measurable using instruments (e.g., heart rate, oxygen consumption, electromyograph of muscle, etc.) or predicable using mathematical models (e.g., vision, strength, etc.). Similarly, the mental status of human can also be established by similar terms (e.g., mental capacity, mental workload, mental fatigue, etc.). Under the conception of human status, different aspects of the human can be aggregated together to present the virtual human completely. The changed human status caused by a physical job or a mental job can be measured or predicted to assess different aspects of the job. It should be noted that the definition of human status is still immature and it requires great effort to form, extend, and validate this conception.

The main difference between the fatigue analysis in our study and the previous methods for posture analysis is: in previous methods (Wood et al., 1997; Iridiastadi and Nussbaum, 2006a; Roman-Liu et al., 2005), intermittent procedures were used to develop the fatigue model with job specific parameters; in contrast, all the related physical exposure factors are taken into consideration in a continuous approach in our model. In this way, the analysis of the manual handling operation can be generalized without limitations of job specific parameters. Furthermore, the fatigue and recovery procedures can be decoupled to simplify the analysis in a continuous way. Although only a specific application case is presented in this section, the feasibility of the general concept has been verified by the introduction of human status and the validation of the fatigue model.

It should be noted that the recovery of the physical strength has not been considered yet. Although there are several work-rest allowance models in the literature, substantial variability was found among the prediction results for industrial operations (El ahrache and Imbeau, 2009) and it is still ongoing to develop a general recovery model.

5.4 Multi-objective posture prediction

5.4.1 Mathematical description

The general purpose of the posture analysis based on multiple-objective optimization (MOO) is to find a set of $\mathbf{q}$ in order to minimize several objective functions simultaneously (5.1).

$$\min_{\mathbf{q}\in\Omega} \quad F(\mathbf{q}) = \begin{bmatrix} f_1(\mathbf{q}) \\ \vdots \\ f_i(\mathbf{q}) \\ \vdots \\ f_n(\mathbf{q}) \end{bmatrix} \tag{5.1}$$

subject to equality and inequality constraints in Eq. 5.2

$$\begin{cases} g_i(\mathbf{q}) \leq 0 & i = 1, 2, \cdots, m \\ h_i(\mathbf{q}) = 0 & j = 1, 2, \cdots, e \end{cases} \tag{5.2}$$

where m is the number of inequality constraints and e is the number of equality constraints. $\mathbf{\Omega}$ is the design space of $\mathbf{q}$ where all the $\mathbf{q}$ satisfies all the constraints.

Two human performance measures are used to create the global objective function: fatigue (stress) and discomfort. In addition to these two performance measures, there are several other objective functions, such as energy expenditure (Ren et al., 2007), joint displacement (Yang et al., 2004), visibility and accessibility (Chedmail et al., 2003), etc. In our current application, only fatigue and joint discomfort are taken into consideration for the posture prediction and evaluation, since the physical fatigue effect acting on the posture prediction is the main phenomena that should be verified. If several objective functions are involved in the posture prediction, it would be difficult to analyze the fatigue independently.

Objective function - fatigue

$$f_{fatigue} = \sum_{i=1}^{DOF} \left(\frac{\Gamma_i}{\Gamma_{cem}^i} \right)^p \tag{5.3}$$

In the literature, normalized muscle force is often used as a term to determine the muscle force. This term represents the minimization of muscle fatigue (also called stress) in the literature, and a similar measure has been used in Ayoub and Lin (1995) and Ayoub (1998) for simulating lifting activities. In our application, the summation of the normalized joint torques is used based on the same concept in Eq. 5.3. DOF is the total number of the revolute joints for modelling the human

body. For each joint, the term normalized torque $\frac{\Gamma_i}{\Gamma^i_{cem}}$ represents the relative load of the joint. The summation of the relative load is one measure to minimize the fatigue of each joint.

In traditional methods, Γ^i_{cem} is assumed to be constant in the maximum strength of the joint Γ^i_{max}. In our application, the fatigue process is mathematically modeled by a differential equation (Eq. 3.2) in order to integrate the fatigue effect.

It should be noted that the fatigue model should be sufficiently precise to reproduce the fatigue accurately in virtual human simulation. More precision requires more parameters to identify the model, while simpler models bring more prediction errors. Thus, there must be a compromise between the precision and the complexity of the model. In Ma et al. (2009), different muscle fatigue models in the literature have been discussed, from the simple to complex ones. The existing muscle fatigue models are either too sophisticated for ergonomics analysis or too simple to integrate with the influences from external loads over time. Although the fatigue model involved in multi-objective optimization is not as precise as physiological mechanism based models, it provides a way to combine the temporal parameters (t), the physical load (Γ_load), and the individual characteristics (k and Γ_{max}). The only two parameters need to be determined for each joint are the maximum strength Γ_{max} and the fatigue ratio k, which offers a relatively simple but precise method to integrate muscle fatigue into virtual human simulation.

Besides fatigue, the recovery of the physical capacity should also be modeled to predict the work-rest schedule in order to complete the design of manual handling operations. The recovery model in Eq. 6.2 predicts the recuperation of the physical capacity (Wood et al., 1997; Carnahan et al., 2001).

Objective function - discomfort

Another objective function is joint discomfort. The discomfort measure is taken from VSR (Yang et al., 2004). This measure evaluates the joint discomfort level from the rotational position of joint relative to its upper limit and its lower limit. The discomfort level is formulated in Eq. 5.4, and it increases significantly as joint values approach their limits. QU (Eq. 5.6) and QL (Eq. 5.7) are penalty terms corresponding to the upper limit and lower limit of the joint. γ_i is the weighing value for each joint. The detailed notation of the variables in the discomfort model is listed in Table 3.

$$f_{discomfort} = \frac{1}{G}\sum_{i=1}^{DOF}\left[\gamma_i(\Delta q_i^{norm})^2 + G\ QU_i + G\ QL_i\right] \tag{5.4}$$

$$\Delta q^{norm} = \frac{q_i - q_i^N}{q_i^U - q_i^L} \tag{5.5}$$

$$QU_i = \left(0.5\sin\left(\frac{5.0\left(q_i^U - q_i\right)}{q_i^U - q_i^L} + \frac{\pi}{2}\right) + 1\right)^{100} \tag{5.6}$$

$$QL_i = \left(0.5\sin\left(\frac{5.0\left(q_i - q_i^L\right)}{q_i^U - q_i^L} + \frac{\pi}{2}\right) + 1\right)^{100} \tag{5.7}$$

In these equations, Δq_i^{norm} is the joint position relative to the neutral position of a joint after normalization (Eq. 5.5). q_i^U and q_i^L are the upper joint limit and lower joint limit, respectively. $G \times QU_i$ is a penalty term associated with joint values that approach their upper limits, and $G \times QL_i$ is a penalty term associated with joint values that approach their lower limits. G is a constant with a value 1×10^6.

An example calculated from joint discomfort is shown graphically in Fig. 5.11. It is apparent that the joint discomfort reaches its minimum value at a neutral position and it increases when approaching its upper and lower limits.

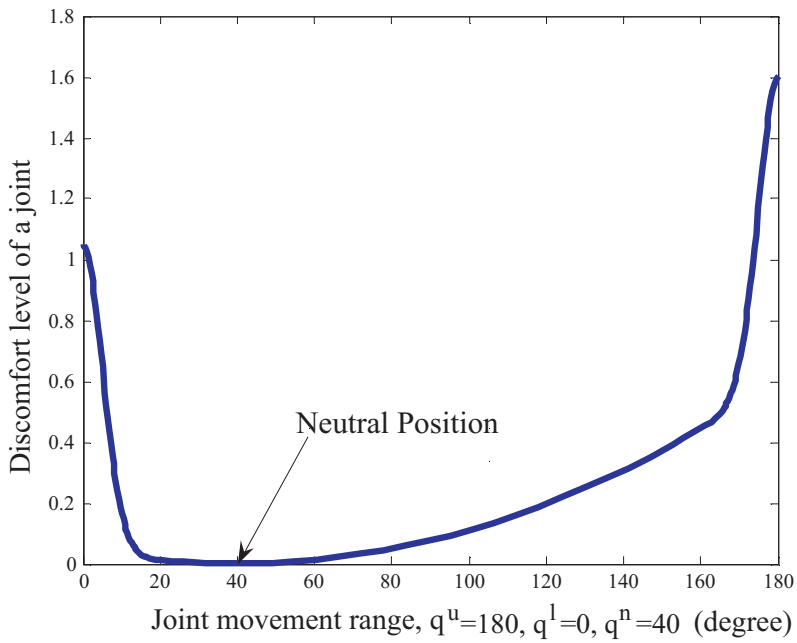

Figure 5.11: Joint discomfort example

The overall objective function (Eq. 5.8) uses fatigue and discomfort measures to determine the optimal geometric configuration of the posture. The biomechanical aspect of the posture is evaluated by the fatigue objective function, and meanwhile, the geometrical constraints for the human body are measured by the discomfort measure.

$$\min \quad F(\mathbf{q}) = \begin{cases} f_{fatigue}(\mathbf{q}) \\ f_{discomfort}(\mathbf{q}) \end{cases} \tag{5.8}$$

Constraints

In this study, kinematical and biomechanical constraints are used to determine the possible design space.

With respect to kinematics, the Cartesian coordinates of the destination for the posture contributes to one constraint in Eq. 5.9. $\begin{bmatrix} x & y & z \end{bmatrix}^T$ is the Cartesian coordinates of the end-effector (right hand and left hand) indicating the aim of the reach. The function $X(\mathrm{q})$ can be described in direct kinematic approach. The transformation matrix between the end-effector and the reference coordinates can be modeled using modified Denavit-Hartenberg method.

$$\begin{bmatrix} x \\ y \\ z \end{bmatrix} = X(\mathrm{q}) \tag{5.9}$$

Joint limits (ranges of motion) are imposed in terms of inequality constraints in the form of Eq 5.10.

$$q_i^L \leq q_i \leq q_i^U \tag{5.10}$$

With respect to biomechanics, theoretically there are two main constraints. One is the limitation of the joint strength (Eq. 5.11) and another one is the equilibrium equation described in inverse dynamics in Eq. 5.12.

It should be noted that in Eq. 5.11 the upper limit $\Gamma^i_{\max}$ is treated as unchangeable in conventional posture prediction methods. In our optimisation method, the upper limit is replaced by Γ^i_{cem} to update the physical capacity caused by fatigue.

$$0 \leq \Gamma_i \leq \Gamma^i_{\max} \tag{5.11}$$

In terms of equality constraints, another constraint is the inverse dynamics in Eq. 5.12. With displacement, velocity and acceleration in general coordinates, the inverse dynamics formulates the equilibrium equation. In Eq. 5.12, $\mathbf{\Gamma}(\mathbf{q}, \dot{\mathbf{q}}, \ddot{\mathbf{q}})$ represents the term related to external loads, $\mathbf{A}(\mathbf{q})$ is the link inertia matrix, $\mathbf{B}(\mathbf{q}, \dot{\mathbf{q}})$ represents centrifugal and coriolis terms, and $\mathbf{Q}(\mathbf{q})$ is the potential term.

$$\Gamma(\mathbf{q}, \dot{\mathbf{q}}, \ddot{\mathbf{q}}) = \mathbf{A}(\mathbf{q})\ddot{\mathbf{q}} + \mathbf{B}(\mathbf{q}, \dot{\mathbf{q}})\dot{\mathbf{q}} + \mathbf{Q}(\mathbf{q}) \tag{5.12}$$

In summary, the MOO problem can be simplified as: for a static posture or quasi static posture, we can assume that $\dot{\mathbf{q}} = \mathbf{0}$, and $\ddot{\mathbf{q}} = \mathbf{0}$, therefore, the joint torque depends only on the joint position and the external load. A set of solution satisfying all the constraints $\mathbf{\Omega} = \{\mathbf{q} |\ g(\mathbf{q}) \leq \mathbf{0}, h(\mathbf{q}) = \mathbf{0}\}$ can

be found. In this case, we are trying to find a configuration $\mathbf{q} \in \mathbf{\Omega}$ to achieve the optimization of both fatigue and discomfort objective functions.

5.4.2 Results

After kinematic and dynamic modeling of the human arm, the posture analysis and posture prediction based on MOO can be carried out.

Optimal posture for a drilling task

In manual handling operations, the workspace parameters are important for determining the posture of the human body. In the case of holding the drill, the distance between the hole and the shoulder is the most important geometrical constraint if the height of the hole and the height of the virtual human are predefined and fixed. In the 0.4m to 0.7m range, the geometrical configuration $\mathbf{q}$ can be determined, and then it is possible to calculate the fatigue measure and the discomfort measure. Both measures are shown in Fig. 5.12. It is obvious that longer distance means greater arm extension. As a result, larger torque is applied to the joints, especially for the shoulder joint, which causes greater fatigue effects (solid curve). Simultaneously, the discomfort level changes with distance. The larger the extension of the arm, the more the shoulder joint moves to its upper limit, however the elbow joint approaches to its neutral position. The combination of both joints shows the declination along the distance (dash curve).

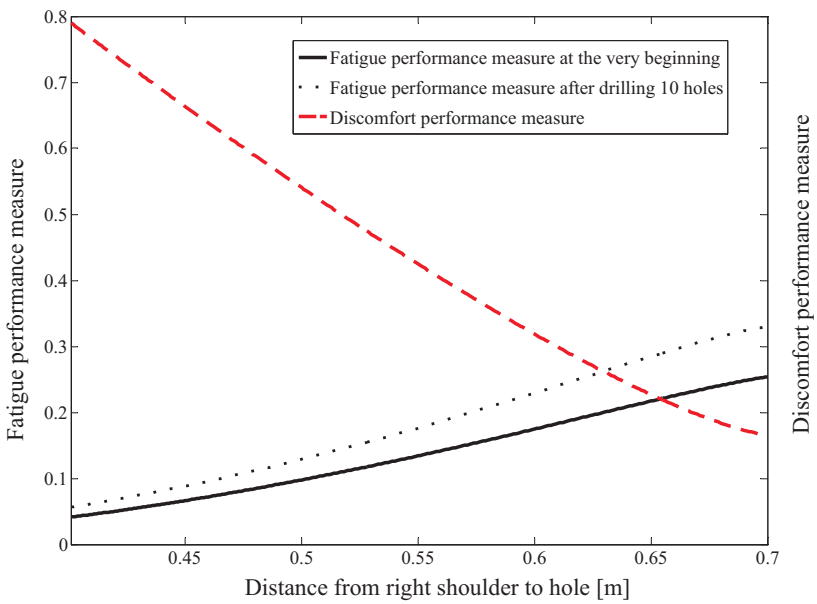

Figure 5.12: Posture prediction

The optimal posture can be determined using the MOO method in Fig. 5.13. Weighted aggregation method is used to covert the Multi-Objective problem into a Single-Objective problem in order to achieve the Pareto optimal in the Pareto Front represented by the solid curve. The single objective is mathematically formed in Eq. 5.13. Both measures are normalized.

$$\min Z = \sum_{j=1}^{N} w_j f_j(\mathbf{q}) = w_1 \frac{f_{discomfort}}{\max(f_{discomfort})} + w_2 \frac{f_{fatigue}}{\max(f_{fatigue})} \tag{5.13}$$

where $w_j \geq 0$ and $\sum_{j=1}^{N} w_j = 1$. Each w_j indicates the importance of each objective. This objective function can be further transformed to a straight line equation: $f_{fatigue} = -\frac{w_1}{w_2} f_{discomfort} + \min Z$.

If we assume that the fatigue and the discomfort have the same importance in the drilling case, the optimal position can be obtained at the intersection point between the solid straight line with slope $-\frac{w_1}{w_2} = -1$ and the Pareto front in Fig 5.13. However, the selection of the weighting value can have a great influence on the choice of optimal posture. The individual preference can be represented by the different weights of the two measures which results in straight lines with different slopes. In Fig. 5.13, two examples with slope $-\frac{w_1}{w_2} = -2$ (dash-dot line) and $-\frac{w_1}{w_2} = -0.5$ (dash line) are illustrated with different intersection points with the Pareto front. Those two points represent different posture strategies for posture control: the former one with less discomfort, and the latter one with less joint stress. All the points in the Pareto font are the feasible solutions for posture prediction. The selection of posture depends on the physical status of individual and the preference of the individual, and the selection might represent the strategy taken by the subject while generating a posture.

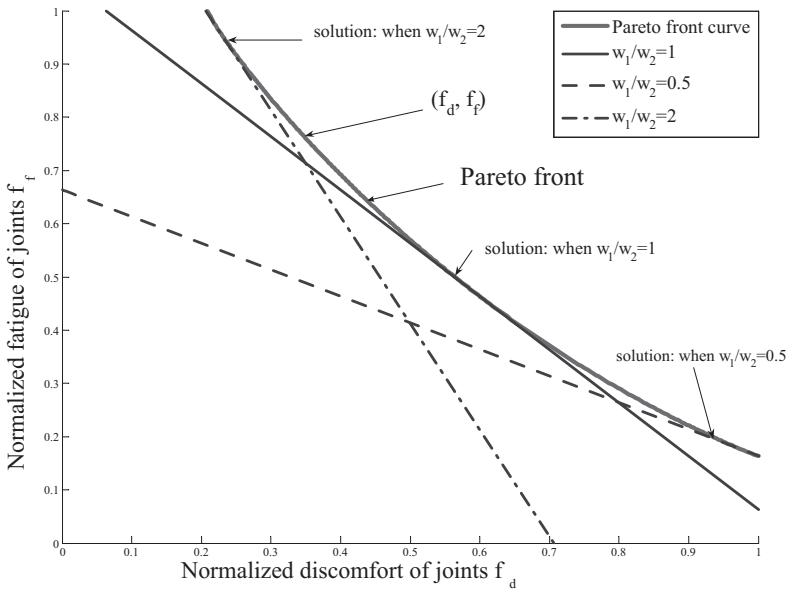

Figure 5.13: MOO prediction in Pareto front

It should be noted that the subjective influence, especially the voluntary effort, might change the posture dramatically. The human can maintain a very difficult posture under voluntary control for a certain period. That situation is outside of the predictive capabilities of the posture prediction method. In addition, in this application case, the design space is relatively large since there is no strong geometrical constraint for the posture. In this way, there are several possible options to choose an optimal posture. With stronger constraints, for example, assembly operation in a very narrow and complicated work space, the accessibility might be the determinant factor to choose the posture for the human. But that leads to another domain of posture prediction which is beyond the scope of the current research.

Optimal posture changed by fatigue effect

Meanwhile, fatigue influences the posture. In order to evaluate the fatigue effect, we keep the same balance between fatigue and discomfort in our application. In Fig. 5.14, the single objective function in Eq. 5.13 along the distance from 0.4 m to 0.7 m is calculated and shown. The solid curve does not consider fatigue, and the dash curve considers fatigue status after maintaining a drilling operation for 30 s. From the left subfigure, it is noticeable that the optimal distances for both situations are different, which maps onto different drilling postures. The optimal distance between the shoulder and the hole is smaller with fatigue than without fatigue. It demonstrates that the manual handling strategy of bringing the arm closer to the human body when there is fatigue to maintain the same load by reducing the moment produced by the mass of the upper arm. This is consistent with the result in Fuller et al. (2008). In this posture, the user can handle the weight of the machine more easily. In the right subfigure, the Pareto front with fatigue is shifted away from the Pareto front without fatigue as fatigue increases resulting from the reduction of physical capacity.

5.4.3 Discussion

In this section, a fatigue model is integrated into a posture analysis and posture prediction method. With this model, it is possible to evaluate and design the posture for manual handling operations by considering fatigue. The fatigue model can predict the reduction of the physical capacity in static posture or quasi-static operation. The reduction of the physical capacity causes the posture to change to maintain the external physical requirement.

One limitation in our framework is that the posture analysis and prediction are limited to the joints, without consideration of the muscles. It is difficult to measure the force of each individual muscle, although the optimization method is employed to solve the underdetermined problem of the muscle skeleton system. The precision of the result is still questionable (Freund and Takala,

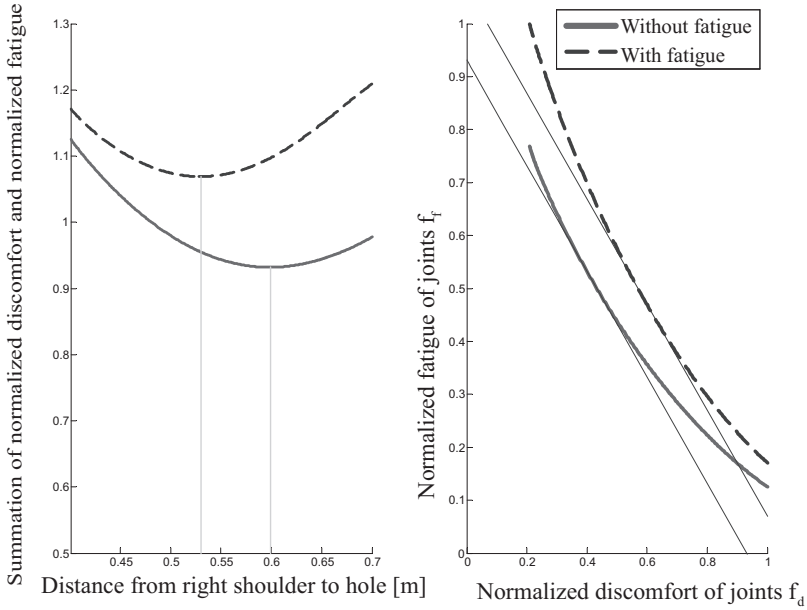

Figure 5.14: Posture prediction under consideration of fatigue effect

2001). From another point of view, the joint torque is generated and determined by a group of muscle attached around the joint. The coordination of the muscle group is very complex, and it is believed that calculating the joint torque can achieve a higher precision than calculating the individual muscle forces. Meanwhile, in several ergonomics measurement, the MET model is also measured by the joint torque (Mathiassen and Ahsberg, 1999) which proves the feasibility of our method. It should be noted that MVC in the torque level depends on current joint state and different joint configurations might generate different maximum strengths. In fatigue evaluation and posture prediction applications, only static posture or quasi-static posture were engaged in those operations, therefore the variation of the joint maximum strength can be neglected since only slight change of posture occurs during those operations. In addition, the proportion of the fatigued motor units might remain almost the same while changing the postures. Hence, the fatigue level in previous posture might be used to determine the current maximum strength under current new posture in quasi-static cases.

Another limitation is that the result of the posture analysis is only applicable for static and slow operations, because the fatigue model is only validated by comparing with existing MET models. For these static MET models, all the measurement was carried out under static posture. Dynamic motion and static posture are different in physiological principle, and fatigue and recovery phenomenon might occur alternatively and co-vary in a dynamic process.

At last, the optimal posture is predicted in the MOO method. Two objective functions, fatigue and comfort, are taken into account to determine the optimal posture during manual handling operations, and both objective functions are considered as strategies leading the human motion. However, differ-

ent strategies might be taken by a subject while performing a task and lead to different setups of the optimization. For example, if a subject is willing to take advantage of passive torques provided by the tendons, there should be no "comfort" criterion that tends to repulse from the joint limits. The MOO optimization approach should be used with caution. In the MOO method, the weighting values of each item are used to construct the overall objective function. However, it requires a priori knowledge about the relative importance of the objectives, and the trade-off between the fatigue and the discomfort cannot be evaluated easily. "It is believed that the human body has certain strategy to lead the human motion, but it is dictated by just one performance measure; it may be necessary to combine various measures" (Yang et al., 2004). Different strategies might be used in leading the motion by different subjects, and there might be different priorities while using these strategies. In case very constrained environment, it is possible that the accessibility is the determinant strategy for choosing the posture or trajectory. Therefore, two main problems arise for the motion prediction. One is how to model the performance measure. Another one is how to combine all the performance measures together. Human motion is very complex due to its large variability. Each single performance measure is difficult to validate in an experiment. Furthermore, for the combination, the correlation between different performance measures requires lots of effort to define and verify. MOO method provides a reference method in ergonomics simulation leading to a safer and better design of work.

5.5 Summary

In this chapter, posture analysis and posture prediction for an EADS drilling task based on the fatigue model have been presented after the detailed digital human modeling process.

In digital human modeling process, a virtual human is modeled from the geometrical level to the graphical level. Necessary information can be integrated into the virtual human step by step in this process. Although we only presented a model with limited precision, it could verify the possible application of our fatigue model in posture analysis and posture prediction. Much higher precision can be achieved, once more effort can be contributed into modeling process. This part is out of discussion in our current research work, since it is not the main focus of our research.

In posture analysis, using the kinematic modeling and inverse dynamics, the forces and torques at the joints of the arm can be calculated for a manual handling operation. Based on the fatigue model, the reduction of the physical strength caused by the external load along time can be assessed by assessing the differences of human physical status before and after an operation. Agreement has also been found between the simulated result and the experimental results. It is promising that this method provides a new approach for fatigue evaluation for a certain population.

In posture prediction part, a new method based on the MOO method for posture prediction and analysis is presented. Different from the other methods used in virtual human posture prediction, the effect from fatigue is taken into account. The fatigue model based on motor-units pattern is integrated into the MOO method to predict the reduction of physical capacity. Meanwhile, the work-rest schedule can be evaluated with the fatigue and recovery model. Given the validation of the fatigue model, this method is suitable for static or relative slow manual handling operations. Finally, it is possible to predict the optimal posture of an operation to simulate the realistic motion. In the future, the fatigue for dynamic working processes will be validated and integrated into the work evaluation system.

In summary, based on the fatigue model, it is promising to carry out posture analysis and posture prediction by considering the fatigue effect along time.

Chapter 6

Muscle recovery model

Contents

6.1 Introduction 115
6.2 Muscle recovery model 116
6.3 Application 122
6.4 Discussion 125
6.5 Summary 128

6.1 Introduction

During a manual handling operation, recovery represents the processes which are the opposite of those leading to fatigue, and describes a return to the unfatigued state.

Recovery is defined as:

Definition 5 Recovery

Increase of the functional capacity of an organ or organism, of which the functional capacity was reduced as a result of fatigue; recovery occurs by ending, reducing or changing the action which results in reduction of the functional capacity of an organ or of an organism. (Rohmert, 1973)

Fatigue level and recovery level are defined and used to complete the recovery process clearly. Fatigue level (degree of fatigue) is the state of functional capacity or an organ or an organism reached through fatigue; recovery level is the state reached through recovery. In fact, both are the same thing in nature indicating the current state of an organ, but in different contraction conditions.

The same variables as in measuring fatigue can be used to indicate recovery in physical process, and indeed these measurements have been used as recovery levels to construct different recovery models in the literature. For example, force has been measured to model the recovery process in some

researches (Edwards et al., 1977; Wood et al., 1997; Duong et al., 2001); the remaining endurance time is used as recovery level in Milner et al. (1986); working heart rate, breathing depth, systolic blood pressure, oxygen uptake, and blood lactate are also used as indicators for modeling recovery processes since the work has been done by Rohmert and his colleagues (Rohmert, 1973; Rohmert and Rutenfranz, 1983); the median frequency in surface EMG is taken to model the recovery process (Elfving et al., 2002). The recovery processes occur exponentially with respect to time in those physiological processes, and some previous studies have used exponential time dependences to describe recovery. However, these models are from mathematical regression under specific operation conditions, and they cannot be easily extended to other manual operations.

In Ergonomics, combining MET models and recovery models, different work rest allowance models have been developed in order to determine suitable work cycles and further to reduce MSDs caused from prolonged static muscular exertions. Rest allowance (RA) in static work represents the time needed for adequate rest following a static exertion, and it is generally expressed as a percentage of holding time ($RA\% = 100 \times resting\ time \div holding\ time$). In account of the differences in the approaches taken by the researchers to build their models, substantial discrepancies in work-rest allowance models have been reported in El ahrache and Imbeau (2009). Information to guide the selection of the most appropriate rest allowance model is lacking. The limitations of the RA models are: the recovery models are constructed from experimental data, and they cannot be explained in muscle physiological principle; there is no parameter representing the individual differences in recovery process which have been found in the preivous research (Elfving et al., 2002).

In this chapter, we are going to propose a recovery model with almost the same parameters as in the fatigue model aiming at giving a general recovery model. This recovery model is theoretically analyzed in comparison with other recovery models from the literature. Potential applications are also given to demonstrate the prediction of RA and the change of physical status in work cycles. Discussion is presented to deal with the limitations and further research work on the recovery model.

6.2 Muscle recovery model

6.2.1 Mathematical description of recovery model

In order to keep consistent to our fatigue model, the same parameters have been used to construct the recovery model (Eq. 6.1). In this recovery model, force or torque is used as fatigue or recovery levels, and the recovery process is formulated in a differential equation, where $R\ (min^{-1})$ is a parameter to describe the rate of recovery of different muscle groups from different individuals. In Eq. 6.1, it is supposed that the rate of recovery R for a specific joint or muscle group of an individual keeps

constant for a certain period, and the recovered capacity per time is proportional to the fatigued part $(\Gamma_{j,max} - \Gamma_{j,cem}(t))$.

$$\frac{d\Gamma_{j,cem}(t)}{dt} = R(\Gamma_{j,max} - \Gamma_{j,cem}(t)) \tag{6.1}$$

The integration of Eq. 6.1 is Eq. 6.2, where $\Gamma_{j,cem_{ini}}$ is the remained strength at the very beginning of the recovery process while $t = 0$. Eq. 6.2 indicates the recovery process after an operation. The fatigue level in our research is defined as the percentage of $\Gamma_{j,cem_{ini}}$ relative to $\Gamma_{j,max}$, $\frac{\Gamma_{j,cem_{ini}}}{\Gamma_{j,max}} \times 100$. The recovery level is defined as the percentage of the $\Gamma_{j,cem}(t)$ relative to $\Gamma_{j,max}$, $\frac{\Gamma_{j,cem_t}}{\Gamma_{j,max}} \times 100$.

$$\begin{aligned} \Gamma_{j,cem}(t) &= \Gamma_{j,max} + (\Gamma_{j,cem_{ini}} - \Gamma_{j,max})e^{-Rt} \\ &= \Gamma_{j,cem_{ini}} + (\Gamma_{j,max} - \Gamma_{j,cem_{ini}})(1 - e^{-Rt}) \end{aligned} \tag{6.2}$$

Recovery time is the time necessary to restore the capacity to the full recovery level, and the recovery time depends on the definition of the full recovery level. In our case, parameter p is used to define the full recovery level, therefore the recovery time from fatigued joint to p of $\Gamma_{j,max}(t)$ can be calculated from Eq. 6.2 by Eq. 6.3. If $\Gamma_{j,cem_{ini}} = q\Gamma_{j,max}$, Eq. 6.3 can be transformed to Eq. 6.4.

$$t = -\frac{1}{R}\ln\left(\frac{p\Gamma_{j,max} - \Gamma_{j,max}}{\Gamma_{j,cem_{ini}} - \Gamma_{j,max}}\right) \tag{6.3}$$

$$t = -\frac{1}{R}\ln\left(\frac{p-1}{q-1}\right) \tag{6.4}$$

We define a half-time $t_{1/2}$ at which the recovery level $p = \frac{1+q}{2}$ can be obtained (the muscle recovers 50% of the difference between 100% recovery level and the initial fatigue level), and the recovery half-time can be calculated in seconds in Eq. 6.5:

$$t_{1/2} = \frac{\ln 2}{R} \times 60 \tag{6.5}$$

The recovery processes (R remains constant) starting from different fatigue levels (0%, 25%, 50%, and 75%) are shown in Fig. 6.1 based on our recovery model. It is obvious that at the beginning of the recovery, the physical capacity is restored relative faster than that at the end of the recovery. There are large differences between the duration necessary to recover to 90% of the maximum capacity, and it takes almost the same time to higher recovery level, e.g. 99%.

Figure 6.1 represents different recovery processes of an specific individual, while Fig. 6.2 represents different recovery processes of different individuals (different rates of recovery) from a specific fatigue level (50%). It shows graphically that different individual might require different time to achieve the same recovery level, meanwhile there might be no big difference while approaching to high recovery level.

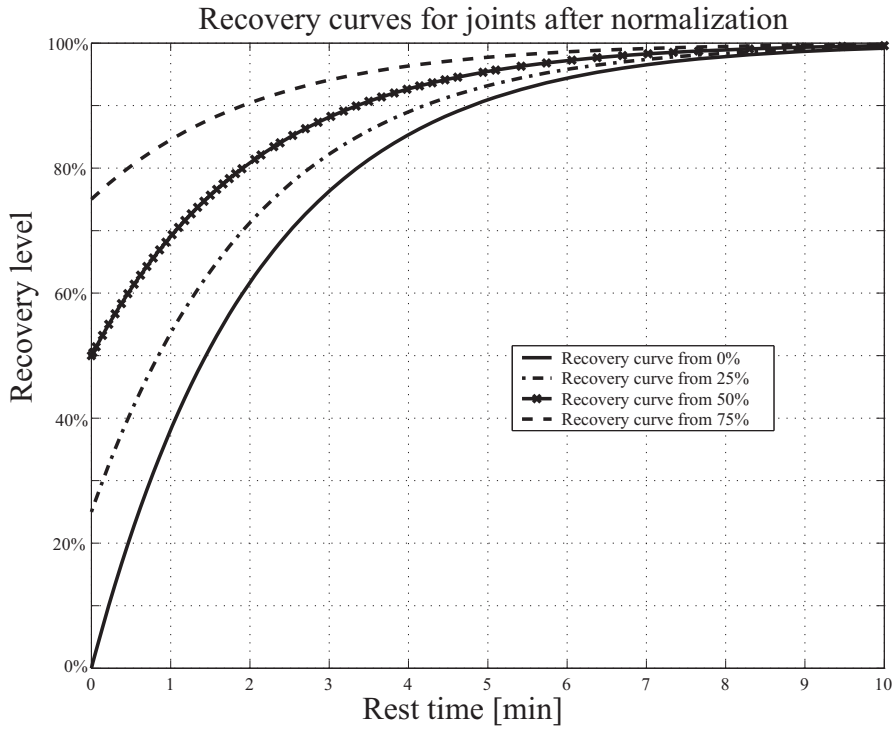

Figure 6.1: Recovery curves of joint from different fatigue levels

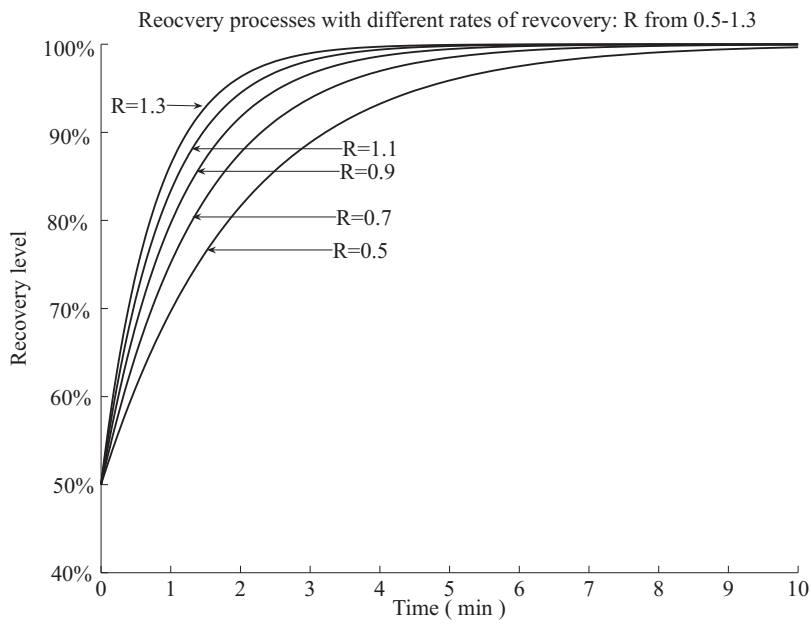

Figure 6.2: Recovery curves of joint under different rates of recovery

6.2.2 Analysis of the recovery model

In this subsection, the proposed recovery model is going to be compared with different recovery models, qualitatively or quantitatively. The aim of the comparison is to reveal the agreement of our model with other models in the literature, and it can provide a promising result for the validation of the recovery model.

Wood's model

Wood et al. (1997) proposed a model to predict the amount of fatiguable strength during repetitive jobs. Repetitive jobs compose of several same work cycles. Each work cycle has the same work arrangement in which there are working interval and rest interval. Assume that there are n work cycles, and the recovery of maximum force capacity in the ith rest interval is modeled in Eq. 6.6 theoretically.

$$GS_{(i+1)} = GE_i + (MAXG - GE_i)(1 - \exp(-0.085RT)) \tag{6.6}$$

where GS_{i+1} (kg) is the grip strength at the start of gripping interval $i + 1$; GE_i (kg) is the grip strength at the end of gripping interval i ; RT (s) is the duration of the rest interval ; $MAXG$ (kg) is the individual maximum grip strength capacity.

This model has been used in Carnahan et al. (2001) in assembly line design for gripping jobs to predict the amount of grip strength recovered at the end of a rest interval. During this interval, the worker is not exerting a grip force. When fit to the results from the experiment, this model explained 94% of the variance.

Eq. 6.6 can be easily transformed to $GS_{(i+1)} = MAXG + (GE_i - MAXG)\exp(-0.085RT)$, which is exactly in the same way as in Eq. 6.2. R in this model is approximately 5.1 min^{-1} for the gripping strength.

Liu's model

Liu's motor units pattern model (Liu et al., 2002) provides a general approach to analyze fatigue from muscle physiological mechanism. Suppose that in recovery period, there is no active motor units and no active commands from CNS, therefore, the recovery can be simplified to Eq. 6.7 from Eq. 1.10,.

$$\frac{dM_F}{dt} = -R\,M_F \tag{6.7}$$

Replace M_F by $(F_{max} - F_{cem})$, since both represent the fatigued motor units in human muscles. Equation 6.8 can be obtained.

$$\frac{\mathrm{d}(F_{max} - F_{cem})}{\mathrm{d}t} = -R\,(F_{max} - F_{cem}) \tag{6.8}$$

After simplification, Equation 6.8 can be simplified to Eq. 6.9 which has the same formation as Eq. 6.1, while F_{max} is constant.

$$\frac{\mathrm{d}F_{cem}}{\mathrm{d}t} = R\,(F_{max} - F_{cem}) \tag{6.9}$$

This model has been verified by experiments with right hand maximum gripping strength measurement. R varies from 0.0042 s^{-1} to 0.0125 s^{-1} after fitting from experimental results. It should be noticed that in this experiment, the recovery is not separated from the fatigue process. In contrast, they are mixed together to measure the force reduction in the maximum force exertion. However, the variation of the rates of recovery is still useful to demonstrate the differences in rates of recovery between subjects.

Other models

In Elfving et al. (2002), the recovery of the median frequency of the power spectrum of the EMG after fatigue has been studies to obtain reference data for healthy subjects (n=55). Agreement with exponential time dependence (Eq. 6.10) was with coefficient of determination $r^2 = 0.98$.

$$f = f_e + (f_i - f_e)(1 - \exp(-\frac{t}{\tau})) \tag{6.10}$$

where τ (min) is the relaxation time constant; f_e (Hz) is the frequency at the end of the fatigue contraction; f_i (Hz) is the recording frequency at time t from the start of the recovery.

In this EMG model, the recovery half-time (s) $t_{1/2} = \tau \ln 2 \times 60$ are calculated to indicate the recovery rates. After recalculating from $t_{1/2}$ to R by Eq. 6.5, R varies from 1.06 to 1.13 for mean recovery data of back extension test. From the experiment results, it has been stated that the exponential model showed very good agreement with mean recovery data, indicating an underlying average process with an exponential time dependence. The analysis of recordings of recovery from individuals is also possible by regression, and recordings of recovery from individuals showed large fluctuations.

Furthermore, in Yassierli et al. (2007), strength recovery following shoulder abduction and torso extension has been measured and fitted to exponential curves (Eq. 6.11).

$$S = A - B\exp(-ct) \tag{6.11}$$

where S is the percentage of the initial maximum strength; A, B, and c are constants varying for different individual. From experimental results on strength recovery from 24 young subjects and 24 old subjects, c varies from 0.82 (young subjects) to 1.58 (old subjects) for shoulder abduction and

from 0.35 (young subjects) to 0.41 (old subjects) for torso extension. The results demonstrates the exponential dependence of the recovery, and the recovery rates varies according to muscle groups and ages.

In this subsection, different recovery models have been listed and compared to our theoretical proposition. Although different parameters have been engaged in the models, single exponential function is used in every model to reproduce different aspects of recovery, which can also be realized from our generalized fatigue model. It has been mentioned in Elfving et al. (2002), muscle strength recovers more rapidly than muscle endurance after local muscle fatigue. Recovery of the power spectrum of the EMG seems to be more rapid process than the recovery of muscle force and endurance. The similar statement has been illustrated in Westgaard and Winkel (1996) (see Fig. 6.3).

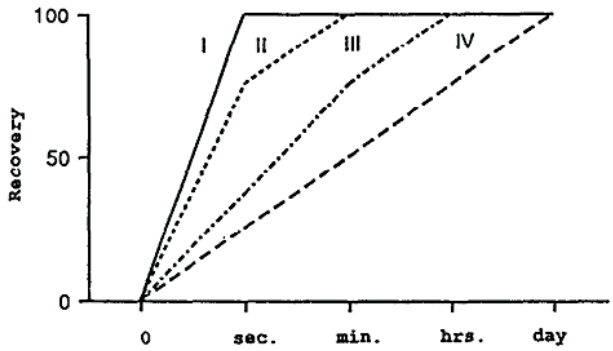

I: PCr, electrolytes, ATP, EMG
II: BF, HR, BP, lactate, muscle temperature
III: MVC, fatigue time
IV: force at muscle stim., muscle glycogen

Figure 6.3: Schematic illustration of recovery time for different parameters after a fatiguing contraction, adapted from Westgaard and Winkel (1996)

Different measurements in constructing the recovery model leads to different parameters, especially recovery rates. The comparison between our recovery model and the other existing models in the literature provides a promising result that our recovery model is able to predict the recovery process in manual handling operations.

6.3 Application

6.3.1 Rest-allowance Model

Theoretical analysis of rest-allowance model

In combination with fatigue model, it is possible to develop a new work rest allowance model to predict suitable rest time for manual handling operation.

Suppose that in a static operation, the actual holding time (Eq. 6.12) can be expressed by the f_{HT} and the maximum endurance time derived from Eq. 3.8.

$$HT = f_{HT}\ MET = -f_{HT}\frac{\ln(f_{mvc})}{(k\ f_{mvc})} \tag{6.12}$$

Then the normalized remained capacity (fatigue level) F^N_{cem} at time instant $t = HT$ is calculated by Eq. 6.13.

$$F^N_{cem} = q = \frac{F_{cem}}{MVC} = \exp(-k\ f_{mvc} * HT) = \exp(f_{HT}\ln f_{MVC}) = (f_{MVC})^{f_{HT}} \tag{6.13}$$

Therefore, according to Eq. 6.3, the required recovery time to recovery level p is expressed in Eq. 6.14:

$$RT = \frac{-\ln\dfrac{p-1}{F^N_{cem}-1}}{R} = \frac{-\ln\dfrac{p-1}{q-1}}{R} \tag{6.14}$$

Then, according to the definition of rest-allowance, the RA is expressed in Eq. 6.15

$$RA = \frac{RT}{HT} = RA(f_{HT}, f_{MVC}) = \frac{k f_{MVC}\ln\dfrac{p-1}{(f_{MVC})^{f_{HT}}-1}}{R f_{HT}\ln f_{MVC}} \tag{6.15}$$

In Eq. 6.15, k and R represent the personal factors on the RA. $\frac{k}{R}$ determines globally the influence from each individual: larger fatigability k requires more time to recover when the other parameters remains the same, since holding time is shorter while the recovery time remains the same; larger rate of recovery R results in shorter recovery time and therefore shorter rest allowance. The engagement of f_{HT} and f_{MVC} in determining RA is relative complicate, and it is graphically shown in Fig. 6.4. Suppose $k = 1$ and $R = 1$, the profile shows the rest allowance for different force levels $f_{MVC} \in (0.1, 1.0)$ and different holding durations $f_{HT} \in (0.1, 1.0)$.

Holding time and recovery time are shown in Fig. 6.5 to explain the profile in Fig. 6.4. Obviously, holding time is the monotonically increasing function of f_{HT}, while f_{MVC} keeps constant; it is also the monotonically decreasing function of f_{MVC}, while f_{HT} remains the same. The profile of the recovery time is calculated under recovery level $p = 99.95\%$. Recovery time is the monotonically increasing function of f_{HT}, and it is the monotonically decreasing function of f_{MVC} as well. However, according

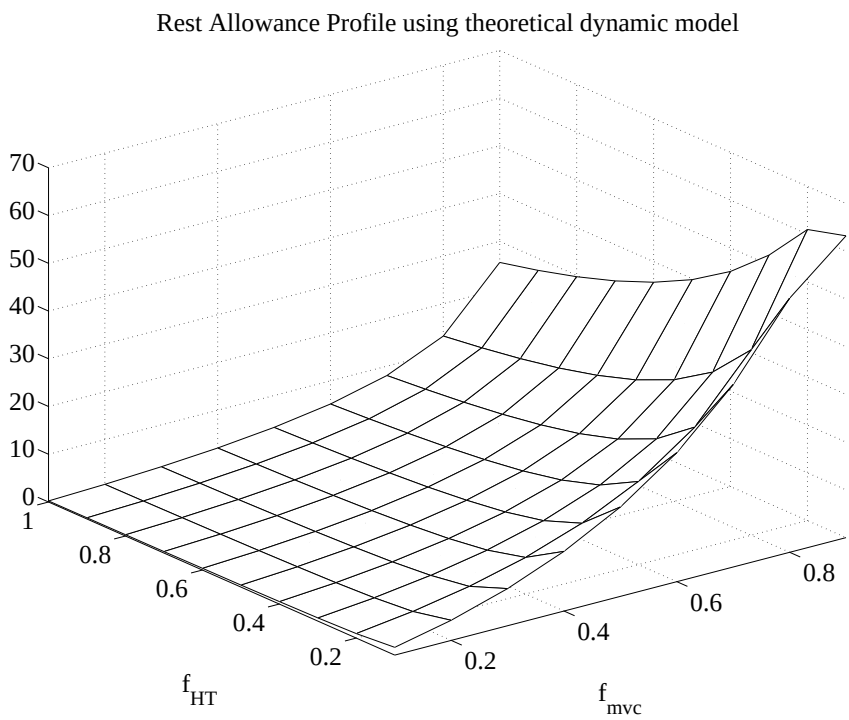

Figure 6.4: Rest allowance profiles using the theoretical approach

to the analysis in Fig. 6.1, there are no substantial differences in recovery time from different fatigue levels to the high recovery level. As a result, the rest-allowance profile reaches to its lowest point, when f_{HT} approaches to 1 and f_{MVC} approaches to 0, since the endurance time is infinite and the recovery time is relative tiny. Theoretically, the highest point occurs while f_{HT} approaches to 0 and f_{MVC} approaches to 1. However, this case is extremely difficult to be reached in real manual operation.

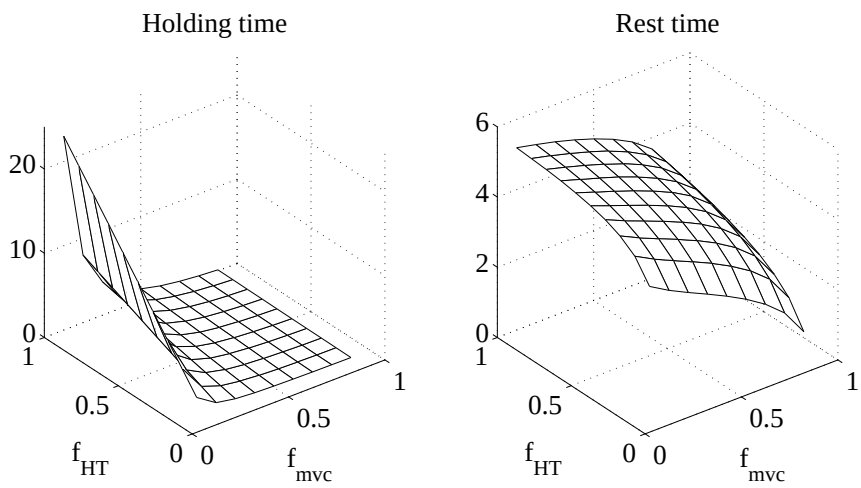

Figure 6.5: Holding time and recovery time using the theoretical approach

Comparison to other Rest-allowance models

Four RA models have been summarized in El ahrache and Imbeau (2009) (see Table 6.1). Each RA model can be expressed as a function of f_{HT} and f_{MVC} according the modification in El ahrache and Imbeau (2009). All these four profiles are shown in Fig. 6.6.

Table 6.1: Rest allowance (RA) models (adapted from El ahrache and Imbeau (2009))

Model	RA(%)
Rohmert (1973)	$RA = 18 \times f_{HT}^{1.4}(f_{MVC} - 0.15)^{0.5} \times 100$
Milner et al. (1985)	$RA = 0.164 \times \left[4.61 + \ln\left(\frac{1}{100 - f_{HT}^{-1}}\right)\right]^{-1} \times 100$
Rose et al. (1992)	$RA = 3 \times MHT^{-1.52} \times 100$
Byström and Fransson-Hall (1994)	$RA = \left[\frac{\%MVC}{15} - 1\right]$

It should be noticed that all the RA models mentioned above are obtained from experimental data, and the substantial differences among these profiles indicates large differences in human recovery process. Although those differences can be explained by the different subjects participating the experiment, methods to measure recovery, and modeling approach (El ahrache and Imbeau, 2009), the same problem for those models as in fatigue MET models, they can not be generalized to analyze the performance of a certain population. Furthermore, it is believed that individual characteristics are the determinant factors. However, the personal factors are not considered enough in the models based on experiments.

In contrast, in our rest-allowance model, four parameters are used to calculate the suitable work schedule: k, R, f_{MVC}, and f_{HT}. Personal fatigue and recovery characteristics can be represented by k and R, and furthermore, both relative external load and relative work duration are also taken into consideration as traditional models. The RA model can be therefore generalized for industrial manual handling operations.

6.3.2 Recovery process during manual handling operation

Work-rest schedule is very important in ergonomics application. Combining fatigue and recovery model can determine the work-rest schedule. Different work cycles result in different fatigue evaluation results. In our application case, two working cycles are evaluated. One is drilling a hole in 30 s and recovery 30 s in Fig. 6.7, and another one is 30 s drilling and 60 s recovery in Fig. 6.8.

Based on the virtual human modeling, we take the 3.5 kg and shoulder joint for demonstrate

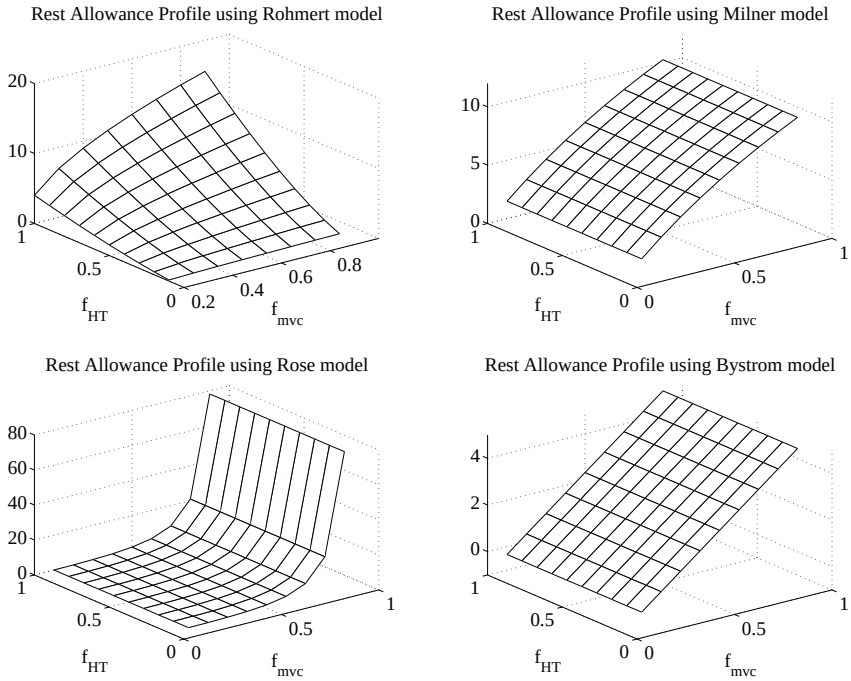

Figure 6.6: Rest allowance profiles using the existing RA models

the influence of recovery period. It is obvious that the longer the rest period is, the better the joint strength can be recovered. Sufficient recovery time can maintain the worker's physical capacity for quite a long time; but insufficient recovery time might cause cumulative fatigue in the joint. In Fig. 6.7, cumulative fatigue during the working procedure can be indicated by the reduction of the joint strength.

And in rest time 60 s, the joint strength can be recovered during the rest period to maintain the job. Once the requirement of the joint strength is over the capacity; the overexertion might cause MSD in human body. It should be mentioned that in actual work; there are lots of influencing factors affecting the recovery procedure, and the rate of recovery changes individually. R is set as 2.4 min^{-1} for 50% population to determine the work-rest schedule.

6.4 Discussion

6.4.1 Recovery model

This recovery model is capable of modeling complex and nonlinear muscle recovery behavior. The model qualitatively reproduce the muscle recovery behavior which has been modeled in the literature. The limitation of the regressed models is that those models were obtained under specific job conditions, and they cannot be extended easily for other different works. In contrast to these

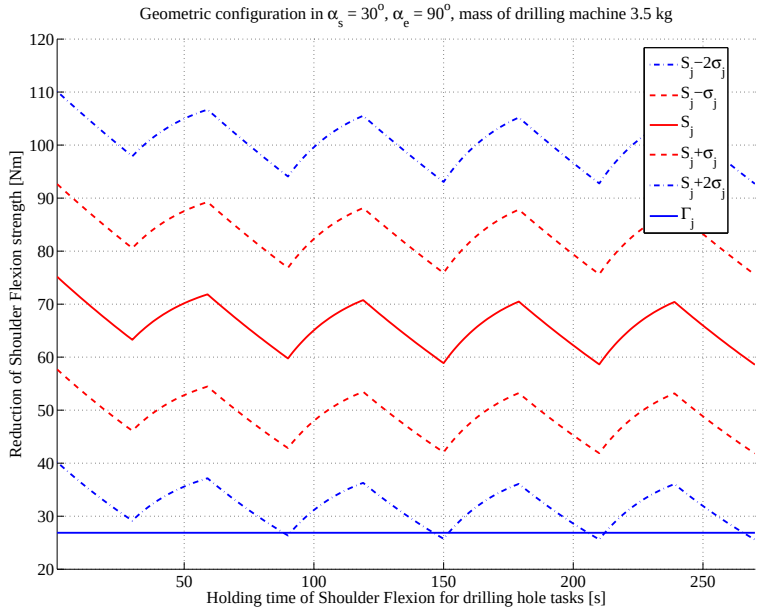

Figure 6.7: Fatigue and recovery in a work cycle

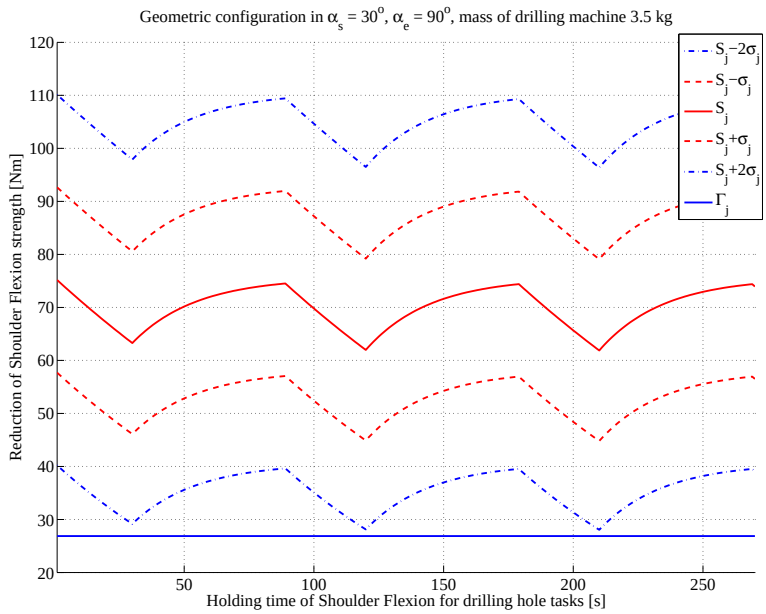

Figure 6.8: Fatigue and recovery in a work cycle

experimental regression models, our theoretical approach is useful as it can be applied generally.

In our recovery model, two terms, the starting fatigue level $\frac{\Gamma_{j,cem_{ini}}}{\Gamma_{j,max}}$ and personal recovery property R, are the main factors determining the recovery process. From the comparison to other recovery models, either in force measurement or in EMG, the similar exponential function has been found consistent with those existing models, therefore we can assume that there is a great possibility that this model can be further experimentally validated. Of course, there are lots of other factors which can generate influences on the recovery process, such as: environmental factors, task types, etc. Until now, these factors are out of consideration in constructing the recovery model, and they are still under investigation for their importances.

In spite of the effects from other factors, another problem is when to apply the recovery model in manual handling operation. According to Rohmert's definition, the recovery occurs by ending, reducing or changing the action which results in fatigue. Therefore, in rest-allowance models and some other theoretical models (half-joint model, rest-allowance models, etc.), recovery happens always just after the termination of the fatigue process. However, in contrast, in some theoretical models (Liu's and Wexler's physiological models), recovery happens simultaneously while the fatigue process occurs. In reality, recovery does happen at the same time with fatigue. Since in most manual handling operations, the external load is relatively large, therefore fatigue is more observable than recovery. We assume that recovery occurs only after the contraction in most physical operations with high strength demands, so we use the recovery model in the rest period between two contractions.

This recovery model has not yet been experimentally validated. The proposition of this model in this chapter aims only to complete the theoretical analysis with the fatigue model. The validation of the recovery model will be one of our future work.

6.4.2 Rate of recovery from individual

Another problem while using the recovery model is how to determine the parameter R for different muscle groups and different population. We propose two approaches: (1) regression from experimental results; (2) mathematical modeling from personal factors.

For the first approach, it is possible to design job specific operations for different muscle groups. Since in recovery period, there is no external load, therefore it might be convenient to measure the recovery level and find R for different individuals. The distribution of R can be further analyzed and then perhaps it is possible to construct basic data set for a certain population for the recovery rates under different job conditions. Since there are large differences in four existing rest-allowance models, it is impossible to use these models to find a suitable R values in the same method as finding the fatigue rate k from MET models.

In the second approach, we assume the parameter R is constant for each individual during a certain period and the rate of recovery is closely related with different factors. A regression model might be useful to predict recovery rates mathematically. However, still great effort is required to achieve the regression model, as the recovery process is very complex and there are different factors engaged in recovery. As a result, the recovery rate R does not only change individually, but also changes over time (Liu et al., 2002).

The rate of recovery depends on muscle groups, gender, age, and muscle training history. From Section 6.2, we have found that different muscle groups might have different recovery parameters. Furthermore, Short and Sedlock (1997) found that trained subjects had faster recovery rates than untrained subjects, while Fulco et al. (1999) reported longer endurance, slower fatigue rate, and faster early recovery rate in women than in men. Additionally, the recovery process is mainly determined by the metabolic regulation in muscles. Early recovery of MVC force is closely linked with muscle oxidative phosphorylation, and it has been found that muscle oxygen consumption occurs primarily during recovery between intense contractions rather than during contractions (Fulco et al., 1999). Different muscle fiber compositions have different muscle oxygen consumption characteristics and lead to different early recovery rates. In Xia and Frey Law (2008), the fatigue and recovery parameters of different fibers are estimated, and the rates of recovery of the muscle fibers are ordered as: type IIb ($0.02\ s^{-1}$) > type IIa ($0.01\ s^{-1}$) > type I ($0.002\ s^{-1}$). In Bol et al. (2009), R has been assumed from 0.0 to 1.0 s^{-1} for different muscle fibers. It is still a challenging work to find a suitable model to predict R.

6.5 Summary

In this chapter, a recovery model which keeps the consistency with the fatigue model has been presented. In comparison to other fatigue models, it is promising that this recovery model could be used to predict recovery process correctly. With this model, it is possible to complete the analysis of the fatigue and recovery process for static manual handling operations. Furthermore, personal recovery rate might be found and modeled after experimental validation. This model is computational efficient and it can be used in ergonomics application for work-rest allowance prediction and biomechanical applications.

Chapter 7

General conclusions and perspectives

Contents

7.1 Conclusions 129
7.2 Perspectives 130

7.1 Conclusions

This thesis deals with the issues of posture analysis and posture prediction in virtual human simulation, especially for manual handling operations in static cases. The main contributions of our research work in virtual human simulation are:

1. human status and its mathematical description;
2. update of human status in virtual human simulation;
3. simplified muscle fatigue and recovery model for ergonomic applications;
4. posture analysis and posture prediction with consideration of fatigue effect.

In Chapter 2, we presented a new conception (human status) and a new approach for human simulation (update of human status in a close loop). The Human Status aggregates all the capacities together to configure the initial conditions for virtual human simulation, and it generalizes the discussion in virtual human simulation. The change of the human status before and after an operation can be used in evaluating the influence from the physical work, and it can be used task independently for assessing the difficulty of different physical or mental operations. Furthermore, the update of the human status can be taken to generate new simulation based on the renewed human status. Fatigue

effect is one concrete application of human status with consideration of the reduction of the physical strength.

In Chapter 3 and 6, we presented a new simplified muscle fatigue and recovery model in order to realize the fatigue evaluation. The simplified fatigue model and recovery model have been explained from basic muscle physiological principle, and furthermore, it includes only the parameters which are used in conventional ergonomic tools as MSD risk factors. That means our model provides a connection between the internal parameters in the muscle and the external parameters from industrial operations. Both models have been theoretically validated, and the high agreement between our model and the existing model provides a promising result for applying our model in ergonomic situations. The fatigue model has been validated experimentally in Chapter 4. The direct measurement of fatigue is used to construct the exponential fatigue function of different individuals. High correlations between measured result and theoretical analysis promise that the fatigue model is available for assessing physical fatigue of upper limbs in static manual handling operations.

In the development of the fatigue and recovery model, two new parameters have been created to indicate the fatigue resistance and recovery rate of an individual. Although only 40 subjects have been tested for the fatigue resistance in upper limb muscle groups, great interests have been aroused for measuring the distribution of these parameters for a certain population and it is believed that both parameters are suitable to quantify fatigue and recovery properties in static cases. If the distribution was achievable, these parameters could be very important for evaluating the fatigue and recovery of a certain population.

The application of the human status and the models is given in Chapter 5. As discussed before, the predicted change of human status can represent the different influence from physical work on human body. Different strengths and different fatigue resistances can lead to significant different result. A study case of industrial drilling in airplane assembly line has been simulated in the posture analysis application. A good agreement has also been found between the theoretical evaluation results and the experimental results in Chapter 4. Furthermore, since it is believed that there are certain strategies guiding the human motion, multi-objective optimization method for predicting posture with consideration of fatigue effect was also demonstrated. The influence of fatigue effect on posture is predictable in this method, and the result is found in agreement with the results from experiments.

7.2 Perspectives

Until now, only physical human status is considered in our framework, and it is also limited to joint strengths. In the future, the other aspects of human status should be examined and established

to extend the scope of the conception, especially for mental aspects, since it would be useful for evaluating mental work load objectively.

Going back to our fatigue and recovery model, only the upper limb has been tested in the experiments in our current research. For the future research, more experiments should be carefully designed to test the availability of our model in other muscle groups, such as back/hip, neck etc. The recovery model is only theoretically compared with other existing models in the literature. More effort should be contributed to the experimental validation of the recovery model. After the experimental validation, the combination of the fatigue and recovery model can be useful for work-rest allowance determination. Concerning the fatigue resistance and rate of recovery, more measurements are necessary to determine the distribution of them.

Most of the operations examined in this thesis were done under static or quasi-static conditions. In dynamic operations, due to the alternation of static posture and dynamic movement, the fatigue and recovery process might be different from the cases mentioned in this thesis. Therefore, it could be interesting to find out the differences between dynamic and static conditions in order to understand the usefulness and limitations of our current models. Certain change might be necessary to make our model suitable in dynamic cases.

The integration of the fatigue and recovery model into computer-aided ergonomics requires also some work. Databases containing strength, fatigue resistance, and rate of recovery need to be established to describe the fatigue and recovery properties of a certain population. New algorithms should be developed to make the update of human strengths possible in a continuous working process.

For human behavior prediction, there are still other guidances leading the human motion, such visibility, accessibility, etc. These aspects should also be taken into account in order to assess an operation completely. The modeling of these aspects and the influences from the work history on these aspects provide one potential research field, and how these aspects influence the human behavior is another point of interest for posture prediction.

Furthermore, the health issues in muscles just cover one part of the occupational disorders. One of our research direction would be constructing detailed musculoskeletal systems. In this way, the force reaction of muscles, tendons, and bones could be analyzed. It is expected that the detailed biomechanical analysis could help us in locating possible sources for the MSDs.

In summary, there are still lots of work to do in order to understand better the interactions between the operations and the humans. The final aim of virtual human simulation is able to predict the human's operation as real as possible and as quick as possible. Only in this way, the potential risks generated by the operations can be reduced to acceptable level, and computer aided ergonomics can benefit the human being.

Bibliography

Abdel-Malek, K., Yu, W., Jaber, M., 2001. Realistic posture prediction. 2001 SAE Digital Human Modeling and Simulation.

Åhsberg, E., Gamberale, F., 1998. Perceived fatigue during physical work: an experimental evaluation of a fatigue inventory. International Journal of Industrial Ergonomics 21 (2), 117–131.

Åhsberg, E., Gamberale, F., Kjellberg, A., 1997. Perceived quality of fatigue during different occupational tasks: development of a questionnaire. International Journal of Industrial Ergonomics 20 (2), 121–135.

Anderson, D., Madigan, M., Nussbaum, M., 2007. Maximum voluntary joint torque as a function of joint angle and angular velocity: Model development and application to the lower limb. Journal of Biomechanics 40 (14), 3105–3113.

Armstrong, T., Buckle, P., Fine, L. J., Hagberg, M., Jonsson, B., Kilborn, A., Silverstein, B. A., Sjogaard, G., Viikari-Juntura, 1993. A conceptual model for work-related neck and upper-limb musculoskeletal disorders. Scandinavian Journal of Work, Environment and Health 19 (2), 73–84.

Arthur, K., 2000. Effects of field of view on performance with head-mounted displays. Ph.D. thesis, University of North Carolina.

Ayoub, M., 1998. A 2-D simulation model for lifting activities. Computers & Industrial Engineering 35 (3-4), 619–622.

Ayoub, M., Lin, C., 1995. Biomechanics of manual material handling through simulation: Computational aspects. Computers & Industrial Engineering 29 (1-4), 427–431.

Badler, N., 1997. Virtual humans for animation, ergonomics, and simulation. Proceedings of the 1997 IEEE Workshop on Motion of Non-Rigid and Articulated Objects 36.

Badler, N. I., Phillips, G. B., Webber, B. L., 1993. Simulating humans: computer graphics animation and control. Oxford University Press, USA.

Bishu, R., Kim, B., Klute, G., 1995. Force-endurance relationship: does it matter if gloves are donned? Applied Ergonomics 26 (3), 179–185.

Bol, M., Pipetz, A., Reese, S., 2009. Finite element model for the simulation of skeletal muscle fatigue. Materialwissenschaft und Werkstofftechnik 40 (1-2), 5–12.

Bongers, P. M., De Winter, C. R., Kompier, M. A. J., Hildebrandt, V., 1993. Psychosocial factors at work and musculoskeletal disorders. Scandinavian Journal of Work, Environment and Health 19, 297–312.

Borg, G., 1998. Borg's perceived exertion and pain scales. Human Kinetics.

Borg, G., 2004. Handbook of Human Factors and Ergonomics Methods. CRC Press, Ch. Scaling Experiences during Work: Perceived Exertion and Difficulty, pp. 11.1–11.7.

Bubb, H., Engstler, F., Fritzsche, F., Mergl, C., Sabbah, O., Schaefer, P., Zacher, I., 2006. The development of RAMSIS in past and future as an example for the cooperation between industry and university. International Journal of Human Factors Modelling and Simulation 1 (1), 140–157.

Buckle, P., Devereux, J., for Safety, E. A., at Work, H., 1999. Work-related neck and upper limb musculoskeletal disorders. Office for Official Publications of the European Communities.

Buckle, P. W., Devereux, J. J., 2002. The nature of work-related neck and upper limb musculoskeletal disorders. Applied Ergonomics 33 (3), 207–217.

Burdorf, A., 1992. Exposure assessment of risk factors for disorders of the back in occupational epidemiology. Scandinavian Journal of Work, Environment and Health 18 (1), 1–9.

Burdorf, A., Laan, J., 1991. Comparison of methods for the assessment of postural load on the back. Scandinavian Journal of Work, Environment and Health 17 (6), 425–429.

Byström, S., Fransson-Hall, C., 1994. Acceptability of intermittent handgrip contractions based on physiological response. Human factors 36 (1), 158–171.

Carnahan, B., Norman, B., Redfern, M., 2001. Incorporating physical demand criteria into assembly line balancing. IIE Transactions 33 (10), 875–887.

Chaffin, D., 1997. Development of computerized human static strength simulation model for job design. Human Factors and Ergonomics in Manufacturing 7 (4), 305–322.

Chaffin, D. B., 1969. A computerized biomechanical model-development of and use in studying gross body actions. Journal of Biomechanics 2 (4), 429–441.

Chaffin, D. B., Andersson, G. B. J., Martin, B. J., 1999. Occupational biomechanics, 3rd Edition. Wiley-Interscience.

Chatizwa, I., 1996. Gender and ergonomics in agricultural engineering. Proceedings from AGROTEC/FAO workshop - Gender and agricultural engineering.

Chedmail, P., Chablat, D., Le Roy, C., 2003. A distributed approach for access and visibility task with a manikin and a robot in a virtual reality environment. Industrial Electronics, IEEE Transactions on 50 (4), 692–698.

Chen, Y., 2000. Changes in lifting dynamics after localized arm fatigue. International Journal of Industrial Ergonomics 25 (6), 611–619.

Conover, W., 1980. Practical nonparametric statistics. New York, Wiley.

Corlett, E. N., 1995. Evaluation of human work. London: Taylor & Francis, Ch. The evaluation of posture and its effects, pp. 662–713.

Corlett, E. N., Bishop, R. P., 1976. A technique for assessing postural discomfort. Ergonomics 19 (2), 175–182.

Costill, D., Coyle, E., Fink, W., Lesmes, G., Witzmann, F., 1979. Adaptations in skeletal muscle following strength training. Journal of Applied Physiology 46 (1), 96–99.

Dahmane, R., Djordjevič, S., Šimunič, B., Valenčič, V., 2005. Spatial fiber type distribution in normal human muscle histochemical and tensiomyographical evaluation. Journal of Biomechanics 38 (12), 2451–2459.

Damsgaard, M., Rasmussen, J., Christensen, S., Surma, E., de Zee, M., 2006. Analysis of musculoskeletal systems in the AnyBody Modeling System. Simulation Modelling Practice and Theory 14 (8), 1100–1111.

Ding, J., Wexler, A., Binder-Macleod, S., 2000a. Development of a mathematical model that predicts optimal muscle activation patterns by using brief trains. Journal of Applied Physiology 88 (3), 917–925.

Ding, J., Wexler, A., Binder-Macleod, S., 2003a. Mathematical models for fatigue minimization during functional electrical stimulation. Journal of Electromyography and Kinesiology 13 (6), 575–88.

Ding, J., Wexler, A. S., Binder-Macleod, S. A., 2000b. A predictive model of fatigue in human skeletal muscles. Journal of Applied Physiology 89 (4), 1322–1332.

Ding, J., Wexler, A. S., Binder-Macleod, S. A., 2003b. Mathematical models for fatigue minimization during functional electrical stimulation. Electromyography Kinesiology 13 (6), 575–588.

Ding, Y., Ceglarek, D., Shi, J., 2002. Design evaluation of multi-station assembly processes by using state space approach. Journal of Mechanical Design 124 (3), 408–418.

Duong, B., Low, M., Moseley, A., Lee, R., Herbert, R., 2001. Time course of stress relaxation and recovery in human ankles. Clinical Biomechanics 16 (7), 601–607.

Dysart, M., Woldstad, J., 1996. Posture prediction for static sagittal-plane lifting. Journal of Biomechanics 29 (10), 1393–1397.

Edwards, R., Hill, D., Jones, D., Merton, P., 1977. Fatigue of long duration in human skeletal muscle after exercise. The Journal of Physiology 272 (3), 769–778.

El ahrache, K., Imbeau, D., 2009. Comparison of rest allowance models for static muscular work. International Journal of Industrial Ergonomics 39 (1), 73–80.

El ahrache, K., Imbeau, D., Farbos, B., 2006. Percentile values for determining maximum endurance times for static muscular work. International Journal of Industrial Ergonomics 36 (2), 99–108.

Elfving, B., Dedering, Å., 2007. Task dependency in back muscle fatigue–Correlations between two test methods. Clinical Biomechanics 22 (1), 28–33.

Elfving, B., Liljequist, D., Dedering, Å., Németh, G., 2002. Recovery of electromyograph median frequency after lumbar muscle fatigue analysed using an exponential time dependence model. European Journal of Applied Physiology 88 (1), 85–93.

Enoka, R., 1995. Mechanisms of muscle fatigue: central factors and task dependency. Journal of Electromyography and Kinesiology 5 (3), 141–149.

EuropGip, 2006. Musculoskeletal disorders in europe: definitions and statistics. Tech. rep., http://www.eurogip.fr/docs/TMS_07-Eurogip-25-EN.pdf.

Forsman, M., Hansson, G., Medbo, L., Asterland, P., Engström, T., 2002. A method for evaluation of manual work using synchronised video recordings and physiological measurements. Applied Ergonomics 33 (6), 533–540.

Foxlin, E., Inc, I., 2002. Motion Tracking Requirements and Technologies. Handbook of virtual environments: Design, implementation, and applications, 163–210.

Freund, J., Takala, E., 2001. A dynamic model of the forearm including fatigue. Journal of Biomechanics 34 (5), 597–605.

Fulco, C., Rock, P., S.R., M., Lammi, F., Cymerman, A., Butterfield, G., Moore, L., Braun, B., Lewis, S., 1999. Slower fatigue and faster recovery of the adductor pollicis muscle in women matched for strength with men. Acta Physiologica Scandinavica 167 (3), 233–239.

Fuller, J., Lomond, K., Fung, J., Côté, J., 2008. Posture-movement changes following repetitive motion-induced shoulder muscle fatigue. Journal of electromyography and kinesiology, doi:10.1016/j.jelekin.2008.10.009.

Garg, A., Hegmann, K., Schwoerer, B., Kapellusch, J., 2002. The effect of maximum voluntary contraction on endurance times for the shoulder girdle. International Journal of Industrial Ergonomics 30 (2), 103–113.

Giat, Y., Mizrahi, J., Levy, M., 1993. A musculotendon model of the fatigue profiles of paralyzed quadriceps muscle under FES. IEEE Transactions on Biomechanical Engineering 40 (7), 664–674.

Hicks, A., Kent-Braun, J., Ditor, D., 2001. Sex differences in human skeletal muscle fatigue. Exercise and Sport Sciences Reviews 29 (3), 109–112.

Hill, A., 1938. The heat of shortening and the dynamic constants of muscle. Proceedings of the Royal Society of London. Series B, Biological Sciences 126 (843), 136–195.

Hou, H., Sun, S., Pan, Y., 2007. Research on virtual human in ergonomic simulation. Computers & Industrial Engineering 53 (2), 350–356.

HSE, 2005. Self-reported work-related illness in 2004/05. Tech. rep., Health, Safety and Executive, http://www.hse.gov.uk/statistics/swi/tables/0405/ulnind1.htm.

Hu, B., Zhang, W., 2008. Progress review for project EADS. Tech. rep., Department of Industrial Engineering, Tsinghua University.

International Ergonomics Association, 2000. What is ergonomics.

Iridiastadi, H., Nussbaum, M., 2006a. Muscle fatigue and endurance during repetitive intermittent static efforts: development of prediction models. Ergonomics 49 (4), 344–360.

Iridiastadi, H., Nussbaum, M., 2006b. Muscular fatigue and endurance during intermittent static efforts: effects of contraction level, duty cycle, and cycle time. Human factors 48 (4), 710–720.

Jayaram, U., Jayaram, S., Shaikh, I., Kim, Y., Palmer, C., 2006. Introducing quantitative analysis methods into virtual environments for real-time and continuous ergonomic evaluations. Computers In Industry 57 (3), 283–296.

Jorgensen, K., 1997. Human trunk extensor muscles physiology and ergonomics. Acta Physiologica Scandinavica. Supplementum 637, 1–58.

Jung, E., Choe, J., 1996. Human reach posture prediction based on psychophysical discomfort. International Journal of Industrial Ergonomics 18 (2), 173–179.

Jung, E., Kee, D., Chung, M., 1995. Upper body reach posture prediction for ergonomic evaluation models. International Journal of Industrial Ergonomics 16 (2), 95–107.

Kanemura, N., Kobayashi, R., Hosoda, M., Minematu, A., Sasaki, H., Maejima, H., Tanaka, S., Matuo, A., Takayanagi, K., Maeda, T., et al., 1999. Effect of visual feedback on muscle endurance in normal subjects. Journal of Physical Therapy Science 11 (1), 25–29.

Karst, G., Hasan, Z., 1987. Antagonist muscle activity during human forearm movements under varying kinematic and loading conditions. Experimental Brain Research 67 (2), 391–401.

Karwowski, W., Genaidy, A., Asfour, S., 1990. Computer-aided ergonomics. Taylor & Francis.

Kasprisin, J., Grabiner, M., 2000. Joint angle-dependence of elbow flexor activation levels during isometric and isokinetic maximum voluntary contractions. Clinical Biomechanics 15 (10), 743–749.

Khalil, W., Dombre, E., 2002. Modelling, identification and control of robots. Hermes Science Publications.

Komura, T., Shinagawa, Y., Kunii, T. L., 1999. Calculation and visualization of the dynamic ability of the human body. The Journal of Visualization and Computer Animation 10 (2), 57–78.

Komura, T., Shinagawa, Y., Kunii, T. L., 2000. Creating and retargetting motion by the musculoskeletal human. The Visual Computer 16 (5), 254–270.

Lämkull, D., Hanson, L., Örtengren, R., 2007. The influence of virtual human model appearance on visual ergonomics posture evaluation. Applied Ergonomics 38 (6), 713–722.

Larivière, C., Gravel, D., Gagnon, D., Gardiner, P., Bertrand Arsenault, A., Gaudreault, N., 2006. Gender influence on fatigability of back muscles during intermittent isometric contractions: A study of neuromuscular activation patterns. Clinical Biomechanics 21 (9), 893–904.

Li, G., Buckle, P., 1999. Current techniques for assessing physical exposure to work-related musculoskeletal risks, with emphasis on posture-based methods. Ergonomics 42 (5), 674–695.

Liu, J., Brown, R., Yue, G., 2002. A dynamical model of muscle activation, fatigue, and recovery. Biophysical Journal 82 (5), 2344–2359.

Ma, L., Chablat, D., Bennis, F., Zhang, W., 2009. A new simple dynamic muscle fatigue model and its validation. International Journal of Industrial Ergonomics 39 (1), 211–220.

Ma, L., Chablat, D., Bennis, F., Zhang, W., Guillaume, F., 2008. A new muscle fatigue and recovery model and its ergonomics application in human simulation. Proceedings of IDMME - Virtual Concept 2008.

Mademli, L., Arampatzis, A., 2008. Effect of voluntary activation on age-related muscle fatigue resistance. Journal of Biomechanics 41 (6), 1229–1235.

Maier, M., Ross-Mota, J., 2000. Work-related musculoskeletal disorders. http://www.cbs.state.or.us/external/imd/rasums/resalert/msd.html.

Mathiassen, S., Ahsberg, E., 1999. Prediction of shoulder flexion endurance from personal factor. International Journal of Industrial Ergonomics 24 (3), 315–329.

McAtamney, L., Corlett, E. N., 1993. RULA: A survey method for the investigation of work-related upper limb disorders. Applied Ergonomics 24 (2), 91–99.

Milner, N., Corlett, E., O'Brien, C., 1985. Modeling fatigue and recovery in static postural exercise. Ph.D. thesis, University of Nottingham.

Milner, N., Corlett, E., O'Brien, C., 1986. A model to predict recovery from maximal and submaximal isometric exercise. In: The Ergonomics of Working Postures: Models, Methods and Cases: the Proceedings of the First International Occupational Ergonomics Symposium, Zadar, Yugoslavia, 15-17 April 1985. CRC Press, pp. 126–136.

Mital, A., Kumar, S., 1998. Human muscle strength definitions, measurement, and usage: part II-the scientific basis(knowledge base) for the guide. International Journal of Industrial Ergonomics 22 (1-2), 123–144.

Mottram, C., Jakobi, J., Semmler, J., Enoka, R., 2005. Motor-unit activity differs with load type during a fatiguing contraction. Journal of Neurophysiology 93 (3), 1381–1392.

Nomura, J., Sawada, K., 2001. Virtual reality technology and its application on aircraft assembling. Annual Reviews in Control 25, 99–109.

Payandeh, S., Dill, J., Zhang, J., 2007. Using haptic feedback as an aid in the design of passive mechanisms. Computer-Aided Design 39 (6), 528–538.

Pontonnier, C., Dumont, G., 2008. From motion capture to muscle forces in human elbow aiming at improving ergonomics of working stations. Proceeding of Virtual Concept & IDMME 2008.

Ren, L., Jones, R., Howard, D., 2007. Predictive modelling of human walking over a complete gait cycle. Journal of Biomechanics 40 (7), 1567–1574.

Rodgers, S. H., 1987. Recovery time needs for repetitive work. Seminars in Occupational Medicine 2 (1), 19–24.

Rodgers, S. H., 2004. Handbook Of Human Factors And Ergonomics Methods. CRC Press, Ch. Muscle fatigue assessment: functional job analysis technique, pp. 12.1–12.10.

Rodríguez, I., Boulic, R., 2008. Evaluating the influence of induced passive torques in the simulation of time-varying human poses. Computers & Graphics 32 (4), 474–484.

Rodríguez, I., Boulic, R., Meziat, D., 2003a. A model to assess fatigue at joint-level using the half-joint concept. In: Visualization and Data Analysis, Proceedings of the SPIE. Santa Clara, CA USA, pp. 21–27.

Rodríguez, I., Boulic, R., Meziat, D., 2003b. Visualizing human fatigue at joint level with the half-joint pair concept. In: Visualization and Data Analysis, Proceedings of the SPIE. Vol. 5009. Santa Clara, CA USA, pp. 37–45.

Rohmert, W., 1960. Ermittlung von Erholungspausen für statische Arbeit des Menschen. European Journal of Applied Physiology 18 (2), 123–164.

Rohmert, W., 1973. Problems in determining rest allowances Part 1: use of modern methods to evaluate stress and strain in static muscular work. Applied Ergonomics 4 (2), 91–5.

Rohmert, W., Rutenfranz, J., 1983. Erholung und pause. Praktische Arbeitsphysiologie. Stuttgart: G Thieme.

Rohmert, W., Wangenheim, M., Mainzer, J., Zipp, P., Lesser, W., 1986. A study stressing the need for a static postural force model for work analysis. Ergonomics 29 (10), 1235–1249.

Roman-Liu, D., Tokarski, T., 2005. Upper limb strength in relation to upper limb posture. International Journal of Industrial Ergonomics 35 (1), 19–31.

Roman-Liu, D., Tokarski, T., Kowalewski, R., 2005. Decrease of force capabilities as an index of upper limb fatigue. Ergonomics 48 (8), 930–948.

Roman-Liu, D., Tokarski, T., Wójcik, K., 2004. Quantitative assessment of upper limb muscle fatigue depending on the conditions of repetitive task load. Journal of Electromyography and Kinesiology 14 (6), 671–682.

Rose, L., Ericson, M., Glimskär, B., Nordgren, B., 1992. Ergo-index-development of a model to determine pause needs after fatigue and pain reactions during work. Computer Applications in Ergonomics, Occupational Safety and Health, 461–468.

Russell, S. J., Winnemuller, L., Camp, J. E., Johnson, P. W., 2007. Comparing the results of five lifting analysis tools. Applied Ergonomics 38 (1), 91–97.

Sato, H., Ohashi, J., Iwanaga, K., Yoshitake, R., Shimada, K., 1984. Endurance time and fatigue in static contractions. Journal of human ergology 13 (2), 147–154.

Schaub, K., Landau, K., Menges, R., Grossmann, K., 1997. A computer-aided tool for ergonomic workplace design and preventive health care. Human Factors and Ergonomics in Manufacturing 7 (4), 269–304.

Seymour, N., Gallagher, A., Roman, S., O'Brien, M., Bansal, V., Andersen, D., Satava, R., 2002. Virtual reality training improves operating room performance: results of a randomized, double-blinded study. Annals of Surgery 236 (4), 458–464.

SHARP, 2005. Safety and health assessment and research for prevention : work-related musculoskeletal disorders of the neck, back, and upper extremity in washington state, 1995-2003. Tech. rep., Washington State Department of Labor and Industries.

Shepstone, T., Tang, J., Dallaire, S., Schuenke, M., Staron, R., Phillips, S., 2005. Short-term high- vs. low-velocity isokinetic lengthening training results in greater hypertrophy of the elbow flexors in young men. Journal of Applied Physiology 98 (5), 1768–1776.

Short, K., Sedlock, D., 1997. Excess postexercise oxygen consumption and recovery rate in trained and untrained subjects. Journal of applied physiology 83 (1), 153–159.

Sirca, A., Kostevc, V., 1985. The fibre type composition of thoracic and lumbar paravertebral muscles in man. Journal of Anatomy 141, 131–137.

Smith, B., 2009. Studying visibility as a constraint and as an objective for posture prediction. SAE International Journal of Passenger Cars - Mechanical Systems 1 (1), 1118–1124.

Stanton, N., Hedge, A., Brookhuis, K., Salas, E., Hendrick, H., 2004. Handbook of human factors and ergonomics methods. CRC PRESS.

Staron, R., Hagerman, F., Hikida, R., Murray, T., Hostler, D., Crill, M., Ragg, K., Toma, K., 2000. Fiber type composition of the vastus lateralis muscle of young men and women. Journal of Histochemistry and Cytochemistry 48 (5), 623–630.

Sun, S., Wu, Q., Chai, C., Xiong, Y., 2006. A driving posture prediction method based on driver comfort. In: Computer-Aided Industrial Design and Conceptual Design, 2006. CAIDCD'06. 7th International Conference on. pp. 1–5.

Tilley, A. R., Dreyfuss, H., 2002. The measure of man & woman. Human factors in design. Revised Edition. New York: John Wiley & Sons, Inc.

Vignes, R. M., 2004. Modeling muscle fatigue in digital humans. Master's thesis, Graduate College of The University of Iowa.

Vøllestad, N., 1997. Measurement of human muscle fatigue. Journal of Neuroscience Methods 74 (2), 219–227.

VSR Research Group, 2004. Technical report for project virtual soldier research. Tech. rep., Center for Computer-Aided Design, The University of IOWA.

Wang, Y., Zhang, W., Bennis, F., Chablat, D., 2006. An integrated simulation system for human factors study. In: The Institute of Industrial Engineers Annual Conference. Orlando, Florida, pp. 20–24.

Welch, G., Foxlin, E., 2002. Motion tracking: No silver bullet, but a respectable arsenal. IEEE Computer Graphics and Applications 22 (6), 24–38.

Westgaard, R., Winkel, J., 1996. Guidelines for occupational musculoskeletal load as a basis for intervention: a critical review. Applied Ergonomics 27 (2), 79–88.

Wexler, A. S., Ding, J., Binder-Macleod, S. A., 1997. A mathematical model that predicts skeletal muscle force. IEEE Transactions On Biomedical Engineering 44 (5), 337–348.

Wiktorin, C., Karlqvist, L., Winkel, J., 1993. Validity of self-reported exposures to work postures and manual materials handling. Scandinavian Journal of Work, Environment and Health 19 (3), 208–214.

Wilmore, J., Costill, D., Kenney, W., 2008. Physiology of sport and exercise. Human Kinetics.

Wilson, J., 1999. Virtual environments applications and applied ergonomics. Applied Ergonomics 30 (1), 3–9.

Wood, D., Fisher, D., Andres, R., 1997. Minimizing fatigue during repetitive jobs: optimal work-rest schedules. Human Factors: The Journal of the Human Factors and Ergonomics Society 39 (1), 83–101.

Xia, T., Frey Law, L., 2008. A theoretical approach for modeling peripheral muscle fatigue and recovery. Journal of Biomechanics 41 (14), 3046–3052.

Yang, J., Marler, R., Beck, S., Abdel-Malek, K., Kim, J., 2006a. Real-time optimal reach-posture prediction in a new interactive virtual environment. Journal of Computer Science and Technology 21 (2), 189–198.

Yang, J., Marler, R., Kim, H., Arora, J., Abdel-Malek, K., 2004. Multi-objective optimization for upper body posture prediction. In: 10th AIAA/ISSMO Multidisciplinary Analysis and Optimization Conference. pp. 319–353.

Yang, J., Pitarch, E., Kim, J., Abdel-Malek, K., 2006b. Posture prediction and force/torque analysis for human hands. In: Proc. of SAE Digital human modelling for design and engineering conference. p. 2326.

Yang, J., Rahmatalla, S., Marler, T., Abdel-Malek, K., Harrison, C., 2007. Validation of predicted posture for the virtual human santos™. Lecture Notes in Computer Science 4561, 500–510.

Yang, J., Sinokrot, T., Abdel-Malek, K., 2008. A general analytic approach for santos™upper extremity workspace. Computers & Industrial Engineering 54 (2), 242–258.

Yassierli, M., Iridiastadi, H., Wojcik, L., 2007. The influence of age on isometric endurance and fatigue is muscle dependent: a study of shoulder abduction and torso extension. Ergonomics 50 (1), 26–45.

Zhang, X., 1997. The development of a three-dimensional dynamic posture prediction model for seated operator motion simulation. Ph.D. thesis, The University of Michigan.

Zhang, X., Chaffin, D., 2000. A three-dimensional dynamic posture prediction model for simulating in-vehicle seated reaching movements: development and validation. Ergonomics 43 (9), 1314–1330.

APPENDICES

Appendix A

Modified Denavit-Hartenberg notation

This method is a new geometric notation for the description of the kinematic of open-loop, tree, and close-loop structure robots. The method is derived from the well-known Denavit and Hartenberg (DH) notation, which is powerful for serial robots but leads to ambiguities in the case of tree and closed loop structure robots. The given method has all the advantages of DH notation in the case of open-loop.

A tree structure is composed of n joints and $n + 1$ rigid bodies, noted as C_0, C_1, ..., C_n, with several end-effectors (see Fig A.1). For convenience, these bodies can be enumerated in the following way:

- C_0 is the root the tree, and C_n is one terminal of the tree;
- the numbers of all the rigid bodies and joints are enumerated in an increasing order on each branch of the tree, from the root to the terminal end;
- joint j connects the body C_j to body $C_{a(j)}$, where $a(j)$ indicates the number of the antecedent body in the branch from the root to C_j. For a serial structure, $a(j) = j - 1$;
- all the joints are considered as ideal joints, either rotatory or prismatic. A complex joint can be broken into several simple joints connecting with fake bodies with no weight and no length.

The topology of the system is defined by the a(j), where $j = 1, 2, \ldots, n$. In order to determine all the necessary geometrical parameters describing the transformation between different bodies, it is necessary to locate a coordinate system on the tree structure in the following way:

- R_i is the coordinate system fixed on the body C_i;
- $\mathbf{z}_i$ is attached to joint i;

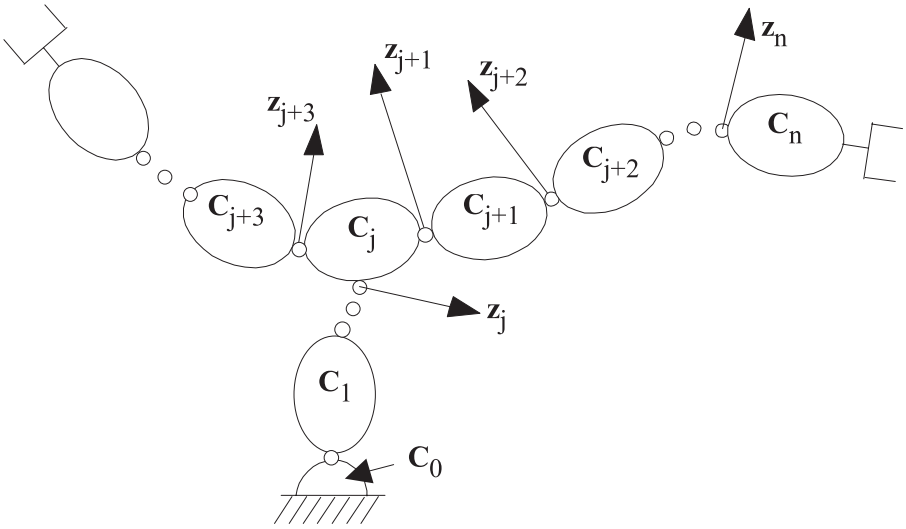

Figure A.1: Associated notations to a tree structure

- $\mathbf{x}_i$ is the common perpendicular to $\mathbf{z}_i$ and the axis which locates following $\mathbf{z}_i$ in the branch and in the rigid body C_i. If body C_i, $i = a(j)$, does not have a tree structure, $\mathbf{x}_i$ is the common perpendicular to $\mathbf{x}_i$ and $\mathbf{x}_j$. When there are more than one body attached to C_i, the proposition is to chose the chain leading to the main end-effector.

In this case, we can define the transformation matrix between two successive coordinates. In the modified DH notation system, six parameters are used to describe the transformation between two Cartesian coordinates. $\mathbf{u}_j$ is the common perpendicular to $\mathbf{z}_i$ and $\mathbf{z}_j$. If $\mathbf{x}_i$ is chosen as the common perpendicular to $\mathbf{z}_i$ and $\mathbf{z}_j$, this is the simple case in serial chain $\mathbf{u}_j = \mathbf{x}_i$, and the last four parameters which are the parameters used usually in DH notation system, are enough to describe the transformation matrix. If $\mathbf{x}_i$ is chosen as the common perpendicular to $\mathbf{z}_i$ and $\mathbf{z}_k$ (see Fig. A.2), $\mathbf{u}_j$ is necessary to be constructed to establish the transformation matrix.

- γ_j: angle between axes $\mathbf{x}_i$ and $\mathbf{u}_j$ around the axis $\mathbf{z}_i$.
- b_j: distance between axes $\mathbf{x}_i$ and $\mathbf{u}_j$ along the axis $\mathbf{z}_i$.
- α_j: angle between axes $\mathbf{z}_i$ and $\mathbf{z}_j$ around the axis $\mathbf{u}_j$.
- d_j: distance between axes $\mathbf{z}_i$ and $\mathbf{z}_j$ along the axis $\mathbf{u}_j$.
- θ_j: angle between axes $\mathbf{u}_j$ and $\mathbf{x}_j$ around the axis $\mathbf{z}_j$.
- r_j: distance between axes $\mathbf{u}_j$ and $\mathbf{x}_j$ along the axis $\mathbf{z}_j$.

The transformation matrix from R_j to R_i is:

$$^{i}\mathbf{T}_j = \mathbf{Rot}(\mathbf{z}, \gamma_j)\mathbf{Trans}((\mathbf{z}, b_j))\mathbf{Rot}(\mathbf{x}, \alpha_j)\mathbf{Trans}(\mathbf{x}, d_j)\mathbf{Rot}(\mathbf{z}, \theta_j)\mathbf{Trans}(\mathbf{z}, r_j) \tag{A.1}$$

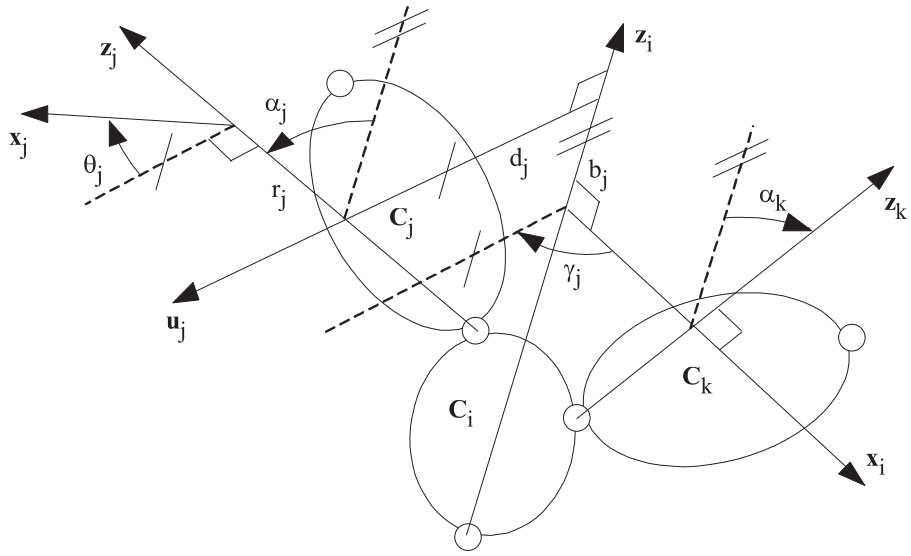

Figure A.2: Geometrical parameters for a body with more than two joints

$$
{}^{i}\mathbf{T}_j = \begin{bmatrix} a_{11} & a_{12} & a_{13} & t_{14} \\ a_{21} & a_{22} & a_{23} & t_{24} \\ a_{31} & a_{32} & a_{33} & t_{34} \\ 0 & 0 & 0 & 1 \end{bmatrix} \tag{A.2}
$$

Where

$a_{11} = \cos\gamma_j \cos\theta_j - \sin\gamma_j \cos\alpha_j \sin\theta_j,$

$a_{12} = -\cos\gamma_j \sin\theta_j - \sin\gamma_j \cos\alpha_j \cos\theta_j,$

$a_{13} = \sin\gamma_j \sin\alpha_j,$

$t_{14} = d_j \cos\gamma_j + r_j \sin\gamma_j \sin\alpha_j,$

$a_{21} = \sin\gamma_j \cos\theta_j + \cos\gamma_j \cos\alpha_j \sin\theta_j,$

$a_{22} = -\sin\gamma_j \sin\theta_j + \cos\gamma_j \cos\alpha_j \cos\theta_j,$

$a_{23} = -\cos\gamma_j \sin\alpha_j,$

$t_{24} = d_j \sin\gamma_j - r_j \cos\gamma_j \sin\alpha_j,$

$a_{31} = \sin\alpha_j \sin\theta_j,$

$a_{32} = \sin\alpha_j \cos\theta_j,$

$a_{33} = \cos\alpha_j,$

$t_{34} = r_j \cos\alpha_j + b_j.$

Use a vector **q** to present generalized variables of the joint chain, and then the joint chain from the root to the end effector can be described as:

$$
\mathbf{q} = [q_1 \ldots q_n]^T \tag{A.3}
$$

with $q_j = (1 - \sigma_j)\theta_j + \sigma_j r_j$ for $j = [1 \ldots n]$, where

- $\sigma_j = 0$ for the rotational joints.
- $\sigma_j = 1$ for the translational joints.

In our geometrical modeling of the virtual human, the geometrical center of pelvis is chosen as the root. Five branches are established to fulfill the functions. The functions of different joint are explained in Table A.1. Two main end-effectors are modeled in this model: left and right hands.

Table A.1: Functions of the joints in human geometrical model

Joint ID	Function
1	torso rotation
2	torso adduction & abduction
3	torso extension & flexion
4	torso rotation
5	torso extension & flexion
6	neck rotation
7	neck adduction & abduction
8	neck extension & flexion
9,14	shoulder flexion & extension
10,15	shoulder adduction & abduction
11,16	shoulder rotation lateral & medial
12,17	elbow flexion
13,18	forearm supination & pronation
19,24	hip flexion
20,25	hip rotation
21,26	hip adduction & abduction
22,27	knee flexion
23,28	ankle extension & flexion

Appendix B

Newton-Euler inverse dynamics for posture analysis

B.1 Mathematical description of task

- There are two external forces on human body while drilling a hole. One is the drilling effort $\boldsymbol{F}_d$, and the other one is the gravity of the drilling machine, symboled as $\boldsymbol{G}_d$.
- The drilling force (Eq. B.1) acting at the center point of the hole (${}^0\boldsymbol{P}_h = [p_x, p_y, p_z]^T$) with magnitude of $5g$, where $g = 9.81ms^{-2}$. The direction of the force is along the symmetric line of the hole pointing out from inner side of the hole, noted as ${}^0\boldsymbol{V}_{hole} = [v_x, v_y, v_z]^T$.

$$ {}^0\boldsymbol{F}_d = 5g\,{}^0\boldsymbol{V}_{hole} \tag{B.1} $$

- The gravity (Eq. B.2) of the machine and its pipes can be quantified as $m_d g$ ($5 < m_d < 7$ maximum) with direction vertically down.

$$ {}^0\boldsymbol{G}_d = m_d\,{}^0\boldsymbol{G} \tag{B.2} $$

where ${}^0\boldsymbol{G} = [0, 0, -g]^T$. The gravity force acts on the gravity center of the drilling machine ${}^0\boldsymbol{W}_d = [W_x, W_y, W_z]^T$.

B.2 Geometric modeling of arm

In order to analyze the fatigue caused by the mechanical work, geometric and dynamic model of arm is going to be presented. According to biomechancial structure of arm, five general joints are

selected to model the arm. They are graphically shown in Fig. B.1. They are:

- q_1: joint generating flexion and extension of shoulder
- q_2: joint generating adduction and abduction of shoulder
- q_3: joint generating supination and pronation of upper arm
- q_4: joint generating flexion and extension of elbow
- q_5: joint generating supination and pronation of forearm

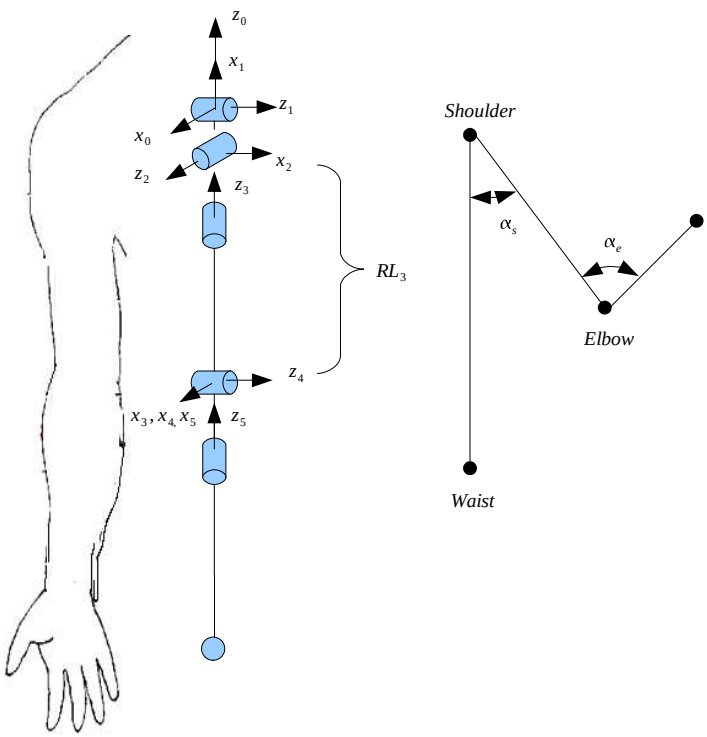

Figure B.1: Geometric modeling of the arm

Each joint has a joint coordinate R_j with an origin O_j, and the coordinate axes are determined based on the rule of Modified DH Notation System. The body between R_j and R_{j+1} is noted as C_j. R_0 is the base coordinate system locating at the shoulder. These coordinate systems are also shown in Fig. B.1. And meanwhile the parameters to describe the transformation between R_{j-1} and R_j are listed in Table B.1.

The transformation matrix from R_j to the R_{j-1} is:

Table B.1: Geometric modeling parameters for the right arm

Joint	σ	d	α	r	θ	θ_{ini}
1	0	0	$-\frac{\pi}{2}$	0	θ_1	$-\frac{\pi}{2}$
2	0	0	$-\frac{\pi}{2}$	0	θ_2	$-\frac{\pi}{2}$
3	0	0	$-\frac{\pi}{2}$	-RL_3	θ_3	$-\frac{\pi}{2}$
4	0	0	$-\frac{\pi}{2}$	0	θ_4	0
5	0	0	$\frac{\pi}{2}$	0	θ_5	0

$$
{}^{j-1}\boldsymbol{T}_j = \begin{bmatrix} \cos\theta_j & -\sin\theta_j & 0 & d_j \\ \cos\alpha_j \sin\theta_j & \cos\alpha_j \cos\theta_j & -\sin\alpha_j & -r_j \sin\alpha_j \\ \sin\alpha_j \sin\theta_j & \sin\alpha_j \cos\theta_j & \cos\alpha_j & -r_j \cos\alpha_j \\ 0 & 0 & 0 & 1 \end{bmatrix} \tag{B.3}
$$

This matrix can also be noted as:

$$
{}^{j-1}\boldsymbol{T}_j = \begin{bmatrix} {}^{j-1}\boldsymbol{s}_j & {}^{j-1}\boldsymbol{n}_j & {}^{j-1}\boldsymbol{a}_j & {}^{j-1}\boldsymbol{P}_j \\ 0 & 0 & 0 & 1 \end{bmatrix} = \begin{bmatrix} {}^{j-1}\boldsymbol{A}_j & {}^{j-1}\boldsymbol{P}_j \\ 0 & 1 \end{bmatrix} \tag{B.4}
$$

with ${}^{j-1}\boldsymbol{s}_j$, ${}^{j-1}\boldsymbol{n}_j$ and ${}^{j-1}\boldsymbol{a}_j$ representing x, y, and z axes of R_j in R_{j-1}. ${}^{j-1}\boldsymbol{P}_j$ represents the vector of $O_{j-1}O_j$ in R_{j-1}.

In order to finish the geometric modeling of arm, several parameters of the arm need to be obtained from anthropometry. These parameters are:

- Length of forearm: h_f
- Radius of forearm: r_f
- Length of upper arm: h_u. This equals to RL_3
- Radius of upper arm: r_u

With parameters listed in Table B.1, the geometrical model of hand can be constructed based on robotic techniques. In spite of the parameters above, there are some other parameters representing some important center points of the arm in Table B.2. The values are determined in corresponding joint coordinates.

These parameters can be obtained from anthropometry database. In our case, several simple functions can be used for estimate these parameters. If the human has a height of H, then according

Name	Coordinates	Symbol	Coordinates
Flexion/Extension Center of Shoulder	R_1	$\boldsymbol{S_{s1}}$	$[0,0,0]^T$
Flexion/Extension Center of Elbow	R_4	$\boldsymbol{S_{e4}}$	$[0,0,0]^T$
Mass Center of Forearm	R_3	$\boldsymbol{S_{f3}}$	$[0,0,-\frac{h_f}{2}]^T$
Mass Center of Upper arm	R_5	$\boldsymbol{S_{u5}}$	$[0,0,\frac{h_u}{2}]^T$
Holding center of Hand	R_5	$\boldsymbol{S_{t5}}$	$[0,0,-h_f]^T$

Table B.2: Coordinates of several center points in corresponding joint coordinates system

to the equations listed in the book (Chaffin et al., 1999) the other geometric parameters can be obtained from Eq. B.5:

$$\begin{aligned} h_f &= 0.146H \\ r_f &= 0.125h_f \\ h_u &= 0.186H \\ r_u &= 0.125h_u \end{aligned} \tag{B.5}$$

B.3 Parameters for dynamic modeling of arm

To calculate the moment of Inertia of each part of arm. In this part, we simplify that the upper arm and forearm have a uniform density distribution ρ and they have symmetric shape as cylinders. The mass of upper arm and mass of forearm are m_u and m_f correspondingly. With the geometric parameters of them, their cylindrical inertia can be determined with h as height of cylinder and r radius of cylinder (Eq.B.6).

$$\boldsymbol{I}_G = \begin{bmatrix} \frac{mr^2}{4} + \frac{mh^2}{12} & 0 & 0 \\ 0 & \frac{mr^2}{4} + \frac{mh^2}{12} & 0 \\ 0 & 0 & \frac{mr^2}{2} \end{bmatrix} \tag{B.6}$$

If the participant's weight is known as M, according to Chaffin et al. (1999), the mass of forearm and upper arm can be estimated by Eq. B.7.

$$\begin{aligned} m_f &= 0.451 \times 0.051M \\ m_u &= 0.549 \times 0.051M \end{aligned} \tag{B.7}$$

B.4 Calculation of torques at joints

Nomenclature for Inverse Dynamics

- $\boldsymbol{a}_j$: unit vector of axis z_j
- $\boldsymbol{F}_j$: the sum of the external forces on body C_j
- $\boldsymbol{f}_j$: force exerted on C_j via point O_j from C_{j-1}
- $\boldsymbol{f}_{ej}$: force exerted on C_j via point O_j from environment
- G_j: gravity center of C_j
- $\boldsymbol{I}_{Gj}$: tensor of inertia C_j relative to a coordinates system in origin of G_j and parallel to R_j
- ${}^j\boldsymbol{J}_j$: tensor of inertia C_j relative to coordinates system R_j
- $\boldsymbol{L}_j$: vector linking the origin of R_{j-1} and the origin of R_j, $O_{j-1}O_j$
- M_j: mass of body C_j
- $\boldsymbol{M}_j$: moment of forces on body C_j around the point O_j
- $\boldsymbol{MS}_j$: moment of inertia of body C_j around the origin O_j
- $\boldsymbol{M}_{Gj}$: moment of forces on body C_j around the point G_j
- $\boldsymbol{m}_j$: moment exerted on C_j around O_j from C_{j-1}
- $\boldsymbol{m}_{ej}$: moment exerted on C_j via point O_{j-1} from environment around O_j
- $\boldsymbol{V}_j$: velocity of point O_j
- $\dot{\boldsymbol{V}}_j$: acceleration of point O_j
- $\boldsymbol{V}_{Gj}$: velocity of point G_j
- $\dot{\boldsymbol{V}}_{Gj}$: acceleration of point G_j
- $\boldsymbol{\omega}_j$: rotation speed of point O_j
- $\dot{\boldsymbol{\omega}}_j$: rotation acceleration of point O_j
- $\Gamma_{j,max}$: strength of joint j in general coordinates
- $\Gamma_j(t)$: load of joint j in general coordinates

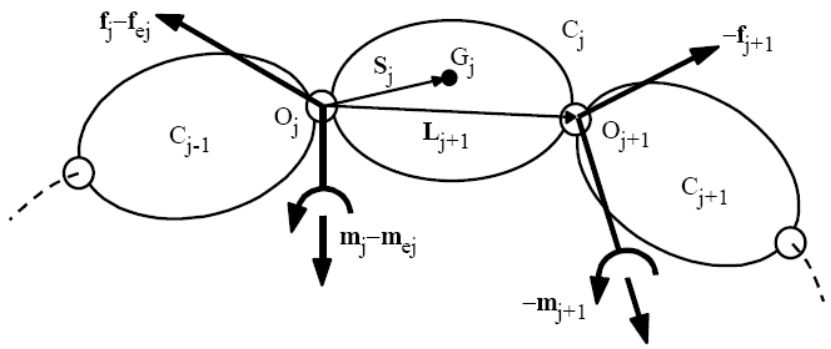

Figure B.2: Dynamic forces exerted on joint body

To calculate the torques at each joint, Newton-Euler inverse dynamics is employed. The general procedure is described in Khalil and Dombre (2002).

For a given solid body with a mass M_j and moment of inertia $\boldsymbol{I}_{Gj}$, the sum of the force and torques on the solid body is:

$$\begin{aligned} \boldsymbol{F}_j &= M_j \dot{\boldsymbol{V}}_{Gj} \\ \boldsymbol{M}_{Gj} &= \boldsymbol{I}_{Gj}\dot{\boldsymbol{\omega}}_j + \boldsymbol{\omega}_j \times (\boldsymbol{I}_{Gj}\boldsymbol{\omega}_j) \end{aligned} \tag{B.8}$$

with $\boldsymbol{\omega}_j$ indicating angular velocity and $\boldsymbol{V}_{Gj}$ as the velocity of the mass center of the body.

Because $\boldsymbol{V}_{Gj} = \boldsymbol{V}_j + \boldsymbol{\omega}_j \times \boldsymbol{S}_j$ and $\boldsymbol{I}_{Gj} = \boldsymbol{J}_j - M_j\hat{\boldsymbol{S}}_j\hat{\boldsymbol{S}}_j$.

$$\begin{aligned} \boldsymbol{F}_j &= M_j\dot{\boldsymbol{V}}_j + \dot{\boldsymbol{\omega}}_j \times \boldsymbol{M}\boldsymbol{S}_j \\ \boldsymbol{M}_j &= J_j\dot{\boldsymbol{\omega}}_j + \boldsymbol{M}\boldsymbol{S}_j \times \dot{\boldsymbol{V}}_j + \boldsymbol{\omega}_j \times (\boldsymbol{J}_j\boldsymbol{\omega}_j) \end{aligned} \tag{B.9}$$

If $\bar{\sigma}_j = 1 - \sigma$,

$$\begin{aligned} \boldsymbol{\omega}_j &= \boldsymbol{\omega}_{j-1} + \bar{\sigma}_j\dot{q}_j\boldsymbol{a}_j \\ \boldsymbol{V}_j &= \boldsymbol{V}_{j-1} + \boldsymbol{\omega}_{j-1} \times \boldsymbol{L}_j + \sigma\dot{q}_j\boldsymbol{a}_j \end{aligned} \tag{B.10}$$

From the base to the end effector, kinematic parameters of each joint coordinate can be determined.

$$\begin{aligned} \dot{\boldsymbol{\omega}}_j &= \dot{\boldsymbol{\omega}}_{j-1} + \bar{\sigma}_j(\ddot{q}_j\boldsymbol{a}_j + \boldsymbol{\omega}_{j-1} \times \dot{q}_j\boldsymbol{a}_j) \\ \dot{\boldsymbol{V}}_j &= \dot{\boldsymbol{V}}_{j-1} + \dot{\boldsymbol{\omega}}_{j-1} \times \boldsymbol{L}_j + \boldsymbol{\omega}_{j-1} \times (\boldsymbol{\omega}_{j-1} \times \boldsymbol{L}_j + \sigma\dot{q}_j\boldsymbol{a}_j) + \sigma(\ddot{q}_j\boldsymbol{a}_j + \boldsymbol{\omega}_{j-1} \times \dot{q}_j\boldsymbol{a}_j) \end{aligned} \tag{B.11}$$

From the end effector to the base, joint force and torque can be determined one by one.

$$\begin{aligned} \boldsymbol{F}_j &= \boldsymbol{f}_j - \boldsymbol{f}_{j+1} + M_j\boldsymbol{G} - \boldsymbol{f}_e \\ \boldsymbol{M}_j &= \boldsymbol{m}_j - \boldsymbol{m}_{j+1} - \boldsymbol{L}_{j+1} \times \boldsymbol{f}_{j+1} + \boldsymbol{S}_j \times M_j\boldsymbol{G} - \boldsymbol{m}_{ej} \end{aligned} \tag{B.12}$$

By excluding the influences from external forces and other joint bodies, the force generated by each joint can be calculated.

$$\begin{aligned} \boldsymbol{f}_j &= \boldsymbol{F}_j + \boldsymbol{f}_{j+1} + \boldsymbol{f}_e - M_j\boldsymbol{G} \\ \boldsymbol{m}_j &= \boldsymbol{M}_j + \boldsymbol{m}_{j+1} + \boldsymbol{L}_{j+1} \times \boldsymbol{f}_{j+1} + \boldsymbol{m}_{ej} - \boldsymbol{S}_j \times M_j\boldsymbol{G} \end{aligned} \tag{B.13}$$

The general force for each joint is:

$$\Gamma_j = (\sigma_j \boldsymbol{f}_j + \bar{\sigma}_j \boldsymbol{m}_j)^T \, {}^j\boldsymbol{a}j \tag{B.14}$$

It is practical to calculate the Γ_j in its corresponding joint coordinate.

$${}^j\boldsymbol{\omega}_{j-1} = {}^j\boldsymbol{A}_{j-1} \, {}^{j-1}\boldsymbol{\omega}_{j-1} \tag{B.15}$$

$${}^j\boldsymbol{\omega}_j = {}^j\boldsymbol{\omega}_{j-1} + \bar{\sigma}_j \dot{q}_j \, {}^j\boldsymbol{a}_j \tag{B.16}$$

$${}^j\dot{\boldsymbol{\omega}}_j = {}^j\boldsymbol{A}_{j-1} \, {}^{j-1}\dot{\boldsymbol{\omega}}_{j-1} + \bar{\sigma}_j(\ddot{q}_j \, {}^j\boldsymbol{a}_j + {}^j\boldsymbol{\omega}_{j-1} \times \dot{q}_j \, {}^j\boldsymbol{a}_j) \tag{B.17}$$

$${}^j\dot{\boldsymbol{V}}_j = {}^j\boldsymbol{A}_{j-1}({}^{j-1}\dot{\boldsymbol{V}}_{j-1} + {}^{j-1}\boldsymbol{U}_{j-1} \, {}^{j-1}\boldsymbol{P}_j) + \sigma_j(\ddot{q}_j \, {}^j\boldsymbol{a}_j + 2 \, {}^j\boldsymbol{\omega}_{j-1} \times \dot{q}_j \, {}^j\boldsymbol{a}_j) \tag{B.18}$$

$${}^j\boldsymbol{U}_j = {}^j\hat{\dot{\boldsymbol{\omega}}}_j + {}^j\hat{\boldsymbol{\omega}}_j \, {}^j\hat{\boldsymbol{\omega}}_j \tag{B.19}$$

$$\begin{aligned} {}^j\boldsymbol{F}_j &= M_j \, {}^j\dot{\boldsymbol{V}}_j + {}^j\boldsymbol{U}_j \, {}^j\boldsymbol{MS}_j \\ {}^j\boldsymbol{M}_j &= {}^j\boldsymbol{J}_j \, {}^j\boldsymbol{\omega}_j + {}^j\boldsymbol{MS}_j \times {}^j\dot{\boldsymbol{V}}_j + {}^j\boldsymbol{\omega}_j \times ({}^j\boldsymbol{J}_j \, {}^j\boldsymbol{\omega}_j) \end{aligned} \tag{B.20}$$

$${}^j\boldsymbol{f}_j = {}^j\boldsymbol{F}_j + {}^j\boldsymbol{f}_{j+1} + {}^j\boldsymbol{f}_{ej} \tag{B.21}$$

$${}^j\boldsymbol{f}_j = {}^{j-1}\boldsymbol{A}_j \, {}^j\boldsymbol{f}_j \tag{B.22}$$

$${}^j\boldsymbol{m}_j = {}^j\boldsymbol{M}_j + {}^j\boldsymbol{A}_{j+1} \, {}^{j+1}\boldsymbol{m}_{j+1} + {}^{j+1}\boldsymbol{P}_j \times {}^j\boldsymbol{f}_{j+1} + {}^j\boldsymbol{m}_{ej} \tag{B.23}$$

The general force for each joint is:

$$\Gamma_j = (\sigma_j \, {}^j\boldsymbol{f}_j + \bar{\sigma}_j \, {}^j\boldsymbol{m}_j)^T \, {}^j\boldsymbol{a}j \tag{B.24}$$

According to the analysis, necessary parameters for calculating the forces are listed in Table B.3.

Table B.3: Dynamic modeling parameters for arm

Number	Mass	${}^{j}\boldsymbol{J}_j$	$\boldsymbol{f}_{ej}$	$\boldsymbol{m}_{ej}$
1	0	$\mathbf{0}_3$	0	0
2	0	$\mathbf{0}_3$	0	0
3	$m_3 = m_u$	$\boldsymbol{J}(m_3, h_3, r_3)$	0	0
4	0	$\mathbf{0}_3$	0	0
5	$m_3 = m_f$	$\boldsymbol{J}(m_5, h_5, r_5)$	${}^{5}\boldsymbol{F}_d + {}^{5}\boldsymbol{G}_d$	${}^{5}(O_5P_h) \times {}^{5}\boldsymbol{F}_d + {}^{5}(O_5W_d) \times {}^{5}\boldsymbol{G}_d$

Appendix C

Joint strength change based on posture change

Based on the strength model in Chaffin et al. (1999), the shoulder flexion strength can be expressed by Eq. C.1.

$$S_s = (227.338 + 0.525\alpha_E - 0.296\alpha_S)G \tag{C.1}$$

where $\alpha_S = q_1$, $\alpha_S = 180 - q_2$, and G (Male:0.2845, female:0.1495) is the parameter for gender adjustment, which is constant for different gender.

When there is posture change which can be represented by $d\alpha_E$ and $d\alpha_S$, the variation of shoulder strength can be expressed by Eq. C.2:

$$dS_s = \frac{\partial S_s}{\partial \alpha_E} d\alpha_E + \frac{\partial S_s}{\partial \alpha_S} d\alpha_S \tag{C.2}$$

The maximum percentage of the change in joint strength is Eq. C.3.

$$p = \frac{\mathrm{d}S_s}{S_s} \leq \frac{\left|\frac{\partial S_s}{\partial \alpha_E}\mathrm{d}\alpha_E\right|}{S_s} + \frac{\left|\frac{\partial S_s}{\partial \alpha_s}\mathrm{d}\alpha_s\right|}{S_s} \tag{C.3}$$

Suppose that $\alpha_E = 120$, $\alpha_S = 40$, $d\alpha_E = 10$, and $\alpha_S = 10$, then

$$p = \frac{0.525 \times 10 + 0.296 \times 10}{227.338 + 0.52 \times 120 - 0.296 \times 40} = \frac{8.21}{277.898} < 3\% \tag{C.4}$$

The profile of the shoulder flexion strength is graphically shown in Fig. C.1. The gray zone on the profile is the strength range of a 50th male population with the change of the posture. The maximum approaches to 81.6 Nm and the minimum approaches to 76.6 Nm. The change of the strength locates in an interval with a length of 6.25%, which means the largest normalized change of the strength is only 3.125% from the mean value of the strength.

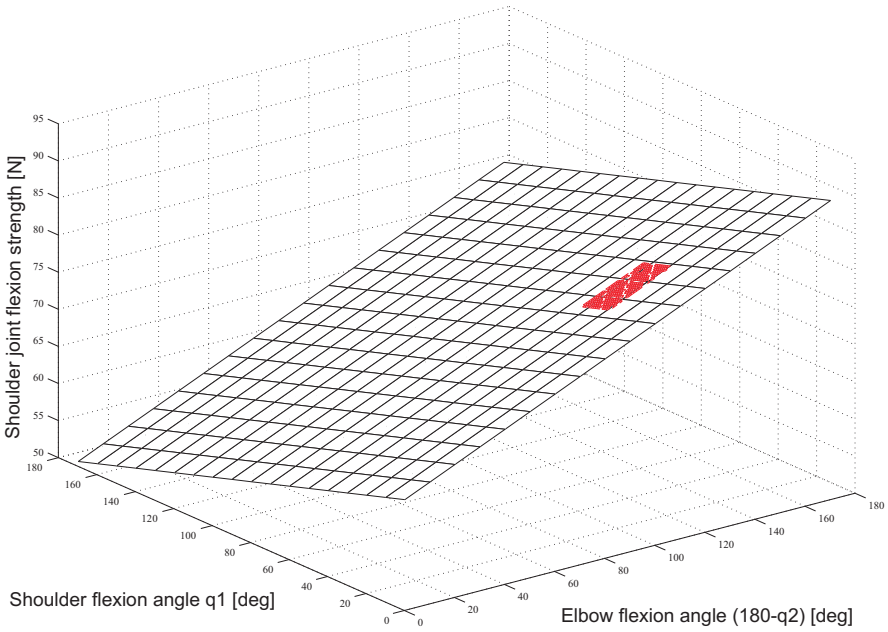

Figure C.1: Shoulder joint flexion strength of adult male population

Appendix D

Original experiment data

Table D.1: Individual force measurement results.(0-180: measurement instant, second; Age: year; Height: cm; Weight: kg; Measured strength: kg)

ID	0	15	30	45	60	75	90	120	150	180	Age	Height	Weight
1	8.2	5.7	5.0	4.7	4.0	2.5	2.4	2.2	2.0	1.6	46	172	80
2	6.0	5.1	4.1	3.6	3.4	2.8	2.8	2.0	1.7	1.0	55	176	75
3	6.3	3.6	3.2	2.8	2.5	2.4	2.2	1.5	1.4	1.2	25	178	95
4	9.0	6.8	5.8	4.4	4.2	3.6	3.6	2.6	1.7	1.1	48	172	72
5	6.0	4.5	3.6	2.6	2.5	2.3	2.2	1.9	1.7	1.6	50	166	80
6	7.6	5.7	4.7	3.6	3.3	2.8	2.7	1.9	1.6	1.4	48	172	70
7	7.3	5.4	3.5	3.2	3.2	3.0	2.8	2.7	2.3	1.8	55	170	72
8	6.2	5.4	5.1	3.6	3.9	3.6	3.5	3.0	2.2	-	38	172	65
9	15.0	12.0	11.0	10.2	9.6	8.7	8.4	8.1	7.6	7.6	51	168	70
10	9.6	7.2	5.9	5.0	4.8	4.5	3.8	3.8	2.7	2.5	42	182	80
11	6.0	3.8	2.9	2.4	1.5	1.4	1.3	1.5	0.9	0.6	25	175	60
12	13.2	10.5	9.6	8.7	7.6	6.6	6.1	5.9	5.8	4.6	43	170	65
13	9.6	8.7	8.3	7.1	6.4	5.7	4.7	3.7	2.8	2.3	48	170	75
14	9.6	9.0	8.2	7.3	6.2	6.0	5.8	5.3	4.1	2.6	54	160	60
15	10.1	8.6	7.9	6.9	6.3	5.9	5.7	4.2	3.5	2.5	41	170	80
16	7.8	3.6	3.3	3.2	3.0	2.6	2.2	1.9	1.7	1.1	43	174	70
17	14.5	12.3	11.2	10.6	10.2	9.8	9.6	8.3	7.7	6.7	28	173	80
18	8.6	6.6	5.2	4.7	4.7	4.3	4.2	3.2	2.3	2.6	53	162	50
19	7.9	4.9	3.8	3.7	3.5	3.4	3.2	2.6	2.2	2.0	38	167	55

Continued on Next Page…

ID	0	15	30	45	60	75	90	120	150	180	Age	Height	Weight
20	7.1	6.1	6.0	5.9	5.7	5.0	4.6	4.0	2.6	1.0	22	183	65
21	5.5	2.8	3.5	3.4	2.2	2.2	2.0	1.6	0.9	0.7	23	172	65
22	7.6	6.4	6.0	4.8	3.7	3.4	3.1	4.0	3.4	2.1	38	179	60
23	6.9	5.0	3.7	3.4	3.4	3.3	3.0	2.6	2.1	1.9	49	170	70
24	7.0	5.4	3.9	3.5	3.0	2.1	2.0	1.1	0.8	0.7	35	168	55
25	5.7	4.9	4.6	3.9	3.8	3.7	3.5	3.2	2.8	2.6	58	176	85
26	9.7	8.2	5.7	4.7	4.5	4.2	3.6	3.2	2.4	1.9	42	170	70
27	6.0	5.5	4.0	3.3	3.2	2.7	2.7	2.3	2.0	2.0	54	170	90
28	7.6	4.0	3.5	3.4	3.2	2.5	2.3	2.1	1.2	1.8	34	171	60
29	6.7	5.2	5.0	4.7	4.0	3.2	3.0	2.1	1.4	0.7	21	172	70
30	7.9	4.0	3.7	3.2	3.2	2.8	2.2	1.9	1.3	0.8	33	177	85
31	9.8	6.9	6.4	5.5	4.1	3.9	3.5	3.2	2.9	1.4	53	170	75
32	7.7	6.1	5.5	5.2	5.1	4.7	4.4	4.1	3.2	3.1	47	170	80
33	9.3	7.6	6.9	6.3	6.0	5.9	5.7	5.0	4.3	3.5	40	165	75
34	7.6	5.6	4.4	4.3	3.7	3.4	3.4	2.4	2.0	1.6	32	172	65
35	8.9	7.3	7.2	6.9	6.4	5.7	4.6	3.9	3.1	2.6	19	175	60
36	7.3	5.6	5.0	3.8	3.0	3.0	2.5	2.0	1.6	-	19	173	57
37	6.9	5.7	5.1	4.6	4.2	3.3	2.8	2.0	2.3	1.9	45	170	70
38	5.0	4.3	3.2	3.1	2.9	2.8	2.7	2.2	1.9	-	47	160	50
39	8.0	6.4	5.0	4.1	4.0	3.2	2.8	2.1	1.2	0.8	53	173	73
40	7.4	6.1	5.6	5.4	5.2	5.0	4.9	4.4	4.1	3.8	52	162	73

Table D.2: Force measurement results and the mean values and standard deviations at each time instant

Time [sec]	0	15	30	45	60	75	90	120	150	180
Mean	8.10	6.21	5.4	4.79	4.38	3.94	3.66	3.14	2.5	1.99
SD	2.21	2.13	2.05	1.94	1.84	1.76	1.71	1.62	1.57	1.57
Max	15	12.3	11.2	10.6	10.2	9.8	9.6	8.3	7.7	7.6
Min	5	2.8	2.9	2.4	1.5	1.4	1.3	1.1	0.8	0.6

Appendix E

Publications

Journal Papers

L. Ma, D. Chablat, F. Bennis, W. Zhang. 2009. A new simple dynamic muscle fatigue model and its Validation. International Journal of Industrial Ergonomics, 39(1), 211-220.

L. Ma, W. Zhang, D. Chablat, F. Bennis, F. Guillaume. 2009. Multi-objective optimisation method for posture prediction and analysis with consideration of fatigue effect and its application case. Computers & Industrial Engineering, 57(4), 1235-1246.

L. Ma, W. Zhang, HZ. Fu, Y. Guo, D. Chablat, F. Bennis. 2009. A framework for interactive work design based on digital work analysis and simulation. Human Factors and Ergonomics in Manufacturing. (in press)

Articles submitted to journals

L. Ma, B. Hu, D. Chablat, F. Bennis, W. Zhang, F. Guillaume. May, 2009. Physical fatigue in a simulated drilling operation and its regression analysis based on muscle fatigue model. Submitted to Applied Ergonomics.

L. Ma, D. Chablat, F. Bennis, W. Zhang, B. Hu, F. Guillaume. April, 2009. Fatigue evaluation in maintenance and assembly operations by digital human simulation. Submitted to Virtual Reality.

L. Ma, D. Chablat, F. Bennis, W. Zhang, B. Hu, F. Guillaume. January, 2009. A general fatigue resistance model for different muscle groups. Submitted to International Journal of Industrial Ergonomics.

Conference papers

L. Ma, D. Chablat, F. Bennis, W. Zhang, F. Guillaume. 2008. A new muscle fatigue and recovery model and its ergonomics application in human simulation. In the proceeding of IDMME-Virtual Concept, October 8-10, Beijing.

L. Ma, F. Bennis, D. Chablat, W. Zhang. 2008. Framework for dynamic evaluation of muscle fatigue in manual handling work. IEEE International Conference on Industrial Technology, April 21-24, Chengdu.

Patent application

L. Ma, D. Chablat, F. Bennis, F. Guillaume. September 2008. Process for quantitative evaluation of muscle fatigue induced by an activity. Application number: 0856595